Department of Applied Physics

Development of Operational and Teaching Software for a Complex Analytical Instrument Using "Virtual Instrument" Technology

James R Holmes

This thesis is presented as part of the requirements for
the award of the Degree of the Master of Science (Physics)
of the Curtin University of Technology

September 2002

Declaration

This thesis contains no material which has been accepted for the award of any other degree or diploma in any university.

To the best of my knowledge and belief this thesis contains no material previously published by any other person except where due acknowledgment has been made.

Signature: …….

Date: ……...

Abstract

It is not always possible to provide students and new users of complex instrumentation with sufficient hands-on use to fully develop the required knowledge of the instrument. Access may also be limited when there is a need to develop data collection and processing procedures. One solution to this problem is to develop a simulation of the instrument in readily accessible computer software.

Modern computer-based technology allows traditional instrumentation to be replaced with "Virtual Instruments" consisting of digital control/acquisition hardware and software that graphically represents the functions of the physical instrument.

In this thesis, operating and analysis software to simulate the operation of complex analytical instrumentation was successfully developed using a numerical model of the instrument. The approach will reduce the need for machine time for operator training and the development of data collection processing procedures.

In particular the thesis developed software to emulate the behaviour of a VG-354 Thermal Ionisation Mass Spectrometer. Graphical programming tools were employed to create a modular set of "Virtual Instruments" that formed the basis of the model. The Simulated Mass Spectrometer produced results that compared well with real data obtained from the physical instrument.

Virtual Instrument peak centring and measurement modules were then developed to operate the Simulated Mass Spectrometer in peak jumping mode. Uncertainties were reduced with improved analysis techniques employing polynomial least-squares fits for peak centring and single-collector isotope ratio measurements. The techniques also have the potential to accommodate hysteresis effects in the magnetic sector analyser, further reducing uncertainty.

Acknowledgments

I would like to thank Associate Professor Robert Loss (principal supervisor) and Professor Kevin Rosman (associate supervisor), of Curtin University of Technology (Isotope Science Group, Department of Applied Physics) for their guidance with the project and the preparation of this thesis.

The John de Laeter Centre for Mass Spectrometry, Western Australia, of which the Curtin University Isotope Science Group is a major part, supplied all equipment, software and samples.

Thanks must be given to the National Instruments team for:

- developing LabVIEW – which is such a stimulating and exciting software system and
- providing one copy of LABVIEW 3.1 and a GPIB interface card to be used free of charge on this project, via a national competition.

Table of Contents

List of Figures

List of Tables

1. Introduction

1.1 Computers in complex analytical instrumentation

Modern analytical equipment can be highly complex, with many processes occurring at once, producing very large quantities of data. The processes can be repetitive and their control must be repeatable to produce accurate and precise data. Analysis of the data sometimes involves a great deal of calculation and manipulation. These factors have contributed to the wide use of computers in the control, data acquisition and data analysis associated with complex analytical instruments.

The computer provides advantages such as:

- Process automation – a lengthy, complicated sequence of actions can be automatically controlled by the computer, allowing the repetition of the process with a high degree of precision. The computer can ensure a certain series of actions is followed every time an experiment is conducted.
- Data recording – the data produced by an instrument can be recorded digitally through a data acquisition system, allowing (for example) high-rate or long-interval data collection. The data can be recalled at any time for analysis. In this form, the data are less subject to human recording errors and can easily be stored, recalled, shared and processed.
- Data processing – once collected the data can be analysed directly, without the need for manual re-entry, eliminating a possible source of error. The data can be processed as they are collected ("real-time"), producing results during the experiment, or after the data collection is over. The available processing power often dictates whether data collected at high rates or in large quantities are processed in real-time or at a later stage.

These tasks can often be performed without operator intervention, if necessary.

However, no system is without disadvantages. With the addition of a computer comes the possibility of equipment becoming obsolete, requiring maintenance or even replacement of the hardware and software used. Well-designed software allows for portability (the ability to

move software between platforms) and ease of maintenance, lessening the impact of these changes.

1.2 Computers in Simulations

In many situations, sufficient hands-on experience for learning or development comes at the expense of operational time or is simply impractical. The problem could be solved with an adequate computer simulation. Simulations also frequently offer a way of gathering data more rapidly than in a live analysis. Some examples:

- Medical procedures – modern ethical concerns regarding animal exploitation limit opportunities for medical students to practice procedures and for researchers to develop improved, less invasive procedures. Computer based models are widely used in medical training, allowing a student to perform the same procedure many times without a live patient or animal substitute (Müller *et al.*, 2000). Human factors affecting surgery can be assessed using simulations (Berguer *et al.*, 1997) and new medical instruments for improved procedures have been developed with simulations (DeCou *et al.*, 2002).
- Driving – ensuring safety while learning to drive can be difficult, with roads constantly becoming more heavily utilised. Early education is now being undertaken using computer-based models (Derra, 1998), teaching hazard perception and other important parts of driving before the student reaches the road. Tests on factors affecting driving, such as mobile phone use (Reed and Green, 1999; Jenness *et al.*, 2002) and visual perception (Hildreth *et al.*, 2000) have been conducted using simulations, gathering data rapidly and safely.
- Military combat – highly expensive military hardware, such as aircraft, is not always suitable for use in training. Simulations allow for the development of tactics and decision-making skills without taking equipment away from operational use and ensure safety during the training (Smith, 1995; Proctor and Gubler, 1998; Miller *et al.*, 2001). The simulation also allows for many different versions of an exercise to be run in much less time than would otherwise be required.
- Instrument development – simulations are proving a popular way to develop new analytical instruments. Examples include a simulation of canopy reflectance developed to assist in the design of a new remote-sensing satellite (Garcia-Haro and

Sommer, 2002) and a prototyping method that allows an instrument to be demonstrated to the target audience before it is constructed (Zubillaga-Elorza *et al.*, 1999).

- Existing laboratory equipment – it is often the case that a complex, expensive instrument is heavily utilised, restricting the time available to develop improved operating procedures and analytical techniques or to teach a new user how to work with the instrument. Simulations allow users to experience the instrument and provide an environment in which to develop and test procedures. For example, Internet based instruction has been employed with new GC-MS users (Waller and Foster, 2000), freeing the instrument for meaningful experiments. The performance of mass-spectrometers has been investigated via simulations (Eng and Karasek, 1983/1984; Blaum *et al.*, 2000). Instruments used in thermal analysis of polymers have been simulated to allow students wider experimentation with the parameters affecting the polymer behaviours (Harrison, 2001).

1.3 Changes in computer-based instruments

Computer software has changed substantially over the last ten years from user interfaces being based on input/output operations involving reading text and responding by typing, to being increasingly based on graphics and selecting and moving using a graphical pointer (e.g. a computer mouse), interacting with “icons” that are graphical representations of objects (Huang *et al.*, 2002). These changes have generally made software more intuitive and simpler to use for both the “expert” the non-"computer expert" (Staggers and Kobus, 2000).

1.3.1 The Graphical User Interface

Modern personal computers and software have lead to a proliferation of applications employing a "Graphical User Interface" (GUI) for interaction with the user. This wide use of GUIs has resulted in some applications becoming more difficult to use rather than easier (Roberts, 1994). This may be ascribed, in part, to a lack of methodology in the design of computer-based multimedia in general (Alty, 1993). Recent studies have determined that icon design plays a large role in the effectiveness of the GUI (Goonetilleke *et al.*, 2001).

An example of the progression from text to graphical user interfaces is the evolution of Microsoft's PC operating systems (Microsoft, 2001):

- MSDOS - this operating system, designed for the first IBM PCs, was based on text commands and subsequent text based output.
- Windows 1 and 2 – these operating systems allowed the user to swap between tasks and employed a mouse for pointing at what was essentially text in a "window." While they used a pointing device, they didn't exhibit the true features of a GUI.
- Windows 3.x – the first true graphical user interface OS from Microsoft, the user interacted with the computer via an input device, typically a "mouse," to "click" or "double-click" on icons (graphical representations of a program or task), which could be organised into groups. "Menus" were also available, selected with the input device, organising tasks within a program into logical structures (often with sub-menus). Later programs starting employing "buttons", clickable graphics appearing to function in a similar way to a physical button, to provide shortcuts for users that preferred not to navigate the menu structure for common commands.
- Windows 9x / NT 4.0 / 2000 – this interface introduced many improvements intended to make the environment more intuitive for the user. The biggest change was the introduction of the "desktop metaphor" (Tollmar and Sundblad, 1995), a design style for the interface where the user interacted with the screen as if it were the top of a desk. For example, all of the icons could be moved around and organised on the screen. "Drag and drop" was introduced; it was a way of interacting with objects by clicking the mouse on an icon or other object and moving it to another object (such as a folder to move or copy a file or application icon to open a file in the application). Also introduced were "context sensitive menus", small lists of common commands that appeared when an object was "right-clicked", displaying choices related specifically to the object clicked. A "task bar" was introduced, including a "start menu" containing shortcuts to all installed programs.
- Windows XP – the latest version of the Microsoft user interface, this OS is oriented around common tasks, which appear in the start bar rather than the shortcuts to the applications used to perform the tasks.

Figure 1.1 shows a Windows 2000 desktop containing icons and windows, with the task bar at the bottom.

Figure 1.1: A Windows 2000 Desktop

1.3.2 Virtual Instrument technology

Computer hardware is now being used in many circumstances to replace analog instruments. For example, data acquisition cards and controllers based on analog to digital or digital to analog (ADDA) conversion can be used to perform many of the tasks of a traditional instrument. Recently, this hardware has been used in conjunction with software to produce "virtual instruments" that reproduce all of the functions of a traditional instrument via computer hardware and a computer software interface. Sometimes the user interface looks and operates like the front panel of a physical instrument (typical in, for example, a data connection to a digital cathode ray oscilloscope or digital voltmeter) but in other cases the entire "instrument" consists of computer-based hardware such as ADDA devices. Some examples of virtual instruments include:

- A virtual phonocardiogram instrument (Guo *et al.*, 2001) that allows the phonocardiogram to be obtained by an operator over the Internet under their control.

- A modification to a technique for the rapid analysis of low-frequency cochlear microphonic (CM) waveforms (Patuzzi and O'Beirne, 1999) where the computer performed processing after the measurements, usually done by dedicated electronics in real-time.
- An integrated system that allows experimental control, data recording and analysis of neurophysiological and neuropsychological Transcranial magnetic (TMS) and electrical (TES) stimulation of the human brain (Kaelin-Lang and Cohen, 2000).
- Virtual instruments for interfacing pH meters of different brands to a personal computer and for measuring proton changes in lightly buffered solutions during enzymatic reactions (Rigobello *et al.*, 1999).
- A scanning and control system for proton beam micromachining (Bettiol *et al.*, 2001).
- A distributed and multi-platform system for water quality monitoring, enhanced with Internet capabilities (Toran *et al.*, 2001).
- An electrochemical analyzer, suitable for analytical square wave (SW) voltammetry, applied to the determination of riboflavin in multivitamin tablets (Economou *et al.*, 2002).

Modern computer-programming tools also make it substantially easier to develop accurate simulations of the analytical instrument, using a numerical model of physical processes or attributes. This enables control and data acquisition software to be developed without the need for the physical instrumentation, reducing the required actual instrument time, and in the process provides software suitable for use in teaching. These tools were fully exploited in this project.

1.3.3 Application of new computer technology to a complex analytical instrument

An example of a complex analytical instrument that was amongst the first to use computer control and data acquisition is a thermal ionisation mass spectrometer (TIMS) such as the Curtin University VG-354 TIMS. A full description of this instrument and the theory behind its operation are provided in Chapter 2 and some brief details of the software are provided in the following sections. In essence, this type of instrument can be used to measure precise and accurate isotope abundance ratios and the concentrations of elements in a very wide variety of samples. The VG-354 TIMS is a typical example of an analytical instrument that still operates

using almost exclusively text-based control and data acquisition software. The software is still based largely on that developed by the original construction factory in the early 1980s, with some ad-hoc modifications (Loss, 1985).

This software suffers from a number of significant problems.

1) It has always been very difficult for users to learn quickly and, even for experienced users, confusing to translate into the real physical behaviour of the instrument particularly when experimental conditions and circumstances were altered.

2) Because this software has grown in a relatively uncontrolled manner without adequate maintenance, it is now increasingly inflexible and difficult to modify to meet new research requirements.

3) The impending problem is that the current computing hardware and operating system platform needed by the current software is no longer supported and increasingly difficult to maintain.

The instrument software has not been updated for a variety of reasons, including software and OS stability and reliability, because it still produces useful measurements and would require an estimated 2 person years to be completely re-written and tested. Relatively complex instruments such as a thermal ionisation mass spectrometer, which take up to several hours to analyse samples, require thousands of hours of testing to test the hundreds of possible analysis modes and pathways through the control and analysis software. The time required for testing consumes valuable time that would otherwise be available for actual measurements. The project aimed to produce software based on mouse operations and graphics.

Current Mass-Spectrometric data acquisition scheme

The JDCMS VG-354 has been controlled by a cumbersome, inefficient, inflexible, text-based computer operating system and software. Machine operation and data analysis was limited to two forms. “Manual operation” required the user to set most of the machine operating parameters and then commence data acquisition. “Automatic operation” enabled the computer based data acquisition system to control the entire machine, collect data and perform data analysis.

This complex instrument provided an excellent test of new generation tools for developing process control and data acquisition software for measurement science.

New Generation Monitor and Control Software

The programming environment required was one that allowed for rapid development of a virtual instrument where the hardware could be simulated by software (Jamieson and Pearce, 1995). Thus a complete control system could be developed and tested away from the instrument and once completed could be connected to the instrument with little modification. This uses substantially less machine time than traditional programming methods. The simulated virtual instrument also enabled the potential development of a "learning tool" by integrating the fully functioning model with computer-based tutorials. This would provide a facility to learn how to use the control software and to operate the instrument without use of the physical instrument.

The software used in this project was National Instruments' LabVIEW (National-Instruments, 1993) as it satisfies the above criteria. The environment is based on Graphical User Interface (GUI) interaction between the user and hardware. This software can also be linked with software modules written in other languages for increased flexibility (eg C++)

Some projects have been undertaken that produced limited virtual instrument software for the VG-354, using more traditional development methods with modern software tools. A mass-scanning program (Turner, 1995) is available and pyrometer control modules (Frew, 1998) have been created.

1.4 Significance

The potential benefits of this work to the scientific community are significant as this type of research and development is still relatively new. The problems associated with GUI and multimedia development are only now being investigated, while the resource-saving methods of developing this control software are widely applicable.

1.5 Research Methodology

Initial research centred on evaluating the functions of the existing system. The operational principles of the mass spectrometer, the modes of operation, data analysis principles and all other elements of producing isotope ratios with the instrument were investigated. The limitations of the current software were also assessed.

An intuitive, user-friendly graphical user interface was designed. The full capability of the LabVIEW/GUI was exploited, to ensure that the result was not simply "text in a window" but rather based on intuitive graphical representations of entities (Blakey, 1994).

1.6 Project Aims

The broad aims of the project were:

(1) To research physically accurate dynamic numerical models of complex analytical instruments (“Simulated Instruments")

(2) To simplify software development and formulate methods to produce highly effective “Virtual Instrument” software for the control of a complex analytical instrument

The objectives achieved in the project were:

(1) to research and develop a numerical model providing data accurately representing the measurements of the ion currents in a Thermal Ionisation Mass Spectrometer (a "Simulated Mass Spectrometer")

(2) to research and develop “Virtual Instrument” software to monitor and control the Simulated Mass Spectrometer in “manual operation” mode, controlling only the fundamental operations, collecting and analysing data from the simulated instrument.

2. Instrumentation

Complex simulated instruments normally function by using a number of simulated inputs, which are processed by a computer program to generate more inputs and finally the required output. The simulated inputs (and even some of outputs) should be designed to correspond as closely as possible to the physical I/Os expected or required on the real instrument. Totally modelling every process requires a detailed understanding of the real operation of the instrument and each of the individual I/Os systems and components; however, for this project it was necessary only to understand the essential operations of the mass spectrometer so that the critical features could be modelled to provide a simulated virtual instrument that would provide useful results.

Similarly, it is important to understand the limitations and benefits of the software tools used to prepare the simulator and how the software interacts with the real instrument. This chapter reviews the operation of a TIMS and describe how the important component parts were incorporated into the simulator. The subsequent chapter briefly reviews the LabVIEW software employed in this project.

2.1 Thermal Ionisation (Sector Field) Mass Spectrometry

A mass spectrometer is an instrument that measures the relative abundances or ratios of atomic sized particles (isotopes, or atoms, or molecules) of different masses in a sample. There are many different designs and types used in a very wide range of applications in areas such as, astrophysics, analytical and fundamental chemistry, drug detection, environmental and atmospheric science, forensic science, geology and geophysics, marine sciences, medicine, metrology and nutritional studies (White and Wood, 1986). Mass spectrometers range in size from centimetre dimensions attached to extraterrestrial spacecraft that analyse atmospheric gases to room sized dimensions needed to measure Lead isotopes and Lead/Uranium ratios in Zircons to determine the ages of rocks.

Irrespective of instrument design or application, most mass spectrometers possess the following major components:

1) Ion Source - vaporising all or part of the sample, then converting the vapour into ions and subsequently focussing and collimating the ions into a beam. This can be performed by methods such as direct thermal heating, radio frequency generated plasmas, ion bombardment and electron impact.
2) Mass Analyser/Separator - passing the ion beam into electrical and/or magnetic filters (eg Electromagnetic sector fields or magnetic quadrupoles) that sort or separate the single ion beams into separate mass/charge ratio beams.
3) Ion Detection - counting the numbers of ions in each of the mass/charge ratio ion beams or converting the ions into a measurable electrical signal. Counting systems often employ electron or photomultipliers while direct collection of ions and amplification of the resultant electrical signal can be used for larger ion beams.

To minimise ion beam scattering, all three operations normally take place under a vacuum of $<10^{-9}$ bar, which requires associated vacuum enclosures, valves, pumps and monitoring and control equipment.

Figure 1 shows a schematic diagram of the major components of a Thermal Ionisation magnetic sector Mass Spectrometer (TIMS) that relies specifically on direct heating to ionise the sample of interest and a magnetic sector field to separate or analyse the resulting ion beams. The figure also shows the co-ordinate system commonly used within the mass spectrometer. The x co-ordinate is in the direction of travel of the ions.

The output from such a mass spectrometer is always in the form of atom ratios. For example, isotope ratios of Lead's four stable isotopes (mass numbers 204, 206, 207 and 208) would usually reported as $^{206}Pb/^{204}Pb$, $^{207}Pb/^{204}Pb$ and $^{208}Pb/^{204}Pb$

Precisions of parts per million are routinely achieved with modern TIMS instruments.

TIMS is the focus of the research reported in this thesis.

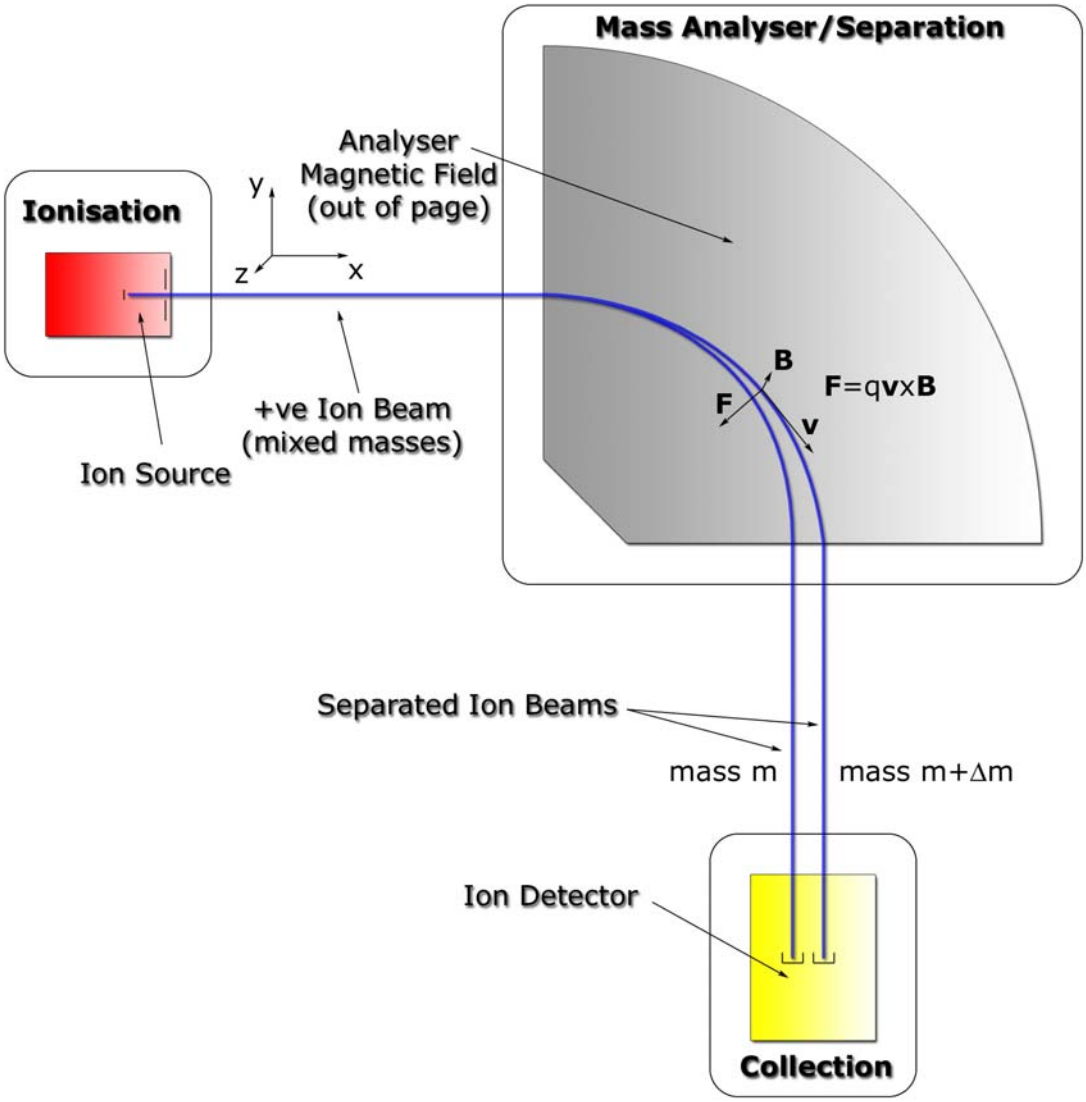

Figure 2.1: Schematic diagram showing the three key components of a Sector Field Mass Spectrometer

2.1.1 Physical Principles and Instrumentation of Mass Spectrometry

Thermal Ionisation

The process of ionising samples can be achieved in a number of ways. These include bombarding the sample with an ion beam; making plasma of the entire sample; and volatilising and ionising the sample from a solid high temperature surface. The most commonly used high temperature surfaces are metal ribbon type filaments, operating between 1000^{O}C and 2000^{O}C.

Surface ionisation for the production of positive ions can be characterised by the Saha-Langmuir equation (Delmore and Appelhans, 1992).

$$\frac{N^+}{N^0} = Ae^{\frac{(\Phi - I)}{kT}} \tag{2.1}$$

where:

N^+, N^0 are the numbers of positive and neutral ions respectively,

A is a constant of proportionality,

Φ is the work function of the material forming the surface (in J),

I is the ionisation potential of the ionised substance (in J),

k is Boltzmann's constant (1.38×10^{-23} J K^{-1}) and

T is the absolute temperature of the surface.

For most systems where $I > \Phi$ the equation indicates that:

- the lower the ionisation potential, the higher the efficiency;
- the higher the work function, the higher the efficiency and
- the higher the temperature, the higher the efficiency

However, most ion formation processes have chemical or volatility issues that complicate the process. For example, low boiling point samples may be vaporised before any significant ionisation occurs. In this case the sample may be converted to a more refractory salt or compound, which increases the probability of producing ionisation, but can lead to other problems such as the sample not readily adhering to the filament.

In single filament ionisation, a number of ionisation processes can be employed. These include:

1) single filament ionisation, self-surface ionisation, where atoms of the filament metal are ionised, such as the rhenium beam from a bare hot rhenium filament.
2) single filament ionisation, of the element deposited directly onto the filament (not electrodeposition) as a compound.
3) single filament ionisation utilizing the silica gel system, in which the element of interest is placed on the filament along with a solution that when heated forms a glassy material and also ions of the element. This is a largely unknown process, which works well for elements with high ionisation potentials, increasing the ionisation efficiency well beyond that obtained by conventional methods. It is possible that the glassy

matrix prepares the element as partially preformed ions (Delmore and Appelhans, 1992). Another possibility is that the matrix holds the element such that it is less volatile and can be fed to the interface between the glass and filament. It is not known whether the ions come from the glass or this interface.

4) multiple filament ionisation, which utilizes two types of closely spaced (< 1mm) filaments (a sublimation and a ionisation filament). The material to be ionised is placed on one or more sublimation filament(s), which are heated by passing small electrical currents through them. Neutral molecules sublime or evaporate from this filament forming a low-pressure neutral atom or molecular cloud near the ionising filament. When these particles strike the ionising filament, molecular bonds may be broken and ions of the element are produced. The chemistry at the ionising surface is largely unknown.

Most single and multiple-filament systems use a rhenium ionising filament, because this metal has a high work function, is available in suitable high purity dimensions and has a very high melting point. However, it is also possible that Rhenium is the best catalyst for the breakdown of the molecules striking the ionising filament (Delmore and Appelhans, 1992).

While it is possible to simulate ionisation processes 1) and 2) above, processes 3) and 4) are very poorly understood. In fact, thermal ionisation of samples is still largely an empirical process; consequently, the simulator was designed to incorporate a number of common input variables, including beam size and signal to noise ratio. The statistical nature of the ion beam generation is discussed in section 2.1.2.

Focussing

Focussing in the ion source is achieved using a series of closely spaced slits and plates held at operator/computer controllable potentials that produce a series of electrostatic fields. The ion focussing and acceleration process can be treated as an ion optical signal-processing model (Regenstreif, 1967; Clement and Compston, 1972), which is how ion sources can be designed. A comprehensive focussing model for ions would require:

- spatial coordinates of the filament and sample,
- electrical potentials, layout and coordinates of seven different plates and slits and
- composition and initial velocities and trajectories of all the ions generated in the source

However, for routine operation of a TIMS instrument it is not necessary to know these parameters. What is required for "real" ion focussing is the production of a maximum ion beam intensity, which is usually achieved either manually or under computer control of the potentials on the focusing plates using a maximising algorithm. While manual ion beam focussing is a useful skill to develop, a real time focussing simulation is well beyond the modelling possibilities of this project. The physical act of focussing could be effectively simulated using seven limited-range random number inputs but this could not effectively simulate the production of other ion beam parameters so focussing was not simulated.

Mass Separation

Mass separation of ions of known mass-to-charge rations in a magnetic field is generally well understood. Assuming the magnetic sector uses a homogeneous magnetic field, the force $\overline{F}$ experienced by the ions is:

$$\overline{F} = q\overline{v} \times \overline{B} \tag{2.2}$$

where q is the charge, $\overline{v}$ is the velocity and $\overline{B}$ is the field strength. This force results in circular motion when both $|\overline{v}|$ and $\overline{B}$ are constant. Therefore, the force must be centripetal and its magnitude is given by:

$$|\overline{F}| = \frac{m|\overline{v}|^2}{r} \tag{2.3}$$

where m is the mass and r is the radius of motion. Combining these equations gives:

$$r = \frac{m|\overline{v}|}{q|\overline{B}|} \tag{2.4}$$

The energy E of the ion can be related to the accelerating potential, V, by

$$E = \frac{1}{2}m|\overline{v}|^2 = qV \tag{2.5}$$

Eliminating v between equations 2.4 and 2.5 gives:

$$\boxed{r = \frac{1}{|\overline{B}|}\sqrt{2V\frac{m}{q}}} \tag{2.6}$$

Equation 2.6 is often called the Mass Spectrometer Equation and shows that the radius of the path depends on the mass to charge ratio (m/q) of the ion.

Sector-shaped magnetic fields have a focussing effect on divergent beams from the ion source (Duckworth *et al.*, 1986 page 337)

Sector fields that employ a non-perpendicular angle of entry for the beam, relative to the magnet, also produce a focussing effect in the "z" direction, normal to the direction of travel of the ions and normal to the plane of travel. This is due to the fringing field at the edges of the magnet pole pieces. An added advantage is that the resolution of the mass spectrometer is doubled with respect to that of a normal-entrance system having the same radius of curvature (Cross, 1951).

This project did not aim to model the intricate details of the mass analyser, as with the focussing of the ion beam in the ion source, but to provide a final set of results suitable for developing analysis routines. Modelling the individual interactions of each ion with the analyser magnetic field would contribute little towards the aims of this thesis.

Ion current measurement

The ion currents from each of the separated ion beams must be measured independently for the ratios of the abundances of each isotope to be determined. A number of detection systems have been designed to achieve this; two of these are the Faraday and Daly detection systems, which are in common use.

The Faraday collector consists of four main parts:
1) Defining slit
2) Secondary electron suppressor
3) Faraday cage
4) Electronic measurement equipment

Figure 2.2 Shows a Faraday collector. The slit allows the focussed ion beam of one isotopic or molecular mass to enter the detector, which passes the suppressor and enters the Faraday cage. The suppressor, typically set at –100 V, prevents loss of secondary electrons formed when positive ions impact the base of the cage. The ion current is converted into a voltage using a DC amplifier that incorporates a 10^{10}-10^{12} Ω input resistor. An ion current of 10^{-11}A

thus produces a 1V output signal, which is measured directly with a high precision digital voltmeter.

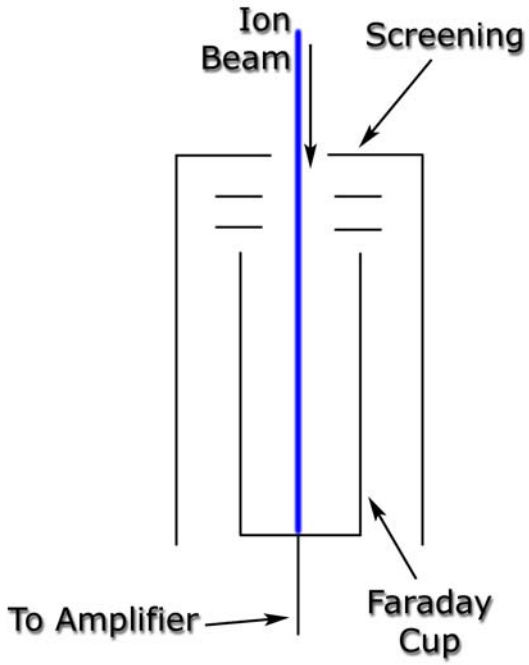

Figure 2.2: Faraday Collector Schematic

The Daly detector, devised by Daly in 1960, allows the beam to be amplified before it is measured (White and Wood, 1986). The ion beam is accelerated into a secondary emitting electrode (usually in the form of a highly polished Aluminium knob) that generates electrons. These secondary electrons are accelerated into a phosphor that is optically coupled with a photomultiplier external to the vacuum system. This system is intended for ion currents below 10^{-12} A, giving a signal to noise ratio far superior to the Faraday collector at these currents. Figure 2.3 shows the schematic of the Daly detector.

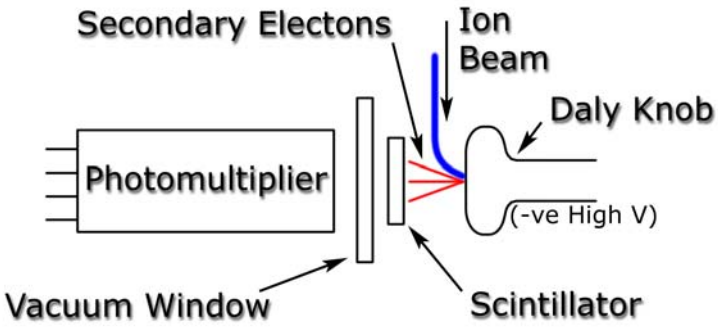

Figure 2.3: Daly Detector Schematic

The two systems have different signal to noise ratios and would need to be modelled differently. The project focussed on the Faraday collector, as this is the collector commonly used with larger ion currents where the uncertainty is more easily modelled, as described in the next section.

2.1.2 Uncertainty in Mass Spectrometric Measurements

Many factors contribute to the uncertainty in the determinations of isotope ratios.

Statistical noise

The ion beam in a mass spectrometer is composed of individual ions, each arriving at the detector at a random time. However, an average rate of arrival can be observed over time, and this is what detectors measure as an ion count or an ion current. This kind of phenomenon is governed by statistics involving the Poisson distribution (Meyer, 1975).

The probability of observing a given number of ions (N) in a chosen interval of time, when the expected mean number of ion is μ, will be:

$$P_\mu(N) = e^{-\mu}\frac{\mu^N}{N!} \tag{2.7}$$

and the variance and standard deviation of the number of counts we observe in the interval are:

$$\begin{aligned}\sigma_N^2 &= \mu \\ \sigma_N &= \sqrt{\mu}\end{aligned} \tag{2.8}$$

For cases where $\mu \geq 30$, the Normal distribution with the same mean and standard deviation, $G_{\mu,\sigma}(N)$, gives a good approximation to the Poisson distribution.

$$G_{\mu,\sigma}(N) = \frac{1}{\sigma\sqrt{2\pi}}e^{(N-\mu)^2/2\sigma^2} \tag{2.9}$$

For a small ion current, eg 10^{-17} A, the number of ions per second can be calculated. If each ion carries a charge of 1.602×10^{-19} C the number of ions per second will be $10^{-17}/1.602\times10^{-19} = 62$ ions per second. This still satisfies the condition for the Normal Distribution approximation, if the period of measurement is about a second. However, an ion

current a factor of ten lower will violate this condition and the Poisson function must be used to describe the likely observed counts.

This situation can cause a further problem for isotope ratio measurements. Many existing systems measure the counts for each isotope and then calculate the ratios of these counts. The mean of these ratios is later taken and their spread dictates the uncertainty in this mean value. This technique can lead to a bias in the measured isotope ratio. Due to Poisson statistics, the number of ions collected for the denominator isotope will influence the measured ratio as described below (Fietzke *et al.*, 1999).

Assume that two isotopes A and B are being measured, one with an expected count *a* and observed count *i* and the other with an expected count *b* and observed count *j*. These counts may be observed in different times, t_A and t_B. The true isotope ratio of A/B (the ratio of the true ion currents), assuming no fluctuations in *a* and *b,* will then be:

$$\left(\frac{I_A}{I_B}\right)_{true} = \frac{a}{t_A}\frac{t_B}{b} \tag{2.10}$$

The expected value of the measured isotope ratio is instead:

$$\begin{aligned}\left(\frac{I_A}{I_B}\right)_{measured} &= \left\langle \frac{i}{t_A}\frac{t_B}{j} \right\rangle \\ &= \frac{t_B}{t_A}\left\langle \frac{i}{j} \right\rangle\end{aligned} \tag{2.11}$$

From Poisson statistics:

$$\begin{aligned}\left\langle \frac{i}{j} \right\rangle &= \sum_{i=1}^{\infty}\sum_{j=1}^{\infty}\frac{i}{j}P_a(i)P_b(j) \\ &= \sum_{j=1}^{\infty}\frac{\sum_{i=1}^{\infty} iP_a(i)}{j}P_b(j) \\ &= \sum_{j=1}^{\infty}\frac{\langle i \rangle}{j}P_b(j) \\ &= \sum_{j=1}^{\infty}\frac{a}{j}P_b(j) \\ &= a\sum_{j=1}^{\infty}\frac{1}{j}P_b(j)\end{aligned}$$

From this, it follows that:

$$\left(\frac{I_A}{I_B}\right)_{measured} = \frac{t_B}{t_A} a \sum_{j=1}^{\infty} \frac{1}{j} P_b(j) \tag{2.12}$$

It must be noted that as an observed count of zero leads to a problem in the calculation, so this treatment functions best for the values of b where $P_b(0)$ is small (eg: above $b = 5$).

The measured ratio differs from the true ratio by a factor of:

$$b \sum_{j=1}^{\infty} \frac{1}{j} P_b(j) \tag{2.13}$$

This factor is then dependent on the value of b. At very low counts, any model that does not include a Poisson calculation will show ratios different from those that would be observed in a physical instrument. For low b the measured isotope ratio is higher than the true isotope ratio.

As the implications of this problem are only realised with low counts, the model was used only with larger counts (i.e. ion currents over 10^{-17} A). This became a limiting parameter of the model's inputs. If future study of low ion currents using the model is to be performed, the model may need modification to include a Poisson calculation. This will be especially significant if a model incorporating a Daly detector is developed.

Electronic noise

As electronic equipment is used in mass spectrometers, noise in the equipment contributes to ion current measurements. This noise might be present in the form of non-linearity in an amplifier or as a baseline noise present in all measurements. Other forms of equipment noise may also be present. These must be corrected for if a measurement is to be accurate. Some of these noise sources were included in the simulation, as described in section 5.1.

Time based variations

The ion current produced by the ion source is subject to temporal variations. This can be a short-term (fractions of a second) effect, such as small bursts of ions being released, or long term (hours for example) such as the gradual decrease in ion current as the sample is depleted in a thermal ionisation source. The impact of these variations depends on the methods used in the measurement. These variations were not investigated in this thesis.

Mass Peak Characteristics

When a mass spectrometer "scans" over the ion beam, either the accelerating HT voltage or the magnetic field is varied to change the physical positions at which the separated ions exit the analyser. When this is done in a steady fashion, a "mass spectrum" of individual "mass peaks" is produced. Ideal mass peaks would be perfectly flat, square and centred exactly on the mass number of the isotope being measured. This would arise from a beam of mono-energetic ions focussed as a single infinitely thin line being swept across the ion detector. Figure 2.4 shows this situation.

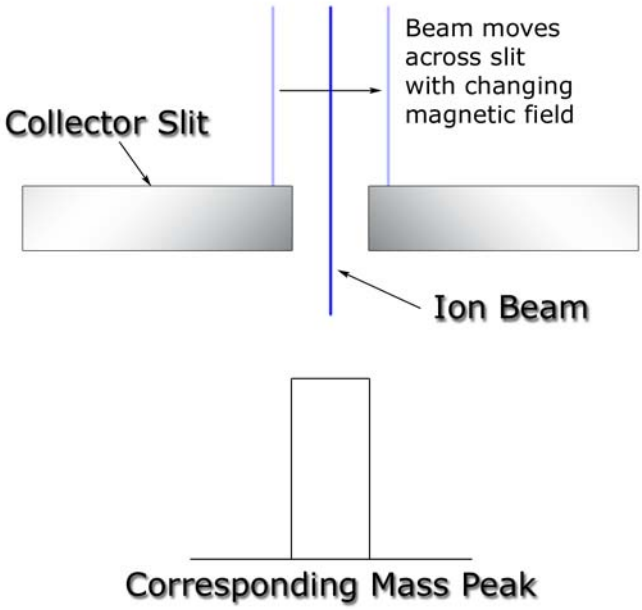

Figure 2.4: Theoretical perfect mass peak

Real or observed mass peaks arise from a beam of finite width entering the ion detector. If the beam were distributed evenly, the peaks would be trapezoidal. This is also not the case in the real world, with the distribution of ions typically approximated by a Gaussian distribution, leading to rounded peak shapes. Both are shown in figure 2.5.

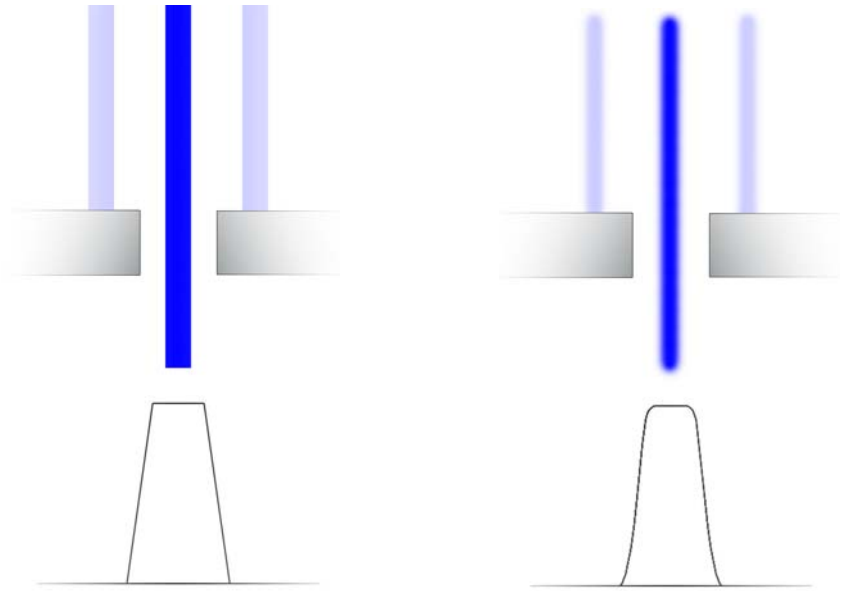

Figure 2.5: Mass peaks for beams of finite width with uniform and Gaussian cross sectional distributions

Figure 2.6 shows a typical ion beam profile as obtained experimentally (Loss, 1986 76 - 77)

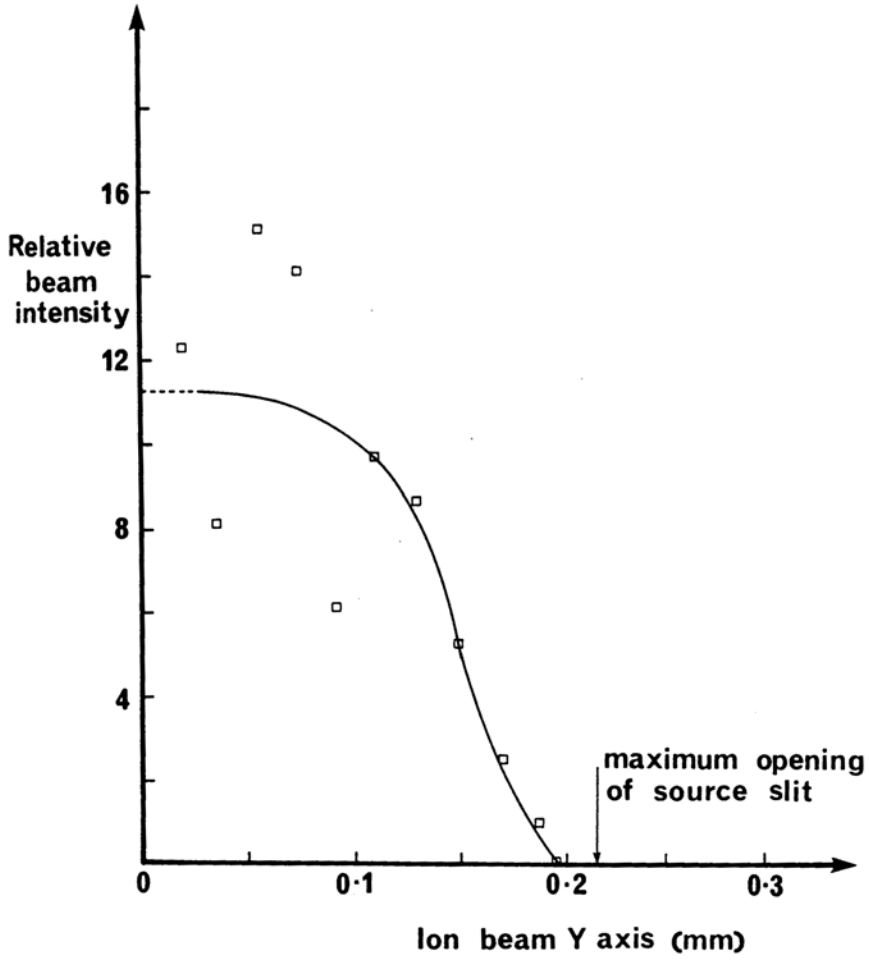

Figure 2.6: Typical mass spectrometer ion beam profile

Real ion beams will also always contain some ions with kinetic energies less than the maximum, leading to additional small tails in the mass peak. In this case, the lower velocities of these ions pass through slightly smaller radii of curvature in the analyser, which adds a "tail" to the mass peak on the low-mass side. These tails can range over as much as three mass units. This becomes a significant problem if a lower mass isotope in very low abundance must be measured (eg Thorium where the mass 232 isotope is of the order of a billion times more abundant in a sample than the mass 230 isotope of interest in Uranium-Thorium dating).

Figure 2.7 shows a measured mass spectrum of Lead (sample NIST SRM 981) obtained from a VG-354 mass spectrometer. The rounded edges of the peaks are clearly visible.

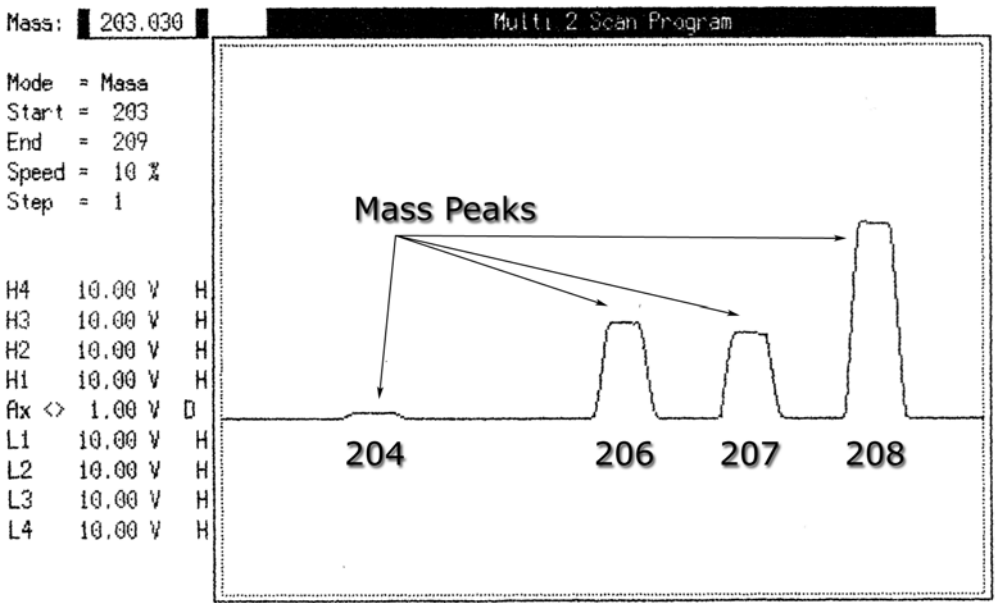

Figure 2.7: Mass Spectrum of NBS-981 Lead printed from VG-354 Mass Spectrometer

The expected mass of a mass peak with respect to the magnetic field applied in the analyser can drift significantly during an analysis unless very stable magnetic fields are used. In addition, hysteresis effects (where the magnetic field produced by a certain current in the magnet is dependent on the previous value of the field) influence linearity in the setting of magnetic field values. Figure 2.8 shows a hysteresis curve where the field value is different for the same current setting depending on whether the current is increasing or decreasing.

Shifts of 0.1 to 0.2 atomic mass units (amu) can be observed so the simulation included peaks off-centre by these amounts.

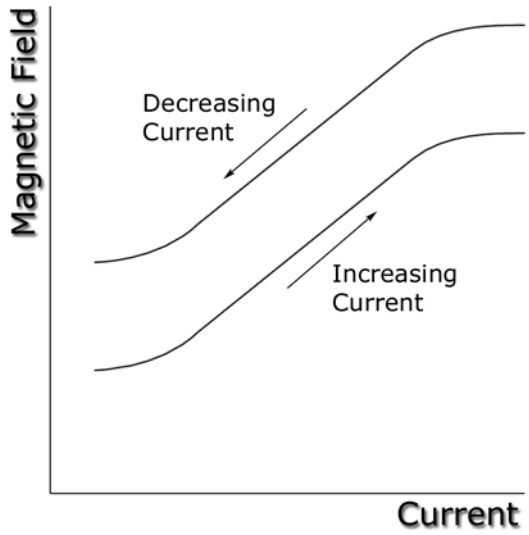

Figure 2.8: Hysteresis curve for a magnetic analyser

Mass Spectrum Interferences

In isotope ratio measurements, an isotope or molecule having a similar mass to one of the isotopes of the element being measured can cause an interference (usually an enhancement) of the measured ion current for the isotope of interest. Conversely, underestimates of isotopic abundances can occur when mass interferences are in the region of baseline measurements. To eliminate these types of interferences, the mass spectrometer must have a sufficient resolution to differentiate between the two relevant masses or samples must be prepared such that these "isobaric interferences" are not present in the sample. Resolutions of 400 are typical for TIMS, not enough (for example) to completely resolve common organic isobars when measuring Lead isotope ratios but often enough to show these as step-like features in the Lead peak.

Fractionation

Isotopic fractionation of the sample during mass-spectrometric analysis has traditionally been attributed to the slightly differing volatilities of isotopes of an element. The effect is an initial enhancement of the isotopic ratio of the lighter to heavier isotopes, which, if volatility is the cause, should be approximately linear with mass. As the isotopic analysis proceeds, the

remaining reservoir becomes enriched in the heavier mass isotopes and eventually the measured isotope ratio can be some tenths of a percent in the opposite direction from that measured initially.

It can be argued (Delmore and Appelhans, 1992) that this is not always the case as the observed fractionation in rare earths is much less than that normally measured for uranium. They argue that the rare earths have simpler chemistry and more stable oxides than uranium and that fractionation arises from dissimilar chemical reaction rates for different isotopes and different volatilities for the resultant oxides. The fact that electrodeposition usually results in samples with much lower fractionation effects (Delmore and Appelhans, 1992) further supports this theory.

A number of mathematical treatments of fractionation have been proposed (Platzner, 1997). No physical basis has lead to the various models – some data merely fit one model better than another.

Different types of ionisation processes and sources introduce different fractionation effects. Gas-source mass-spectrometers will demonstrate a constant fractionation (with respect to time) such that a given ratio is biased by the same amount during the whole period of the measurement. This results from the technique of injecting a small amount of the (unfractionated) sample to be ionised into the ionisation source, leaving the remaining sample's isotope ratios unchanged. However, a thermal ionisation source will normally deplete the lighter isotopes in the sample during the measurement, as they are evaporated preferentially. Thus a given ratio that is initially enhanced will decrease during the run, equal at some time the "true" value representative of the original sample and then fall below the true value and continue to decrease. The opposite will happen for an initially decreased ratio.

In this thesis, fractionation was not investigated as in TIMS the effects are primarily time-based. In comparisons with real results, the absence of fractionation in the model results had to be kept in mind.

2.1.3 Mass Spectrometric Data Analysis Principles

The advent of computers in the control of mass spectrometers has naturally lead to their use in the analysis of the data coming from the instrument. Analysis can be performed as data is measured ("real time") and after the entire process of measurement is finished ("post processing"). In practice, real time analysis is blended with the data collection such as peak intensity measurements and control process, such as peak centring. Although some attempts have been made at parallel control and processing, most mass spectrometric control and analysis occurs at the per second or per tenths of second rates hence these can easily be performed using relatively simple linear processing and control schemes.

In the following section it is assumed that a relatively stable long-lived (i.e. hours) ion beam has been established in a calibrated mass spectrometer. Described are the typical preliminary checks and tests that are performed prior to isotope ratio measurements.

Peak centring

Accurate ion current measurements can only be performed when the ion beam is entirely within a collector, which corresponds to a mass or magnetic field position on the top of a mass peak. To minimize the effect of possible magnetic field drift during measurements the ideal starting mass position is the centre of the mass peak.

"Peak centre" determinations need to be performed regularly during an analysis to ensure that the true ion current is being measured for each isotope. The peak centring process effectively involves determining the approximate shape or mass position of a mass peak and locating its centre, usually by the computer quickly scanning a peak and then repeatedly measuring the ion beam on alternating sides of the peak and adjusting the magnetic field (mass positions) until approximately equal half-height peak values are being measured. The centre is then determined as the magnetic field value halfway between these equal or half height points. This can be a time consuming process and the hysteresis effects resulting from the action of measuring back and forth across the peak can produce incorrect results.

Ion collection: Multiple collector, Peak jumping and Multiple Peak jumping

Where sufficient ion collectors are available, the collectors are usually arranged in a spatial manner such that all of the ion beams can be collected simultaneously in a process known as multiple-collection. The isotopic ratios are then ratios of the respective ion currents or "sums of ion currents" collected over a given period. A series of multiple measurements over some minutes is more accurate, and usually produces a lower single analysis measurement uncertainty because of the simultaneous and therefore greater number of ions collected. The major advantages of this method are the reduced time taken to collect data and the minimization of the effect of ion beam instability on isotope ratio determinations. Higher precision is, however, no guarantee of accuracy in isotope ratios, particularly when fractionation effects become dominant. Another significant limitation to both accuracy and precision is the knowledge of the relative physical and electronic gains of the collector and associated amplification system; these must be well measured and stable over a sufficient period both during and between analyses.

If only a single Faraday collector is available or used, only one ion beam can be measured at any time. To measure an isotope ratio, the magnetic field must be changed so that each ion bean in turn can be deflected into the collector in a process known as "peak jumping". Because the total number of ions beam can change between peak measurements, peak jumping must be done in a predetermined sequence that is repeated many times. An advantage is that the variables associated with the collector and amplification system do not usually change significantly over these time scales and do not need to constantly be compared with other collectors. The peak jumping technique can also be used with single high-gain collectors such as the Daly system, which having a superior signal to noise ration for small ion beams ($< 10^{-12}$ A) enables very small samples to be measured.

The major disadvantage is that failure to account for total ion beam changes during an analysis biases the calculated isotope ratio, as one of the ion currents may be higher or lower than it was at the time when the other isotope was measured. When the ion beams change on a relatively long-term basis, such as exponential type decay or, this problem can be accounted for by some kind of short term averaging or numerical fitting technique. If stable beams can be produced for a sufficient time the peak jumping method can produce accurate and precise results, although a significantly longer period (as compared to multiple collector analysis) is

required to collect the data and the question of the degree of fractionation variability between analyses still applies.

Multiple Peak jumping is a combination of the above two methods where peak jumping is performed using two or more collectors. The major advantage is that where possible collection schemes can be arranged to cancel out possible collector and amplifier biases, which therefore produces the most accurate and precise results. Again, this procedure is only useful for measuring relatively large ion currents, although pulse-counting multiple-collector systems are now becoming available. Subsequent discussion in this work will be restricted to peak jumping data collection schemes.

Curve fitting

Single collector Peak-jumping schemes do not allow all the ion currents to be measured precisely at the same time for each of the isotopes. Hence, reliable determinations of isotope ratios require estimating the ion currents for each of the isotopes at some common point in time. Traditional methods have used simple linear interpolation over a limited time range. Later methods have involved a series of higher order numerical fits to the ion currents, including using a least squares polynomial fit to each isotope's ion current vs. time (Werz and De Bièvre, 1981). Polynomial fitting, in general, can extract the maximum amount of information from ion beam data.

Ratio calculation

The degree of natural variability of a thermally generated ion beam over time generally requires that a method of determining the ion currents at a common time is necessary. The simple ratio of the measured ion currents does not always directly yield the true abundance ratios, as instrumental bias, mass spectral interferences, isotope fractionation and other uncertainty sources complicate the measurement.

Traditional methods have involved calculating the projected ion currents by linear interpolation and using these to calculate intermediate sets of isotope ratios. The process is repeated many times over the course of the measurement to produce sets of ratios which are

analysed statistically producing mean isotope ratios with uncertainties based on the standard error of the mean or a similar statistical measure of data spread.

A major drawback of this method is that of fractionation (as discussed in Section 2.1.2 – *Fractionation*). It is most unlikely that even the mean of the measured ratios is equal to the true ratio of abundances in the sample since one never really knows how far along the fractionation process the sample analysis really begins or ends. In most cases the efficiency of ion beam production and the depletion of lighter isotopes is generally unknown so the bias introduced into the measured ratios is also unknown.

If the ion currents are produced only and measured over the entire period from the first useful ion emissions until the sample is completely exhausted, a technique can be used to assess the effects of fractionation. The ion-currents as a function of time can be integrated over the entire analysis, effectively determining the areas under each of the ion curves. The ratios of the areas for different isotopes may then give the isotope ratios, with minimal effects from fractionation. In practice though, some of the sample will evaporate before the ions are generated and some will remain (perhaps in a non-ionisable form) beyond the point at which ion currents can be measured, although these effects may often be minimal.

The uncertainty for a set of isotope ratio measurements is generally based on the standard error of the mean of the ratios measured. Some form of rejection criteria can be used to reduce the uncertainty resulting from probable outliers arising from factors such as intermittent ion beam instability. However, due to fractionation effects, the uncertainty limits derived from the standard error of the mean of the measured ratios may not even actually include the true value.

In cases that only require the relative differences between isotope ratios, internal isotopic fractionation correction schemes can be employed. This is performed by measuring the degree of isotopic fractionation using one pair of isotopes and comparing this to a reference set of isotopes of that element and then correcting the other ratios by the appropriate amounts. Where absolute ratios are required, the absolute ratios of the reference isotopes must be known. A complete assessment of isotopic fractionation is required for absolute isotopic measurement of all isotopes of an element; this is usually performed using gravimetrically prepared isotopic mixtures.

2.1.4 Physical/Operating Principles of VG-354

Specifications

The VG-354 used in this work is a commercially designed and constructed Thermal Ionisation Mass Spectrometer that, despite its seventeen years, utilizes essentially the same hardware as current models. Figure 2.9 shows the VG-354, demonstrating the physical relationship to the schematic in figure 2.1.

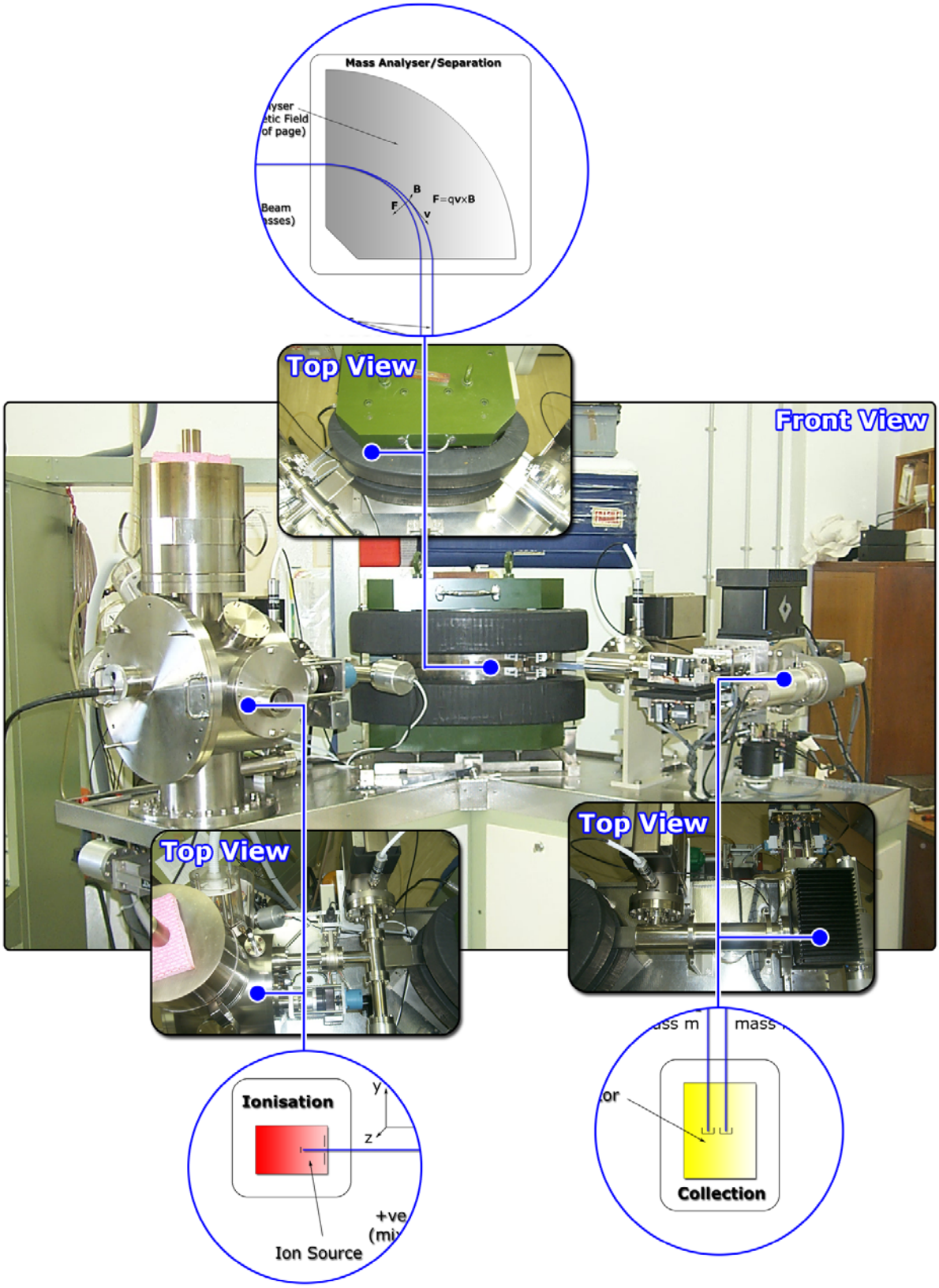

Figure 2.9: Photograph of the VG-354 showing Ion Source, Analyser and Ion Detector

The ion source on the VG-354 consists of a carousel holding up to sixteen sample filaments, and an electrostatic focussing collimator comprising of extra extraction and deflection plates. The ion source schematic is shown in figure 2.10.

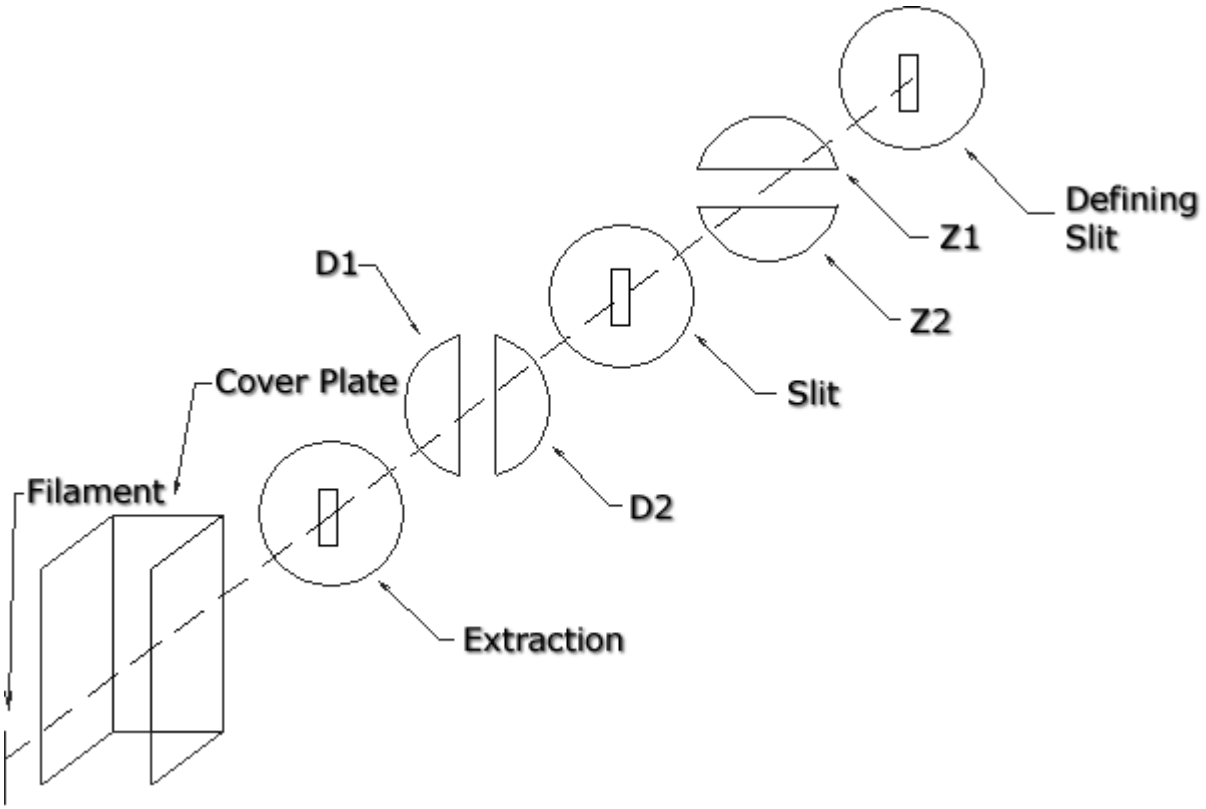

Figure 2.10: VG-354 Ion Source Schematic

The VG-354 magnetic sector analyser deflects ions through 90^{o} along a path of nominal radius 270 mm. The analyser has a geometry factor of two (the ions do not enter the magnetic field at right angles to the polefaces) giving an effective radius of 540 mm. This geometry provides the benefits of Z focussing (as detailed in section 2.1.1 – *Mass separation*). The effective distance from the source slit to the edge of the magnetic field is 540mm. This is also the distance from the other edge of the field to the detector slit. Figure 2.11 shows this configuration.

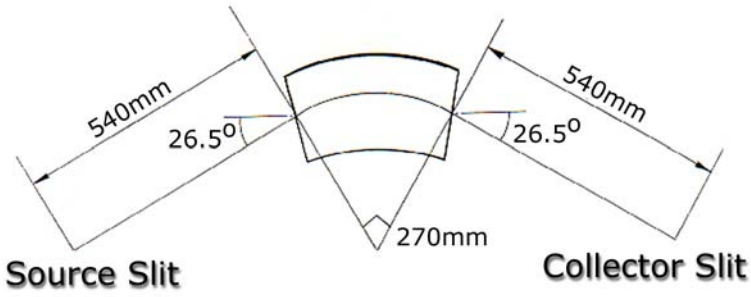

Figure 2.11: Schematic of the VG-354 Magnet

Two kinds of ion detection systems (as discussed in section 2.1.1 – *Ion current measurement*) can be used on the VG-354:

i) Faraday collection: The multiple collector system is a linear array of nine individual Faraday collectors, each with a defining slit. This detector allows the measurement of ion currents from different masses simultaneously, so that a decay or fluctuation in beam current will have little effect on the measured ratios. Data can be collected at a higher rate than for a single collector so more data can be collected from small samples and changes in fractionation can be minimised. The central or "axial" Faraday collector can be used for peak jumping modes if required.

ii) Ion counting system: A Daly detector can be used in place of the central (axial) Faraday collector. This is achieved by moving the axial collector downwards from the central ion axis, allowing the ions beams through to the Daly. This type of detector is restricted to ion beams smaller than 10^{-12}A to prevent damage to the detector. Although it is possible to use it in conjunction with the Faraday collectors it is normally only used in peak jumping mode.

Computer interface

Magnet control and all data acquisition are done through a computer interfaced with the VG-354 via GPIB, a parallel I/O interface detailed in the IEEE 488 Specification (see appendix A). The computer is linked to the "Multi-I/O", a device that interfaces the GPIB with most of the other units in the mass spectrometer, including the magnet, filament controls, high-tension voltage unit, focus controls, and analyser pressure controls. Each collector is connected to an

individual DVM interfaced using GPIB directly to the computer. The new software was required to interface with the existing hardware, as GPIB system has many advantages and replacing the hardware would be prohibitively expensive while providing little benefit.

Operating modes

The computer enables isotope ratio measurements using the VG-354 to be performed in either manual or automatic mode. Manual mode requires the user to select the relevant sample, set the ion accelerating voltage and filament currents/temperatures, and find and focus the ion beams. Once these are performed, the computer will control the magnet, centre mass peaks, and collect and analyse the data. In fully automatic mode, the software performs all of the above functions using predetermined input data for each type of analysis and sample. Measurement success of the automatic mode is dependent on many factors but for routine analyses, successful isotope ratios are possible on 90% or more of samples. The fully automated mode is not normally considered reliable enough for use with critical or one-off samples. The “manual” mode of control was the mode chosen for this thesis.

3. GUI Software Development

The theory covering general software development is relatively abstract and complex and while many computer science formalisms are available to describe the processes undertaken, this section is restricted to describing the essentials of programming for scientific applications. The specifics of an instrument control and measurement-oriented development environment, such as the LabVIEW application used in this work, will also be covered.

3.1 Software Life Cycle

The development of any software should follow the well established "software life-cycle" (Walker, 1989), which can be described by five phases. Appropriate documentation is necessary in all of these phases.

Specifications

In this phase, the tasks or problems to be solved are described in detail. Possible specifications include lists and details of all required inputs and outputs, a description of each type of processing task to be completed and other important characteristics, such as response times. The specifications for this work relate to the aims of the thesis, as described in section 1.6.

Design

This phase involves designing the required procedures and algorithms to achieve each of the specifications arrived at in the first phase. The required procedures and algorithms are independent of any programming language. At this stage, the project is commonly divided into sections called modules. The design in this work is described in chapters 4 and 5.

Coding

Coding follows the specification and design exactly. Sufficient documentation must be provided to enable a reader to trace the flow of the code and understand the algorithms. The time spent in coding should be less than the time spent on the phases preceding it.

Verification and testing

Each part of the application must be tested to ensure that the design and coding meet the specifications intended. Test cases with well-known or expected outcomes are designed and evaluated immediately following or even while a module (algorithm and its corresponding code) is being developed.

Finally when completed the entire project must be tested as completely as possible. Following rigorous testing, the software can be released. It then enters the maintenance phase.

Maintenance

Most large-scale software developments require modification following the testing stage as it generally impossible to test all the permutations and combinations possible within a program. Many projects also involved changes to the specifications as the software is used, and as users' demands expand or change.

Documentation

Documentation to a predetermined audience or user is required for all phases.

One key audience is the user, who must know how to interact with the program. This documentation may be in the form of a users' manual, a help file and/or as pop-up tips or windows from within the program. Every one of the features available in the software must be documented in this manner.

Code structure and function must be explained in appropriate documentation and where possible within the actual code. Documentation should be detailed enough for the original author(s) to understand the code at some future time, and other developers to perform the maintenance phase. Documentation for maintainers can be internal, such as comments inside the code, or external, such as a written manual or guide. Additional external documentation and examples are usually required when algorithms are too complex to be described adequately within the code.

Documentation is enhanced by the use of languages which allow for appropriate levels of "self-documentation", eg: permit the use of variable, object, module and file names that are self-explanatory and structures that are logical to follow.

3.2 LabVIEW

LabVIEW was chosen as the tool to develop the mass spectrometer software. LabVIEW is a fully structured programming language that allows ready documentation, modular programming and logical program flow (Johnson, 1994).

A program written in LabVIEW is called a Virtual Instrument (VI) named because of its function (and even possible visual appearance), representing any physical electronic instrument that can be emulated by program. Applications written in this language are based on two parts: the "*panel*" and the "*diagram*" Figures 3.1 and 3.2 show a simple LabVIEW application to add two numbers and show the result. The *panel* contains all of the objects with which an end-user can interact (called *controls*). The *diagram* contains *terminals*, which are representations of each *control* on the *panel*, objects that manipulate data (called *functions)* and *wires* that join *functions* to *terminals*.

LabVIEW is data flow oriented - the actions of the *diagram* are based solely on whether data is available for the required action. The *terminals* (e.g. variables A, B and output Y in figure 3.2) and *functions* (e.g. the addition symbol in figure 3.2) on the *diagram* are linked by "wiring together" and data can be thought of as flowing through the *wires*. This is significantly different to any previous method of programming such as event driven (eg: Visual BASIC) or sequential (eg: FORTRAN). The data driven sequence of events can lead to issues in the timing of operations that must be carefully planned. However, methods exist to ensure correct sequencing.

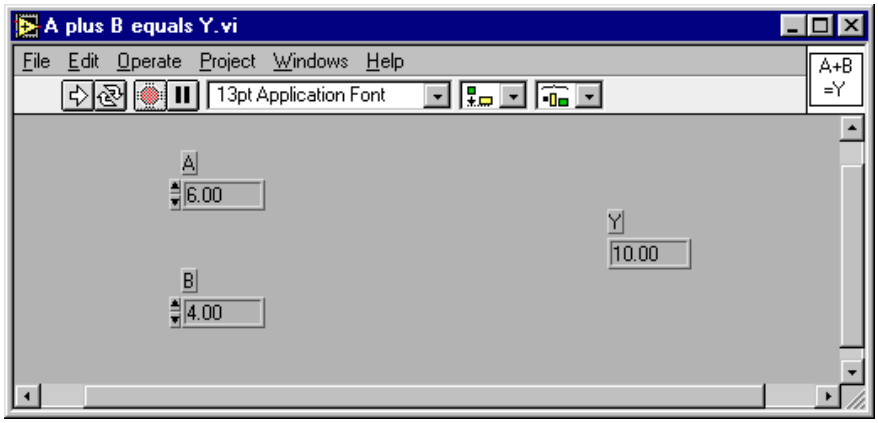

Figure 3.1: Front panel of a program to add the numbers, A and B, in LabVIEW

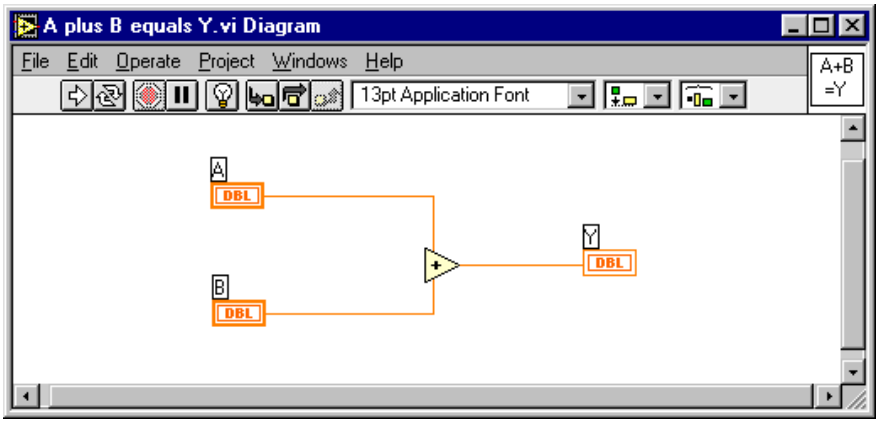

Figure 3.2: Diagram of program in figure 3.1

A "reader" can easily follow this flow of data. Debugging tools are supplied, including highlighted execution where the reader can see the data flow visually through the VI, breakpoints and watches. A wide range of control operations such as loops, case statements and other structures are also available.

VIs (often called modules) can be easily used within or called from another VI, by adding the *SubVI* to the *diagram*. This form of modular programming minimizes the complexity commonly associated with many traditional programming environments, particularly those for scientific instrumentation. Another advantage of LabVIEW over other languages is that any module can be independently tested without the need for any other module. In other languages this process would require the use of a "software driver," a small application that passes inputs to the module and displays its outputs, whereas LabVIEW VIs provide these inputs and outputs internally.

Detailed documentation is possible on many levels in a LabVIEW application. The design layout and structure of the VI can be self-documenting. For example, detailed labels can document the *front panel* or *diagram* on any VI. Pop up help can also be made available at the discretion of users. Finally, operating system style help files can be linked to correctly constructed VIs (but these will need to be compiled outside of LabVIEW).

Figure 3.3 shows a LabVIEW application exhibiting these features. The application plots a sine wave of given amplitude and initial phase angle over the given number of cycles using a specified number of points.

The figure shows the pop up window help that is seen when the mouse is moved over the chart. This explanation is written as part of the documentation of the VI. Inputs are the four controls on the left (Amplitude, Number of cycles, number of samples in waveform and Phase angle) - different styles of controls are shown as an example of the many available. The output indicator is the resulting chart showing the sine wave.

The diagram used to produce Figure 3.3 is shown in figure 3.4; it shows that another VI, the Sine Pattern VI, which is used as a module, generates the sine function. The diagram is documented with an explanation of this module, in the form of a label. Figures 3.5 and 3.6 show the front panel and diagram respectively of the Sine Pattern VI. The sine generator itself employs another LabVIEW feature, a CIN (code interface node). The CIN is a function compiled in C, usually because that language offers benefits for example in mathematical computation or a well-established piece of C code already existed in the literature and conversion to LabVIEW is not required.

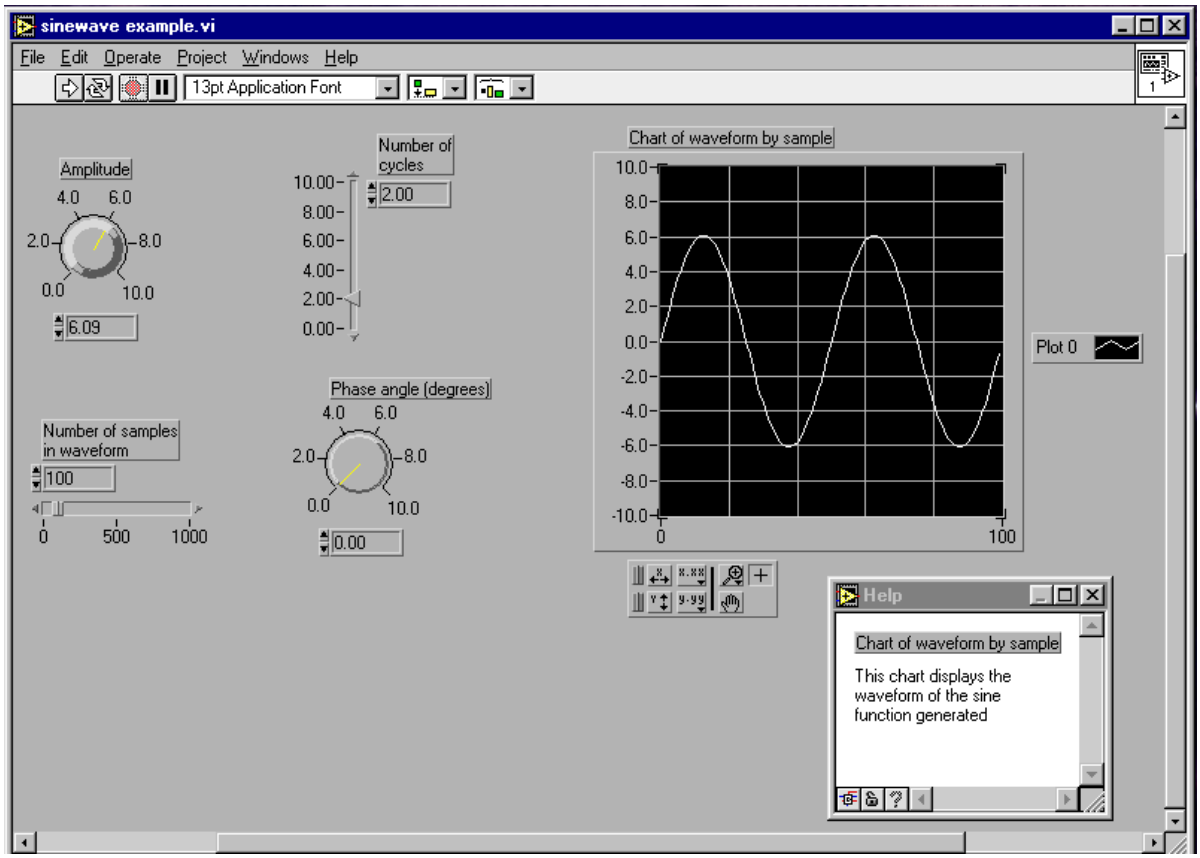

Figure 3.3: Front panel of sine wave plotter showing pop up help

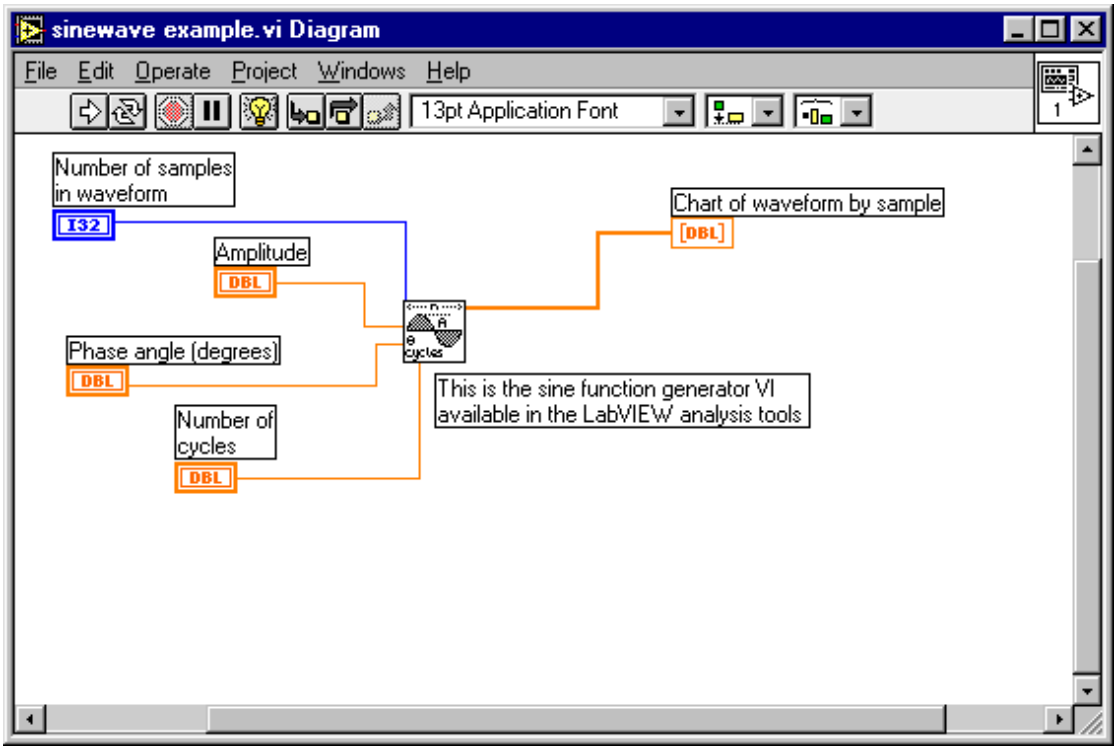

Figure 3.4: Diagram of sine function generator

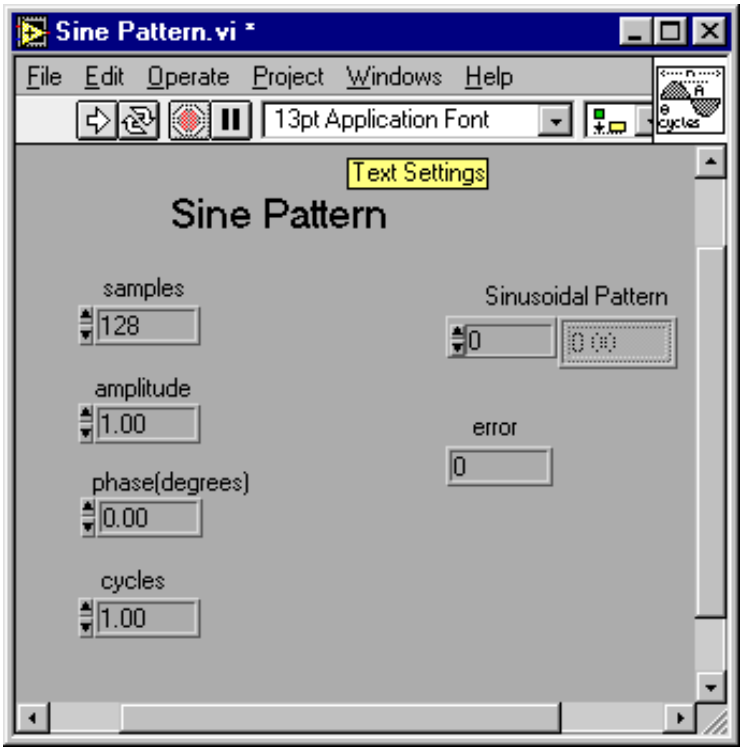

Figure 3.5: Sine Pattern front panel

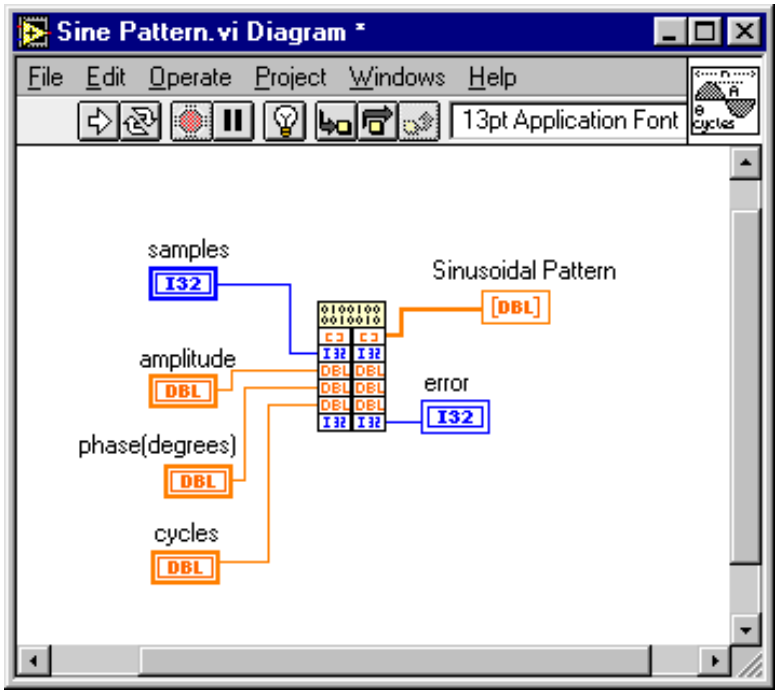

Figure 3.6: Sine Pattern diagram

This and the previous chapter have detailed the background required for performing the work in the thesis. The next chapter begins to detail the work itself.

4. Mass Spectrometer Model Development

The production of a computer based numerical model of a complex instrument such as a mass spectrometer is a major task that is best handled by breaking down the model into manageable sub-units or modules. Each of the modules requires the development of specific algorithms, which may also be broken into sub-modules etc. Dealing with the restrictions imposed by mass-spectrometer hardware, maintaining as physically accurate a model as possible, and efficient management of the code associated with the various modules and sub-modules, represent a major challenge that benefits substantially from careful design before undertaking substantial coding.

The methodology of developing the code for an application using a model instead of the physical instrument was first developed on a "test project" using a single digital voltmeter (DVM) identical to one of the nine DVMs used on the mass spectrometer.

The DVM used was a Solartron 7060, which is a GPIB based instrument, using general GPIB functions but not conforming exactly to IEEE 488.2 (see Appendix A) specifications. The design specifications used for this test project were:

- to take inputs relating to changing the range and triggering the DVM.
- to provide outputs of the voltage measured by the DVM.

A LabVIEW generated random number was used to simulate a changing voltage and incorporated into a basic Virtual Instrument (or "VI", as discussed in section 3.2) as a "model" of the input voltage. The application also was designed to manage the DVM hardware such as, initialising the DVM, converting range requests to the appropriate strings, triggering measurements and reading / writing using the appropriate GPIB calls. The resulting *front panel* is shown in figure 4.1.

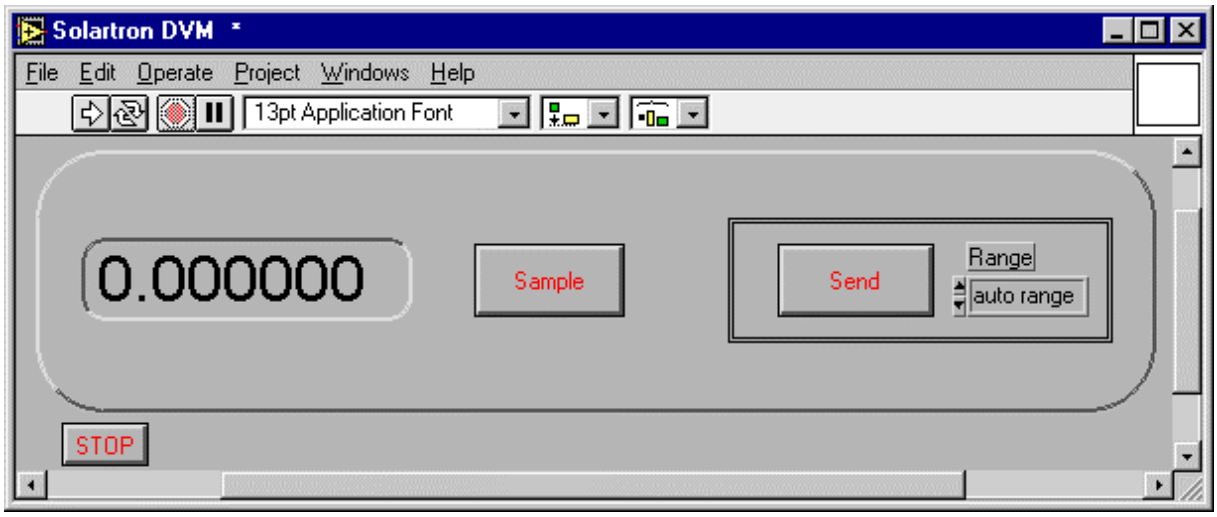

Figure 4.1: Front panel of Solartron DVM application

The corresponding *diagram* in figure 4.2 shows that a number of modules (Including the "Config" and "Read" modules) are used even in this simple application. Figure 4.3 demonstrates the resulting *hierarchy* - the chart that shows which modules are part of other modules and the depth at which the modules lie. Each of the mid-level modules in the hierarchy calls one of the "demo" VIs, which are exact replicas of the GPIB functions available within LabVIEW but have no hardware functionality.

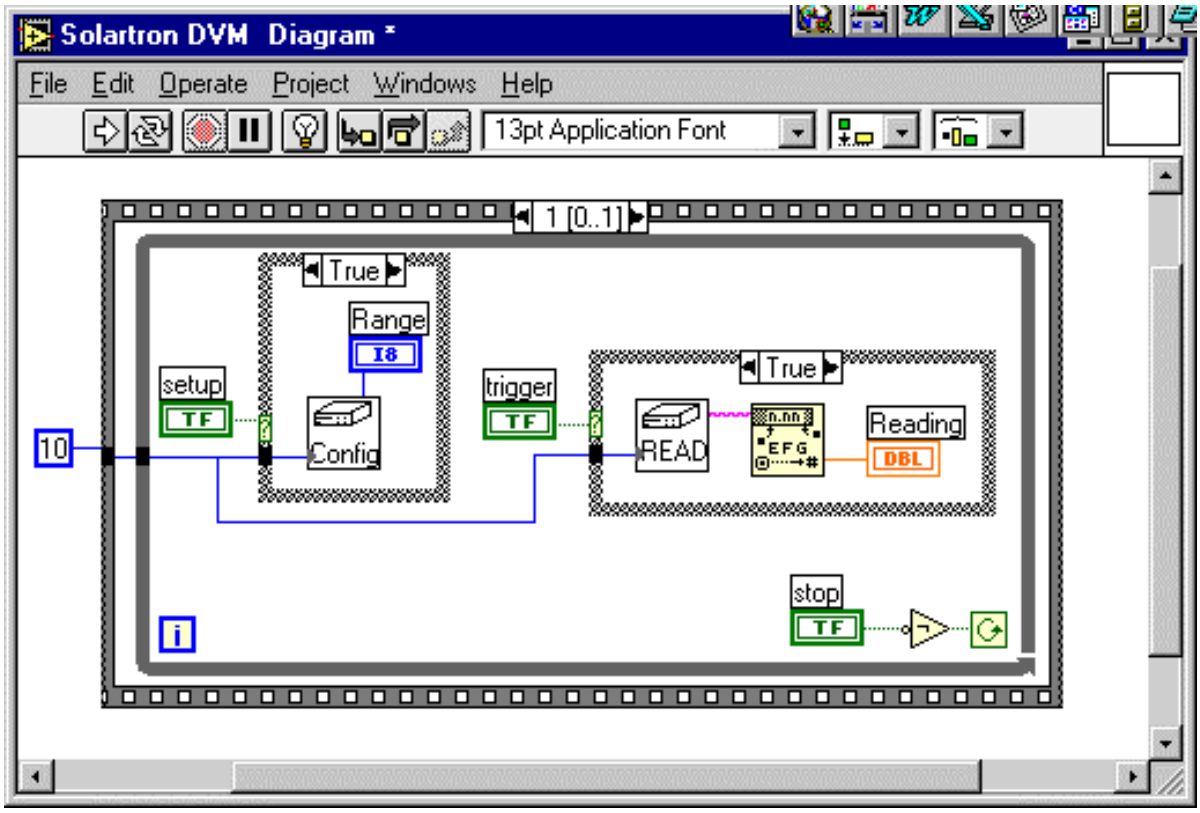

Figure 4.2: "Diagram" of Solartron DVM application

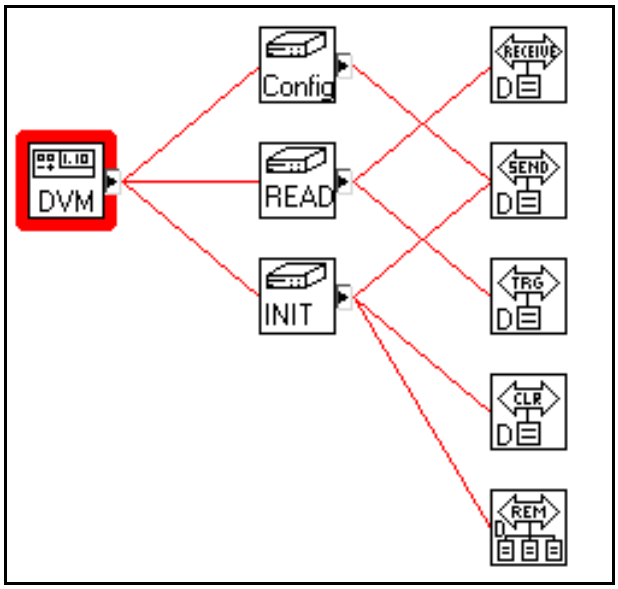

Figure 4.3: Hierarchy of the Solartron DVM Application

The Config module's diagram is shown in figure 4.4. This module calls, for instance, the "Demo GPIB Send" sub-VI, as seen previously in the hierarchy.

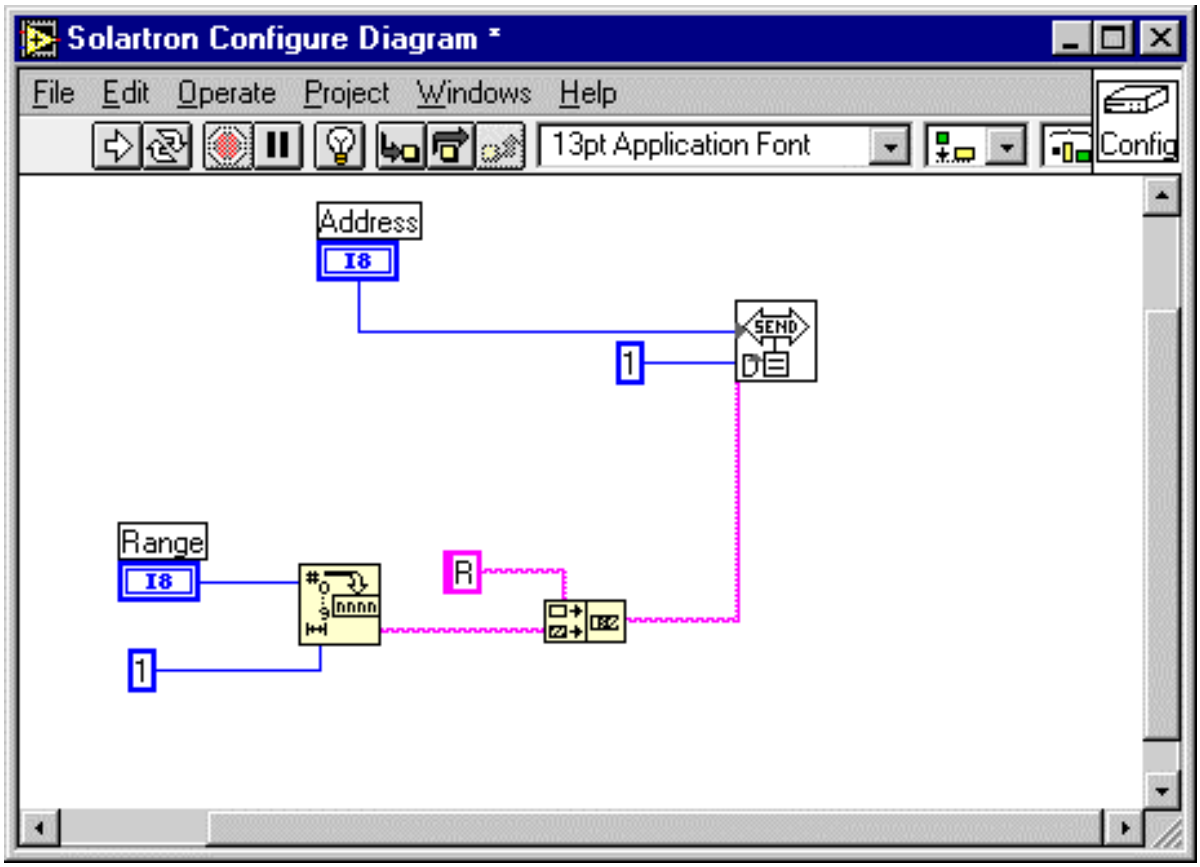

Figure 4.4: Diagram of DVM configuration VI

The pop-up help for the Demo GPIB Send VI, figure 4.5, shows the four inputs (on the left) and resulting three outputs (on the right) available for use.

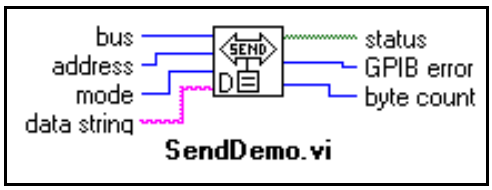

Figure 4.5: Input and outputs of GPIB Demo Send VI

Once the demo program was functioning correctly, the demo GPIB calls were replaced with the actual hardware interface VIs to form a working GPIB instrument driver, developed without using the instrument itself. This gave confidence that the basic methodology was appropriate so work on the mass spectrometer model could begin.

4.1 Single Mass Peak Model Development

The first part of the mass spectrometer simulation development involved a model of a single mass peak.

Single Peak Model Specifications

The model was required to:

- Simulate an ion beam voltage output for a given a mass position in the mass spectrum and display mass scans (ion beam voltage as a function of mass position).
- Simulate as many noise sources in the mass spectrum as possible
- Accept parameters that allowed the shape of the mass peaks to be modified according to hardware/software settings normally present on a mass spectrometer. (eg mass resolution, peak flatness and interval between points.)

Single Peak Model Design

A “Single Peak Model” was developed assuming a Gaussian ion beam cross-sectional distribution and a “noise” source consisting of a uniformly distributed random number

proportional to the square root of the voltage. The noise source wasn't intended to accurately represent the noise in the mass spectrometer at this point.

The first algorithm developed was designed to produce measured voltage data for only one mass peak. The specific modules comprising this algorithm were:

- "Single Point"- calculated a numerical value for the measured voltage at a point on the mass peak
- "Noisy Point" called the Single Point module and added noise
- "Single Peak" scanned the mass by iterating the Noisy point module across the mass peak.

Single Peak Model Coding

The algorithm was tested using a test program written in Visual BASIC (the VB Single Peak Model), as this was a more familiar programming environment at the time. Figure 4.6 shows the inputs (some unused) utilized by the program.

The algorithm accounted for mass resolution of the mass spectrometer and, as a preliminary test, the noise associated with ion counting (as described in section 2.1.2 – *Statistical noise*) using a number based on the Normal Distribution approximation to the Poisson Distribution (a noise proportional to the square root of the voltage).

Figure 4.7 shows a typical mass peak produced by the VB Single Peak Model. The small amount of noise (less than 1 percent of the peak height) can be seen on the top of the peak.

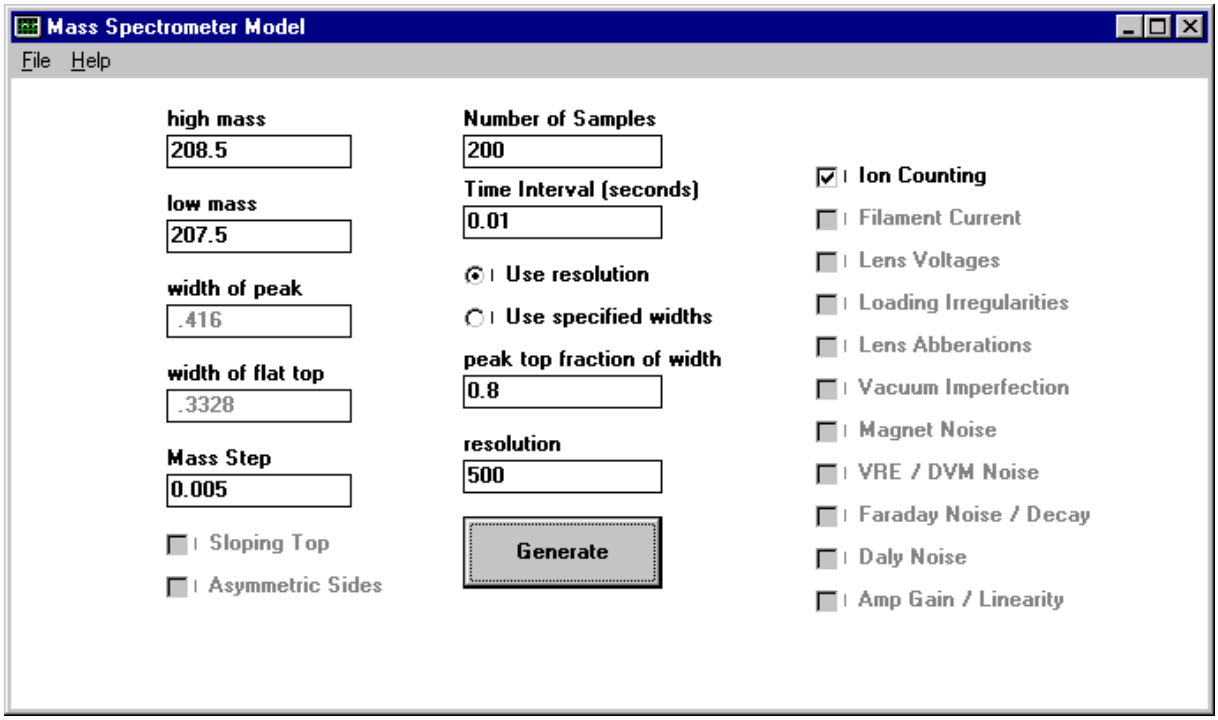

Figure 4.6: User interface for the VB Single Peak Model

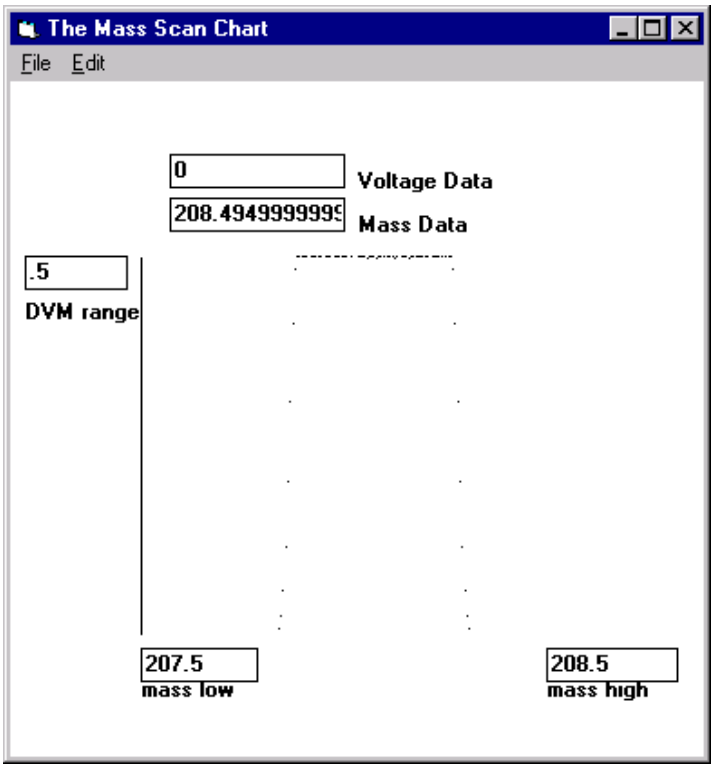

Figure 4.7: Mass peak produced by numerical model code

The VB Single Peak Model was then converted to a set of LabVIEW VIs and the ion counting noise was modified to incorporate the magnitude of noise expected from the number of ions "counted" in the integration time of the DVM. The Gaussian noise functions in LabVIEW were tested to ensure they did indeed produce Gaussian distributions (approximating Poisson distributions at large sample sizes). A sample of 1000 random numbers was generated from a Gaussian distribution of 0 mean and standard deviation 6.00 and the resulting numbers plotted in a histogram as shown in figure 4.8. This figure shows the calculated standard deviation (6.05) and the proportion of the generated numbers falling within the ranges of 1, 2 and 3 standard deviations from the mean (as percentages). Table 4.1 compares the generated numbers to a true standard distribution. The VI used to do the test is shown in figure 4.9, demonstrating first the generation of the numbers (at the left) followed by the statistical test for the numbers within the ranges.

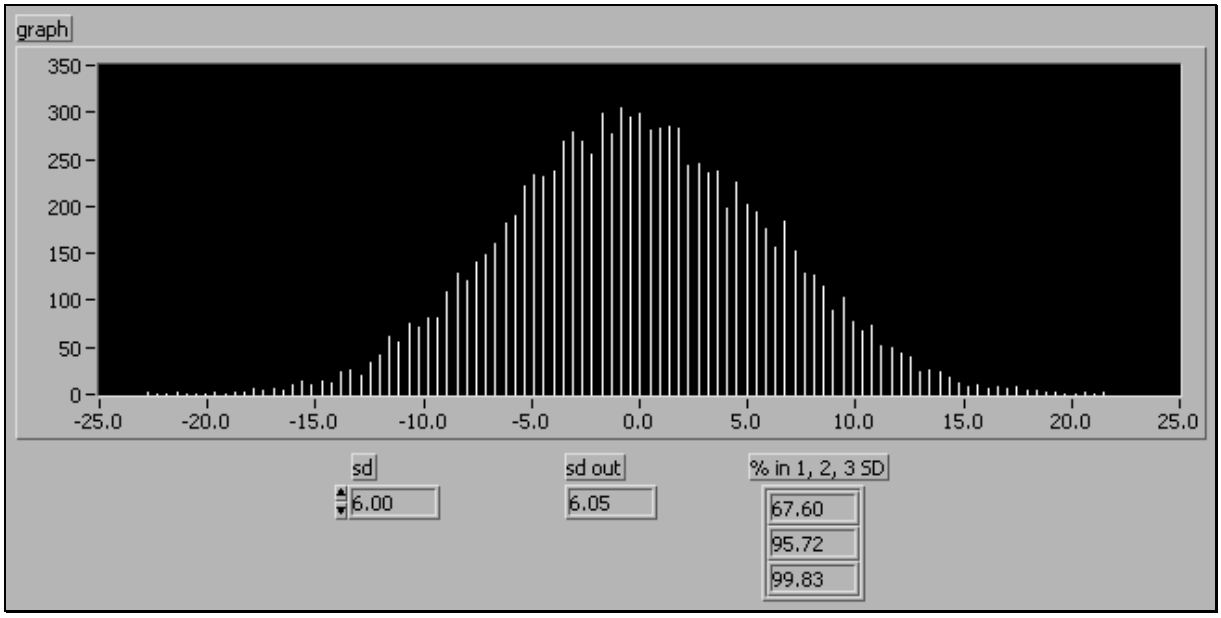

Figure 4.8: Sample Gaussian distribution generated in LabVIEW

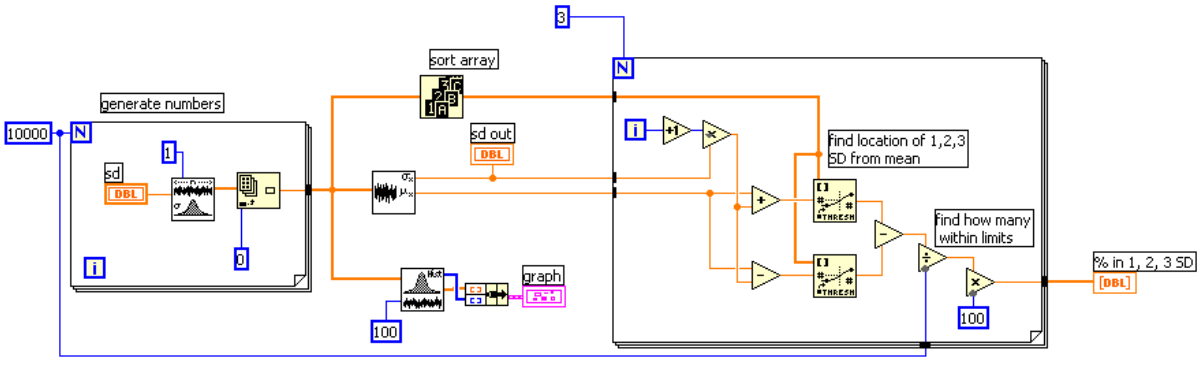

Figure 4.9: Gaussian distribution generation diagram

Table 4.1: Proportion of LabVIEW generated numbers falling between ±1, ±2 and ±3 SD

	Range		
	± 1 SD	**± 2 SD**	**± 3 SD**
LabVIEW results	67.6%	95.72%	99.83%
Normal Distribution	67%	95%	99%

The table demonstrates that the function built in to LabVIEW does indeed generate approximately Gaussian random variables, with the resulting output standard deviation being, in this particular run, less than one percent higher than the input parameter. However, as demonstrated in 2.1.2 – *Statistical Noise*, these functions will not produce accurate results at very low ion currents as the Normal Distribution no longer approximates the Poisson Distribution.

It was decided to leave the addition of the noise sources to the next stage, the development of the Mass Spectrum Model (as detailed in section 4.2), as the Single Peak Model calculated voltages yet the noise sources were based on ion counting. The Single Peak Model as converted to LabVIEW, without noise sources added, is shown in figures 4.10 and 4.11. In this example, a mass 206 peak is shown.

The front panel (4.10) shows how the inputs in a VI need not exactly represent a physical instrument. The VI inputs are not present in a real mass spectrometer; they instead represent factors resulting from the design and operating parameters of the physical instrument. The inputs were: the maximum voltage of the measured peak (in V); the mass of the peak being measured (in amu); the resolution; the fraction of the peak width that had a flat top; the baseline voltage (in V); the step size for incrementing the mass vs. voltage graph (in amu) and the start and end masses of the graph (in amu).

The factors directly affecting the peak shape were the mass, the resolution and the peak top fraction of width. The resolution was defined as the mass of the peak divided by the width of the peak at the base, for ease of calculation within the model.

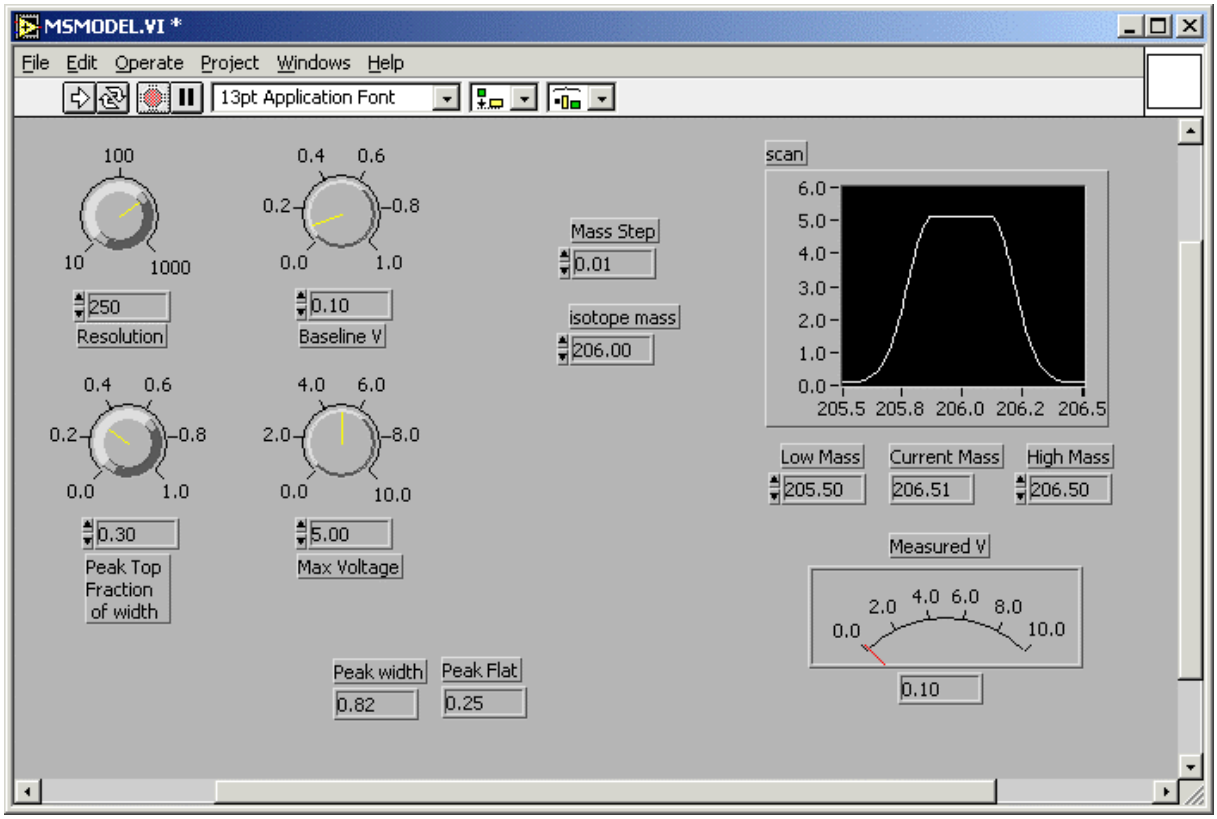

Figure 4.10: Single Peak Model

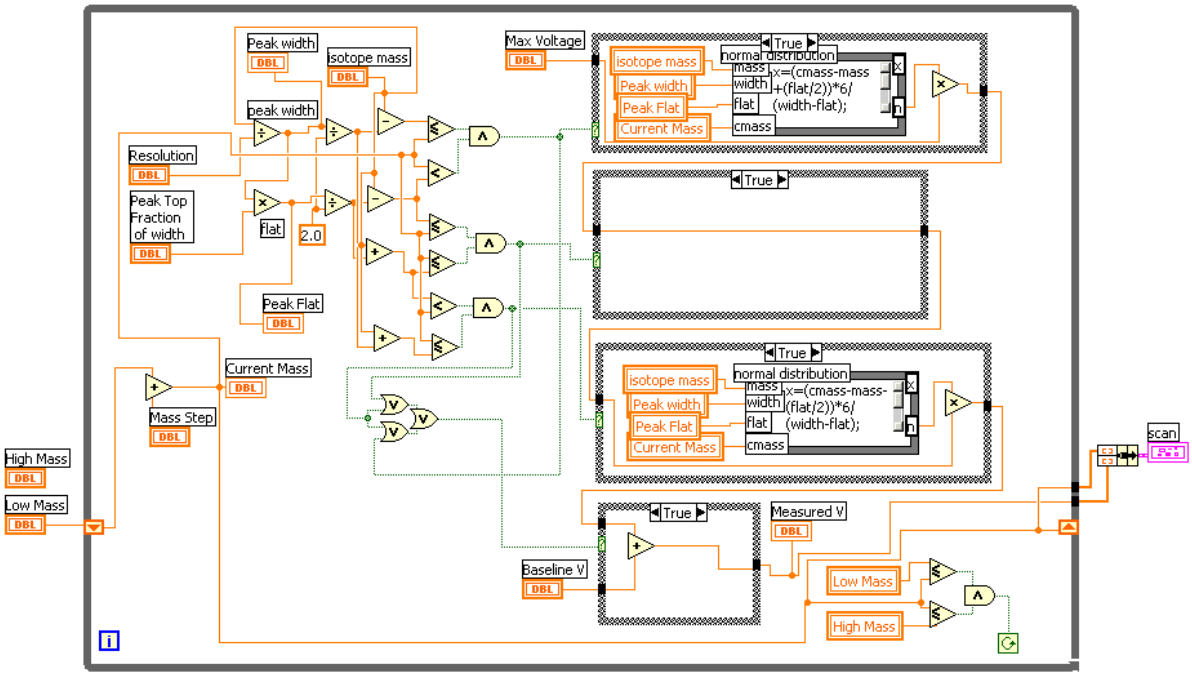

Figure 4.11: Diagram of Single Peak Model in LabVIEW

Verification and Testing

In testing, comparisons were made between simulated and real mass peaks. A sample test peak is shown in figure 4.12, generated with a resolution of 325 and a "peak top fraction of width" of 0.4. The blue outline on the peak links the bottom and top corners of the peak. A typical mass 206 Lead peak, obtained from the VG-354, is shown with this simulated-peak outline superimposed, also in figure 4.12; the figure demonstrates the agreement between the simulated and real peaks. The difference is due to asymmetry in the ion current intensity within the real beam.

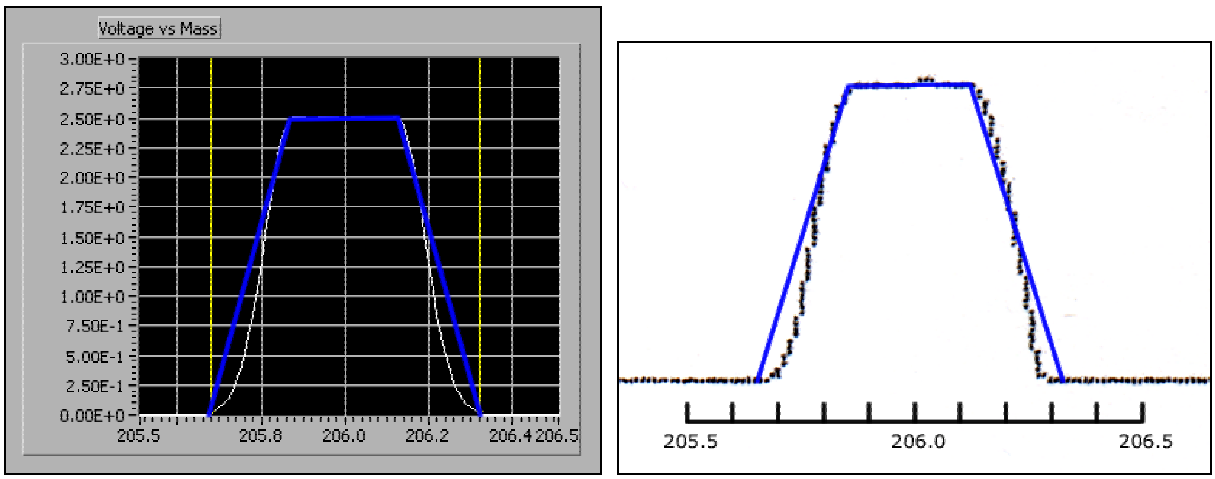

Figure 4.12: Comparison between simulated and real 206 Lead mass peaks

The next step was to introduce the ability to reproduce a physically realistic mass spectrum.

4.2 Mass Spectrum Model Development

Specifications

The LabVIEW Single Peak Model was incorporated into a simple mass-spectrum scanning program (the Simple Scan Program) in the form of the Mass Spectrum Model, in principle able to simulate the generation of the complete mass spectrum for an element. Apart from a limited number of controls to supply input parameters and the actual geometrical shape of the mass spectrum output produced by the Mass Spectrum Model, the Simple Scan Program was not intended to represent the normal operation of a mass spectrometer as used in normal scanning mode. This approach was taken so that the ability of the model and associated noise modules to generate realistic mass spectra could be tested. The Simple Scan Program user

interface had to allow for inputs, such as changing mass or mass resolution, into the model so that the overall change in the shape of the mass spectrum could be assessed and compared to real mass spectra.

In addition to the specifications of the Single Peak Model, the Mass Spectrum Model needed to:

- Output a mass spectrum as specified in a data file
- Produce realistic noise levels on the peaks and baseline
- Generate data for ion beams of a prescribed size.

Mass Spectrum Model Design

The Mass Spectrum Model was designed to allow the noise sources to be configured and enabled at the user's command. The scan parameters also included settings commonly available on a physical instrument such as mass-spectral scanning (start mass, end mass and mass increment). However, the input abundances were taken from a data file. This file was simple tab-delimited text, directly readable by LabVIEW, containing the number of isotopes, the masses and their corresponding abundances as decimal fractions. An example of the file contents for Lead is as follows from the file "NBS-981.txt":

```
4
204	0.014
206	0.241
207	0.221
208	0.523
```

Mass Spectrum Model Coding

All coding was performed in LabVIEW with no external code necessary. The LabVIEW VI and associated hierarchy, containing the Mass Spectrum Model written for the Simple Scan Program, are shown in figures 4.13 through 4.16.

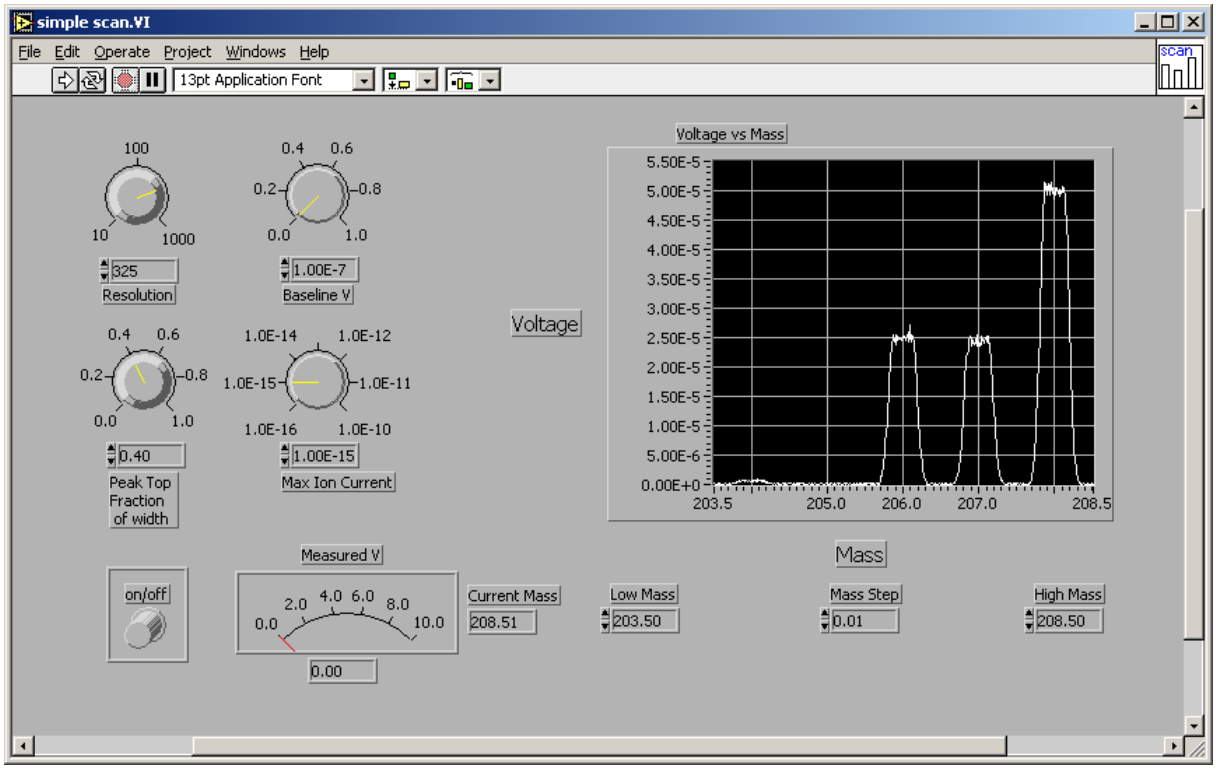

Figure 4.13: Simple Scan Program showing model lead spectrum with noise

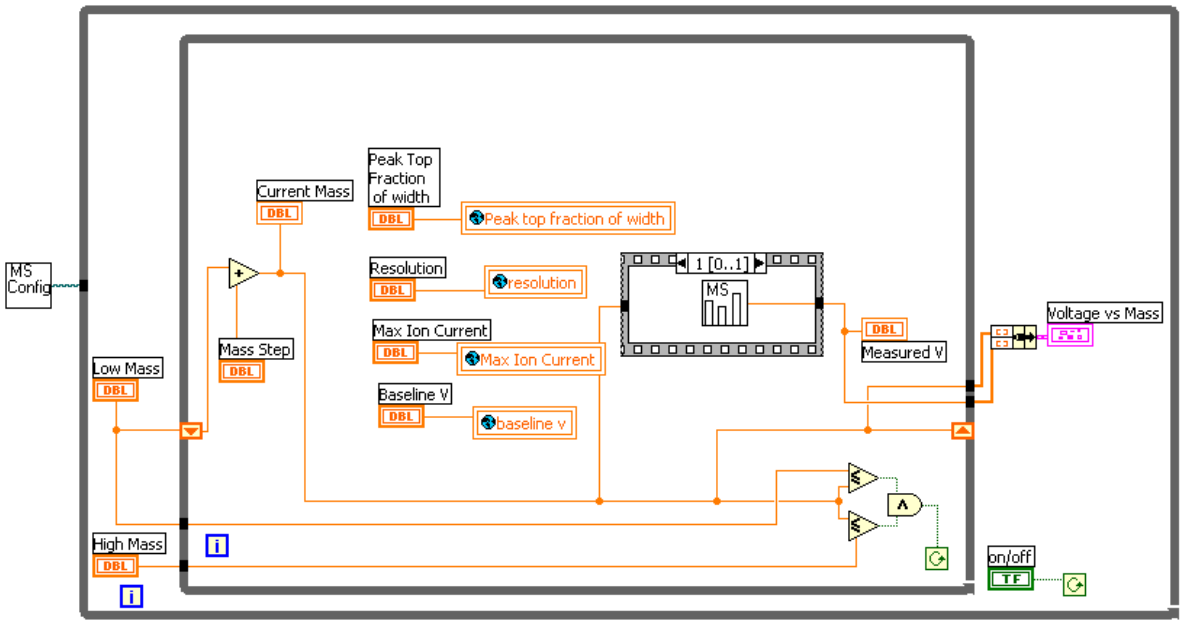

Figure 4.14: Diagram of Simple Scan Program

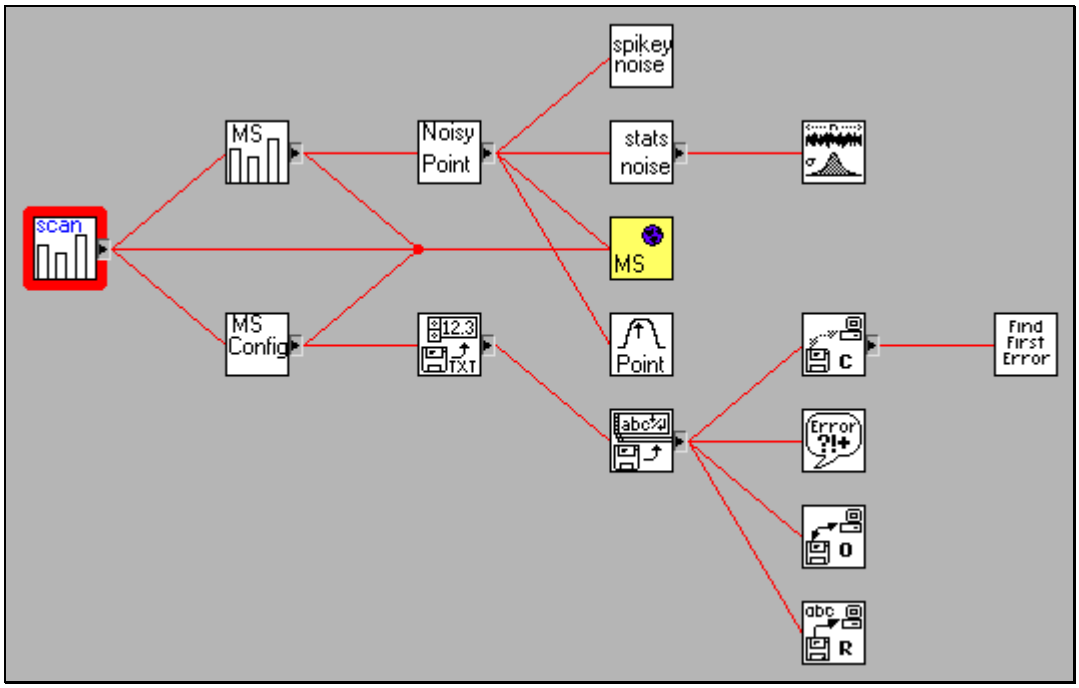

Figure 4.15: Simple Scan Program VI hierarchy

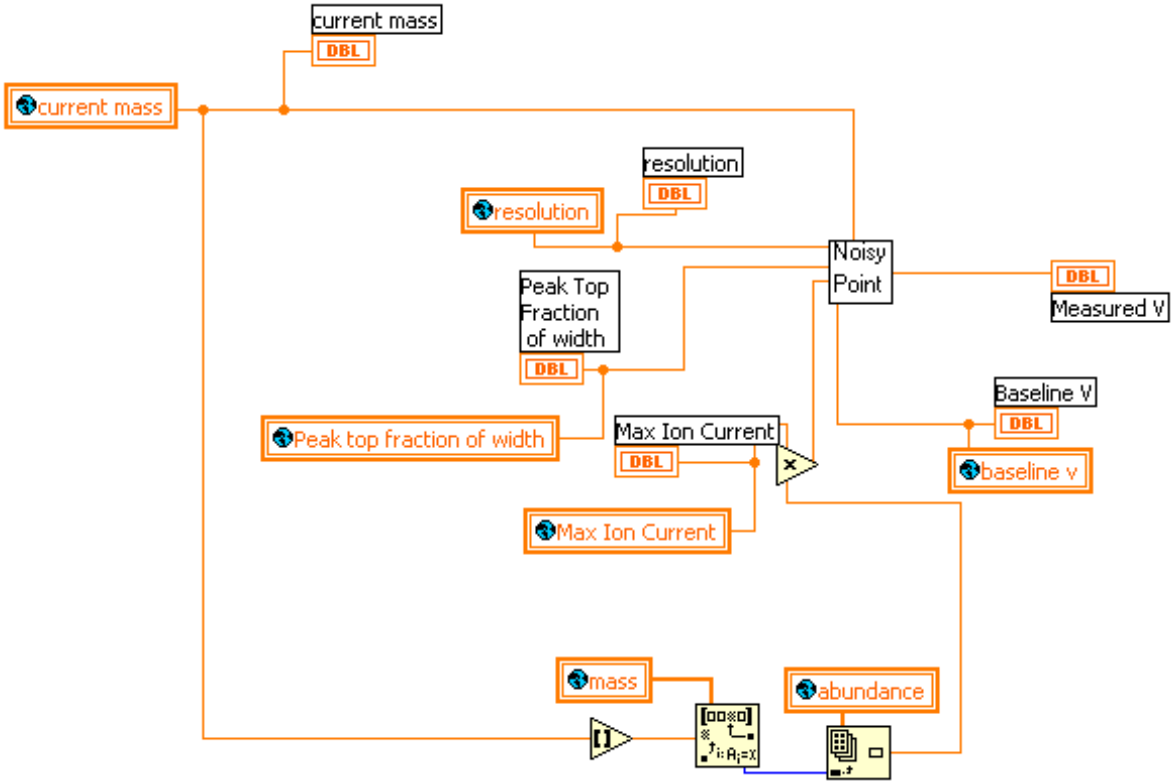

Figure 4.16: Mass Spectrum Model main VI diagram

For ease of integration, global variables (such as the resolution, abundance and current mass shown in figure 4.16) were used throughout the VIs.

Enhancements were added to the model to make it as realistic and useful as possible for the development and testing of new modules. A key enhancement to the model was the requirement to generate synthetic measurement uncertainties consistent with those produced by real thermally ionised beams

All ion beam generation methods and measurement systems are subject to some level of fluctuation or uncertainty, as detailed in section 2.1.2. The development of the statistical noise model is detailed in section 4.1 – *Single Peak Model Coding*; this noise was used in the Mass Spectrum Model.

Baseline or background noise is essentially that produced by the ion detection system when there is no intentional ion beam being directed at the detector. This form of noise is critical in assessing the uncertainty of the baseline and can limit the measurement uncertainty for ion beams with an intensity approaching that of the baseline. Baseline noise in TIMS systems is normally measured between peaks in the mass spectrum and is dependent primarily on the type of detector system being used, the cleanliness of samples and the level of vacuum involved. Unwanted ions arising from interferences or from reflections (from incorrectly constructed or configured instruments) may appear at baseline measurement positions; these were not considered in this model. A simple form of baseline noise was generated by adding a randomly generated number (representative of white noise) to the baseline signal. The magnitude of the noise was made variable so that changes to the type and characteristic of detector being used could be simulated.

A “shot noise” source was also added (also referred to as “popcorn noise”) using a variable sized spike of voltage that had a variable probability (between 0 and 1) of occurring. This kind of noise often arises from thermal effects in amplifiers and other solid-state devices – a properly cooled system can avoid most of these effects.

Magnet hysteresis and peak shifting (due to HT noise) both add small uncertainties but these were also not considered in this model.

The noise sources were set by the user in the VI that determined the relevant signal voltage at any given time (or mass). The “Noisy Point” VI is shown in figures 4.17 and 4.18.

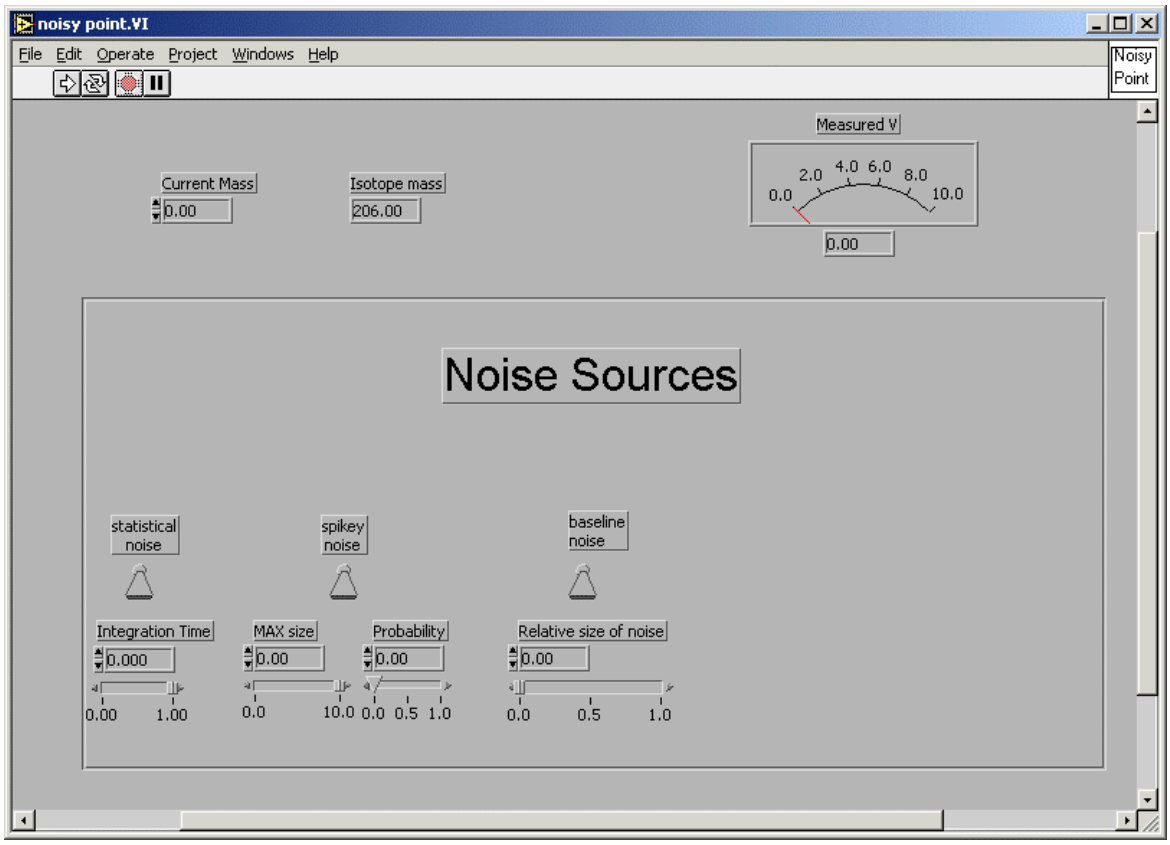

Figure 4.17: Noisy Point showing input parameters

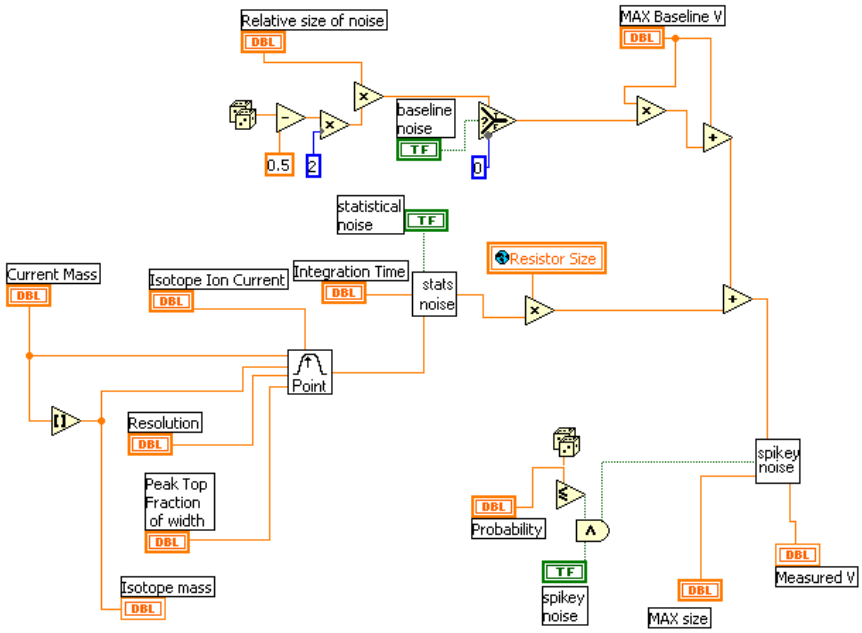

Figure 4.18: Noisy Point Diagram

Mass Spectrum Model Verification and Testing

Testing involved Lead isotope input data with a very simple set of abundances. The data file used contained the following:

```
4
204   0.005
206   0.25
207   0.245
208   0.5
```

A resolution of 325 and peak top fraction of 0.4 were chosen for the tests, as these produced realistic results in the single peak tests. Around 100 tests were performed with combinations of noise types, noise levels and beam sizes ranging from the very large (10^{-10}A) to the very small (10^{-16}A). The tests verified realistic behaviour such as a higher proportion of noise with a smaller beam.

4.3 VG-354 GPIB Based Model

With the Simple Scan Program now capable of realistically a typically scanned mass spectrum, work began on modifying the model program so that the back end of the program would to be able to be replaced by the VG-354 mass spectrometer. Since in practice this would need to be performed via the VG-354 data interface (the GPIB), a set of model GPIB routines was written (called "demo" VIs). These demo VIs were coded to emulate the function of the GPIB and all related devices on the Mass Spectrometer. This was done in conjunction with the incorporation of an existing LabVIEW mass-scanning program into the model.

A mass-scanning program written using LabVIEW, was developed in 1995 by a student as part of an undergraduate and summer studentship project (Turner, 1995). This program was a fully functioning set of routines for use with the VG-354 which controlled only the scanning function of the mass spectrometer and was able to perform simple isotope ratio determinations from the scanned data.

The program contained a set of VI modules that handled GPIB I/O (to set mass and take readings), displaying the scan voltage result graphically and doing a rudimentary analysis of the mass spectrum. The program used only the axial collector (either Faraday or Daly).

The software had been tested with the VG-354 and was found to function correctly. Attention now turned to integrating various components of the model into the mass-scanning program.

4.3.1 Combination of Turner Scan Program and Mass Spectrum Model

The availability of Turner's functioning mass-scanning program saved a considerable amount of time and effort, since the development of the relatively low level interfacing code, such as reading an ion beam voltage or writing a mass to the magnet, was relatively complicated and time consuming. This was largely due to the digital hardware limitations of and interactions between the various VG-354 electronic components; the development of specific functions was required to deal with these limitations. Having a functioning program that had been fully tested meant that the model could be less complicated and the other code could be written with the confidence that the final product's interface code worked.

An example of this is the magnet strength writing routine, which involved two levels of operation. First, the mass number had to be converted to the relevant field strength, through a mass to field calibration table stored in a file. Secondly, the calculated field strength had to be converted to a 20 bit octal DAC setting (a requirement of the hardware). If this had been modelled from scratch, each of the two steps would have been emulated in reverse. Because the program already had a working magnet setting routine, the Mass Spectrum Model could simply note the mass that had been written and refer to it later in the demo GPIB write routine. The diagram of this VI is shown in figure 4.19, demonstrating how the Demo GPIB Write subVI has the same I/O as the real one.

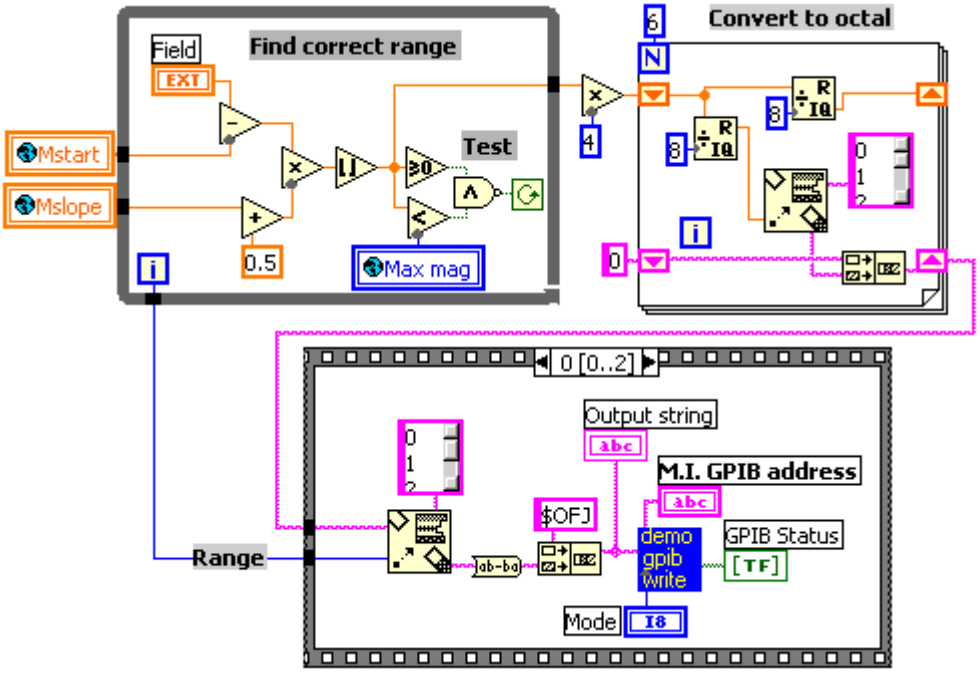

Figure 4.19: Magnet Setting model routine

The Mass Spectrum Model was then modified to allow pre-configuration of the resolution, baseline voltage, peak shape and maximum ion current in a separate VI. The model set-up VI is shown in figure 4.20, demonstrating the ease of using the global variables employed earlier.

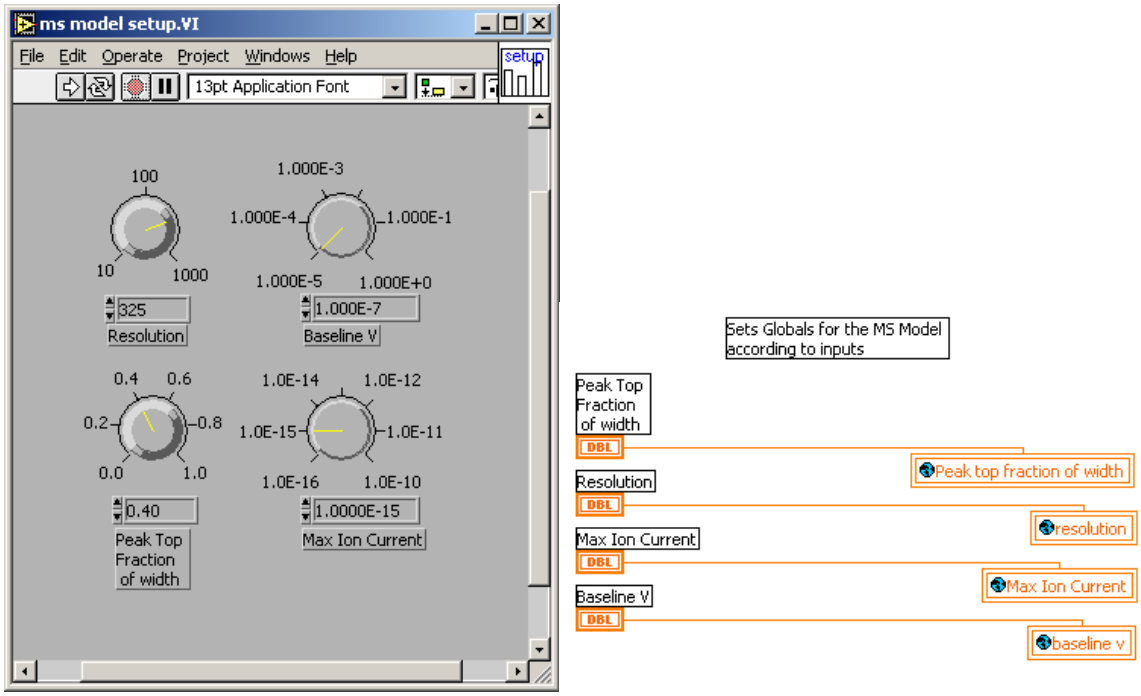

Figure 4.20: Mass Spectrum Model Set-up front panel and diagram

4.3.2 Testing of Mass Spectrum Model based Turner Scan Program

A synthetic mass spectrum approximating NIST SRM-981 Lead, an international isotope reference material, was written in the model configuration data file and loaded into the Turner Scan Program, with a resolution of 325 and peak top fraction of 0.4 as in previous tests. Numerous scans were obtained using various noise and ion beam currents from 10^{-10}A to 10^{-16}A. The abundances used are shown in table 4.2:

Table 4.2: Isotope abundances used in testing the Mass Scanning program

Isotope	Abundance
204	0.014
206	0.241
207	0.221
208	0.523

Figure 4.21 shows a sample scan of the Lead spectrum and figure 4.22 shows results from the simple analysis routine on a subsequent scan from the same set.

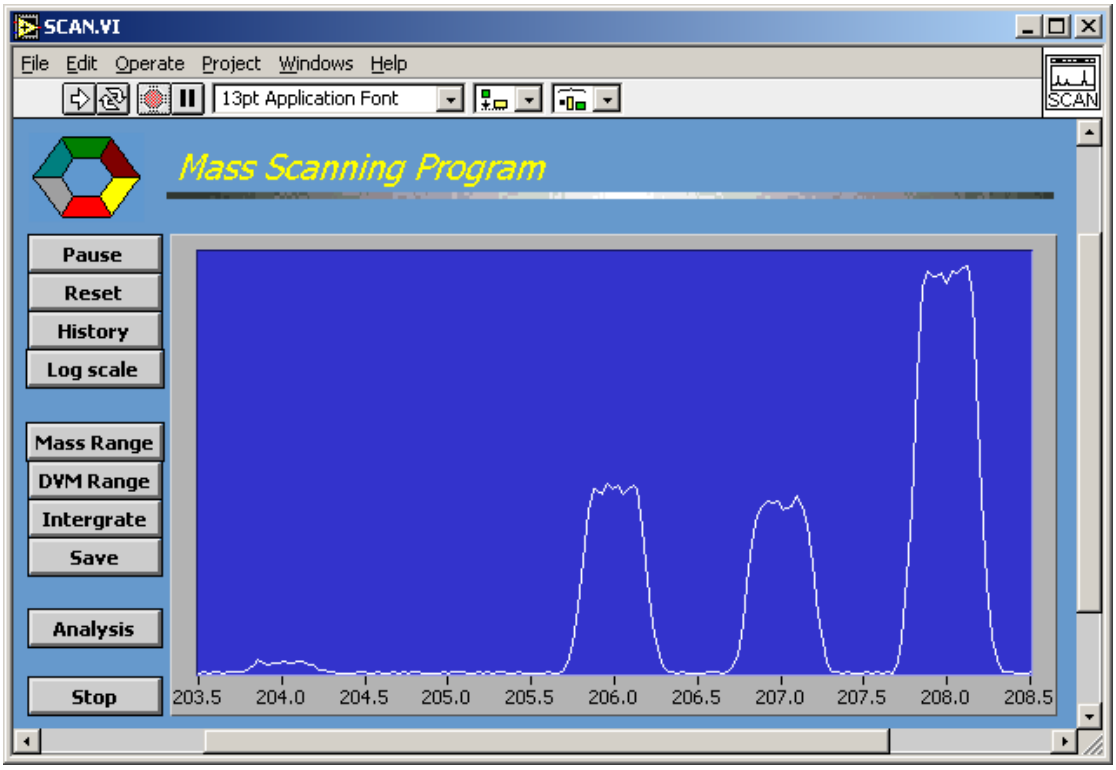

Figure 4.21: Turner Scan Program integrated with Mass Spectrum Model, showing Lead mass spectrum with noise

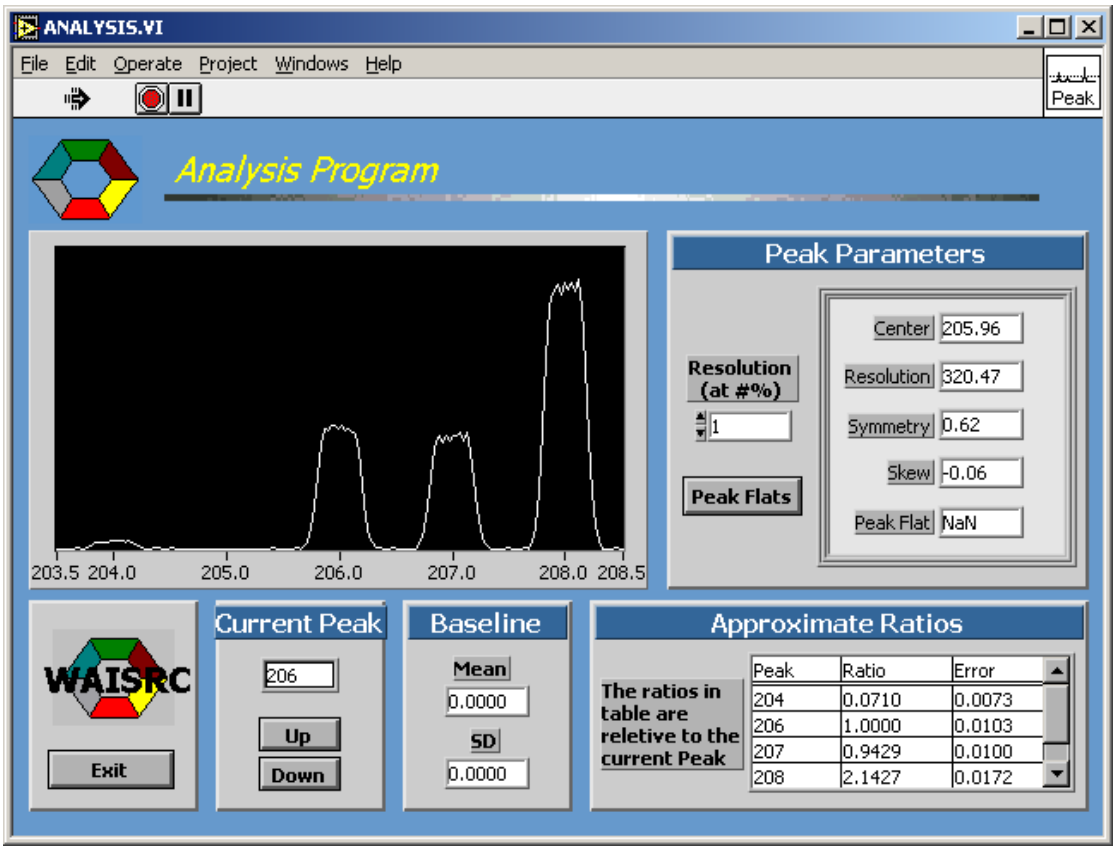

Figure 4.22: Simple Analysis of simulated NBS-981 Lead mass-spectrum (206 Peak)

The 206 peak parameters, as measured by the program, are also shown in figure 4.22. Of note is the resolution, measured at the base of the peak (as specified in the model); the calculated resolution is 320 as compared to an input resolution of 325. The routine also measured the peak centre mass to be 205.96, as compared to the input of 206.00, a difference of 0.02%.

Using 206 as the reference isotope, the input abundances resulted in the isotope ratios shown in table 4.3 alongside the output (in this analysis) from the Turner Scan Program for comparison.

Table 4.3: Comparison of scan program input and calculated ratios

Ratio	Input Value	Output Value	Minimum % Difference
204/206	0.058	0.071 ± 0.007	10%
207/206	0.917	0.94 ± 0.01	1%
208/206	2.17	2.14 ± 0.02	-0.5%

The difference between the input ratio and the closest limit of the calculated value is shown in table 4.3. The calculated values all differ from the input values within uncertainty. The "Error" shown in the analysis program is calculated based solely on the baseline noise, while the spectrum used in the testing had both baseline and ion-counting noise; therefore, the scan program didn't calculate a high enough value. This demonstrates that the "analysis" routine is not to be relied on for accurate results – it provides only a guide to results that might be obtained for a real measurement.

The results showed that the model was working and the noise was contributing to some uncertainty in the measurements. The analysis routine shown was not intended to produce reliable isotope ratios – the program was only a scanning routine - so further work was required to achieve isotope ratio measurements.

5. Measurement Module Development

The development and testing of the peak centring and isotope ratio calculation measurement modules were the final steps performed in this thesis.

Of the various modes and methods of mass-spectrometer operation, the specifications chosen for measurement module development were:

- peak jumping,
- manual operation of filament temperatures, focussing and vacuum systems and
- single-collector measurement.

This measurement method is applicable to any isotope ratio measurement and provided a suitable simple starting point from which other more complex routines, such as variations of peak jumping methods, could be developed

5.1 Peak Centring

Peak centring is the process by which the magnetic field value at the middle of a mass peak is selected (see in Section 2.1.3). One often-used approach is to sequentially step the magnet back and forth across the peak to determine the magnetic field values at the half-height positions at the sides of the peaks and then take the mean value. This approach is time consuming and has the potential to induce hysteresis effects in the analyser magnet. The method may also produce inaccurate results when an asymmetrical peak is being analysed.

Here, another approach was taken to peak centring to attempt to speed up the process. This is especially important for small, rapidly decaying ion beams and for isotopic analyses involving large numbers of mass peaks. The method developed measures the ion beam intensity (i.e. scans) across the mass peak by changing the magnetic field value in one direction only and applies a quadratic polynomial best fit to the intensity to directly determine the peak centre without the need to repeatedly measure ion beam intensities on the sides of the peaks.

The algorithm used was that provided by the “Peak Detector” Analysis VI supplied with LabVIEW. In this algorithm a chosen number of data from the peak scan were used in the

initial fit and the fit moved across the data until the smallest Mean Squared Error was obtained. The concept is illustrated in the following example.

Figure 5.1 shows a theoretical peak consisting of 12 points to which a series of seven point quadratic fits is performed. The first of these fits, "position 1", involves point 1 to 7, the second involves points 2 to 8, the third 3 to 9 etc. Figure 5.2 shows the first four of these fits. The equations shown in figure 5.2 lead to the points of inflection and mean squared errors shown in table 5.1, which clearly demonstrates that the true centre is found with the "position 3" fit, in this case to within 0.002% of the true x value.

Table 5.1: Peak detector conceptual example results

Fit	MSE	x value at point of inflection
Position 1	0.654	6.432
Position 2	0.1292	6.0714
Position 3	0.0952	5.9999
Position 4	0.1394	5.9286
	True Centre	6.0000

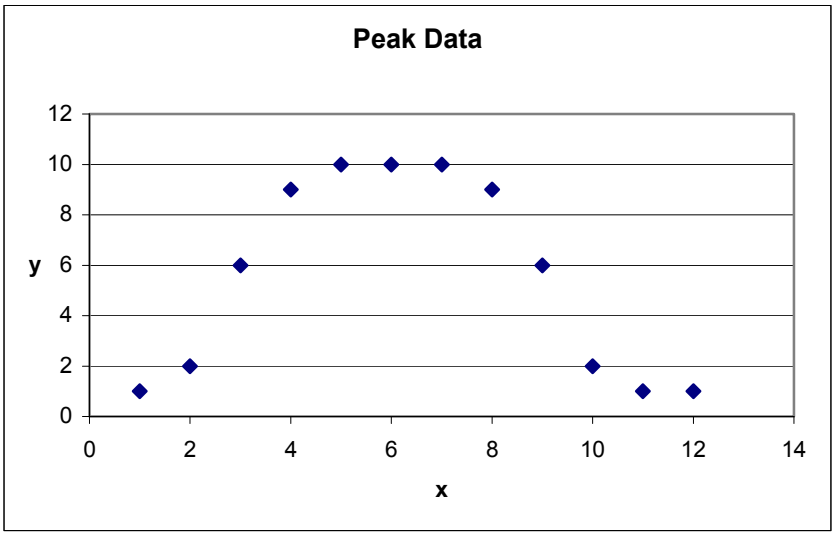

x	y
1	1
2	2
3	6
4	9
5	10
6	10
7	10
8	9
9	6
10	2
11	1
12	1

Figure 5.1: Peak detector conceptual example input data

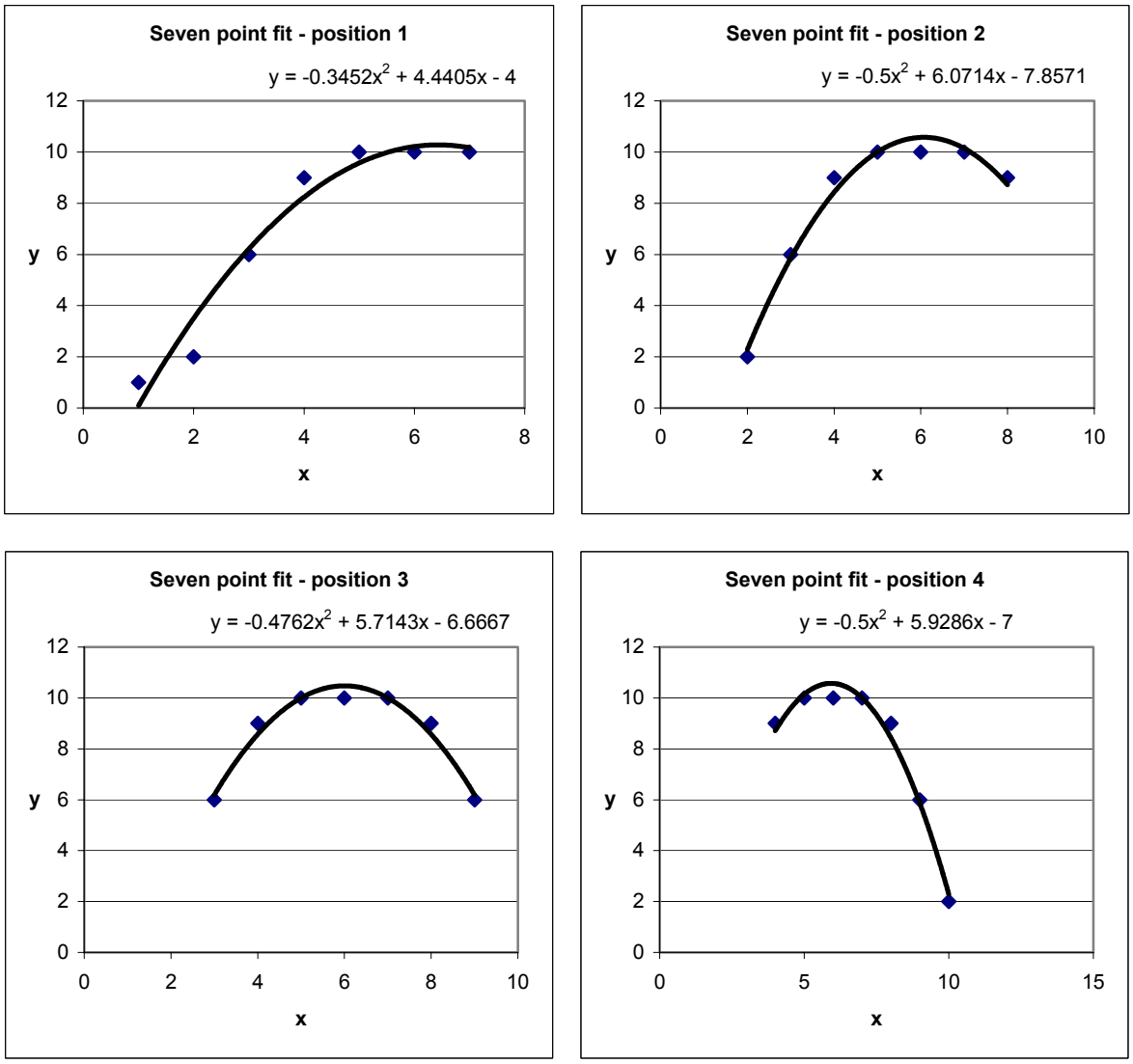

Figure 5.2: Peak detector conceptual example polynomial fits

The peak centring module inputs were:

- the set of isotope masses on which to centre;
- the scan width, in amu, within which to find the centres;
- increment, in mass units, to step through the scan;
- a threshold signal level (in mV) below which peaks were to be rejected, as a percentage of the highest value in a single peak scan (assisting with baseline noise) and
- the number of data to use in the quadratic fit.

The module outputs were:

- the set of points used in finding the peak centre and
- the calculated peak centres, presented as the apparent masses of the peak centres in amu.

Figures 5.3 and 5.4 show the Peak Centre VI.

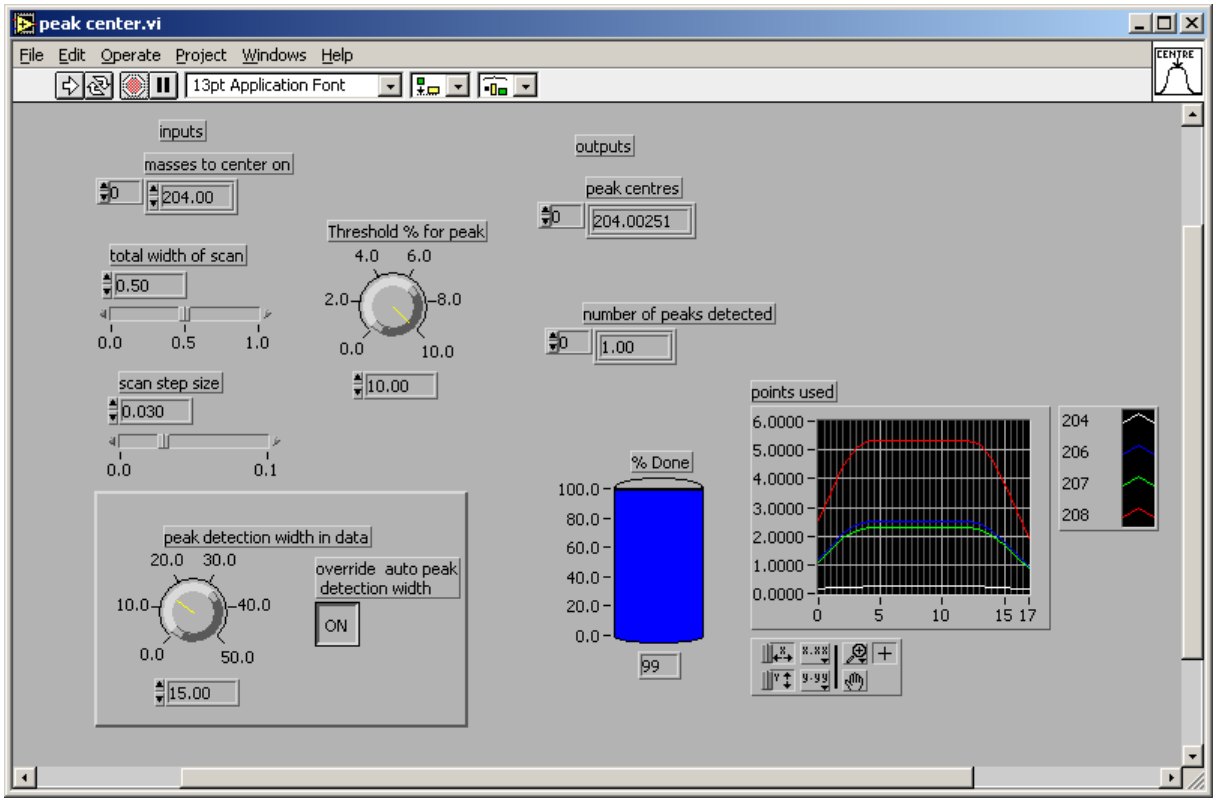

Figure 5.3: Peak Centring VI Front Panel

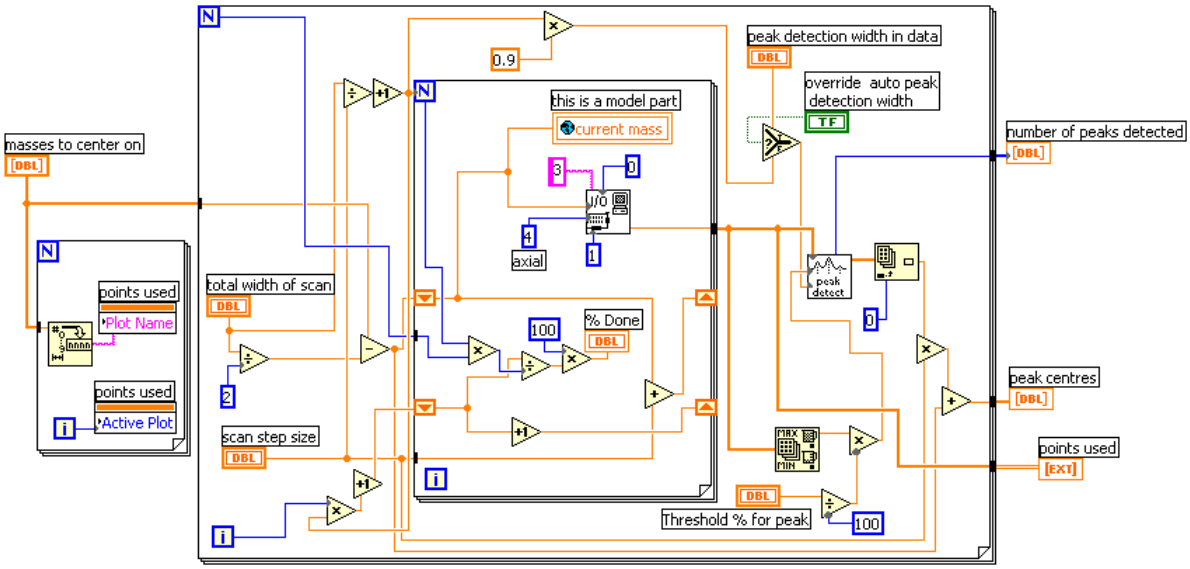

Figure 5.4: Peak Centring VI Diagram

The front panel (Figure 5.3) shows results obtained when a synthetic NBS-981 spectrum (as detailed in section 4.4.2) without noise was fed into the VI.

However, during typical testing, the VI was provided with a noisy 206 peak off-centre by 0.1 mass units. The VI consistently found the peak centre to be within 0.0002 mass units from the true centre, a difference of 1 ppm, which is well below the capability of conventional TIMS magnetic control systems.

At 0.2 amu off centre, the VI needed to scan more points over a wider range, increasing the time that would be required. However, it was able to find the centres to within 0.005 amu. The wider scan would only be necessary for a first pass, as the centres found could be used for a subsequent scan to find the peak to a better precision.

5.2 Isotope Ratio Determination by Ion Beam Curve Fitting

Traditional isotope ratio measurements involve simple linear interpolations and rejection of results that appear to be outliers based on statistical tests. It was decided to try a different approach for this thesis, taking advantage of tools provided in LabVIEW to improve the process.

A technique using least-squares polynomial fitting of the individual ion beam measurements as a function of time was developed to determine the isotopic ratios. This method was then compared against the commonly used technique involving a linear-fit of adjacent peaks.

The ion beam voltage vs. time for each measured isotope was to be fitted to a polynomial of varying degree, using different algorithms. To assess the reliability of the fitting routine, numerous functions were generated and fitted. These functions included exponential functions overlaid with step and sine wave functions to simulate a drastic step-like changes and longer-term variations in filament current and ion beam variability.

The polynomial fit functions used were those available in LabVIEW. Algorithms available for calculating the best fit were *SVD*, *Givens*, *Givens2*, *Householde*r, *LU decomposition* and *Cholesky*.

These algorithms were tested with varying polynomial orders. A typical test of 200 synthetic sample points (including the step and typical time varying beam parameters discussed above) and sixth order polynomial fitting is shown in figure 5.5, in which the test points are labelled "Data" in the legend at the top-right of the graph and the polynomial fit is labelled "Polyfit".

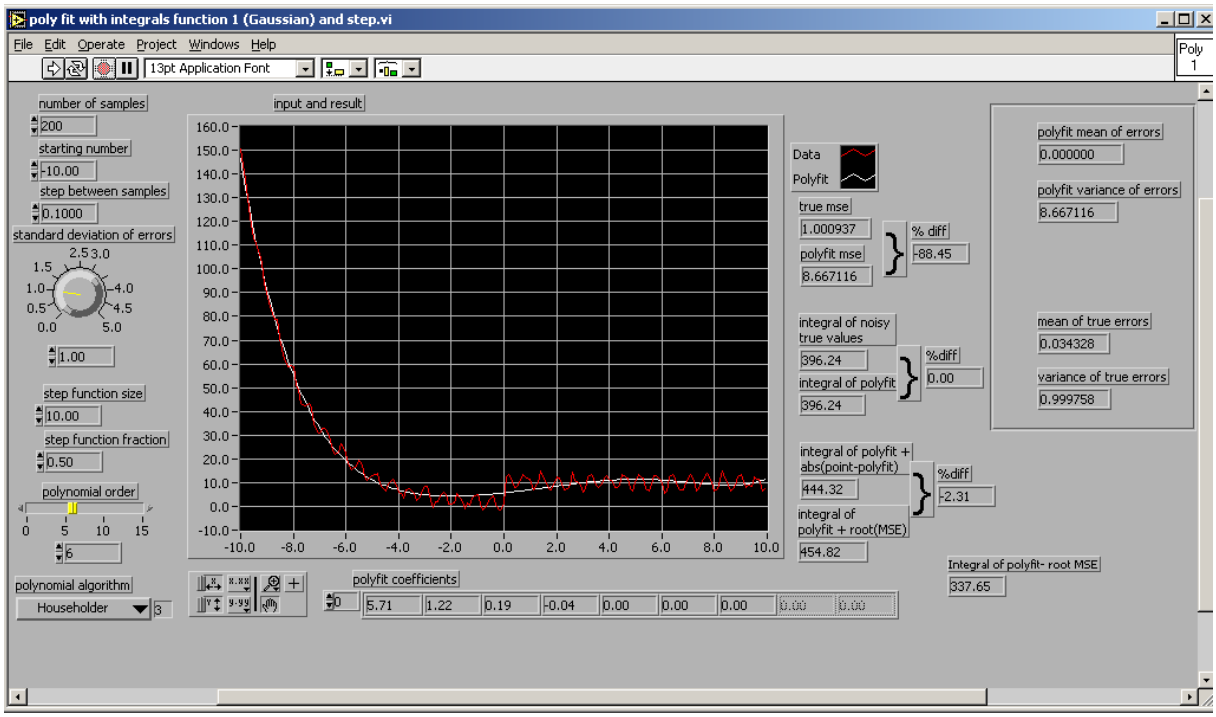

Figure 5.5: Test of polynomial fitting techniques with a predefined function

The figure shows a numerical function calculated at the defined interval with Gaussian noise added to the result to cause deviation from the true value. The fit is also shown, along with various calculations on the original data and the fit data. It was found that the *Householder* algorithm performed the best, generally yielding the lowest MSE relative to the other algorithms.

Once the six algorithms were evaluated, a comparison was undertaken with real ion beam data obtained from the VG-354 during a conventional isotopic analysis of Lead spiked with ^{205}Pb Lead. The spike is an artificially prepared isotope often used in "Isotope Dilution" concentration measurements and would not normally be present in a Lead mass spectrum. The VG-354 software calculated ratios relative to mass number 205 in this particular experiment.

An example of the VG-354 data is given in figure 5.6. The figure shows the results from the VG-354 over time, ratio number 1 being the first measurement of the 206/205 ratio and ratio number 60 being the last. In total, the experiment produced data for the 204/205, 206/205, 207/205 and 208/205 ratios.

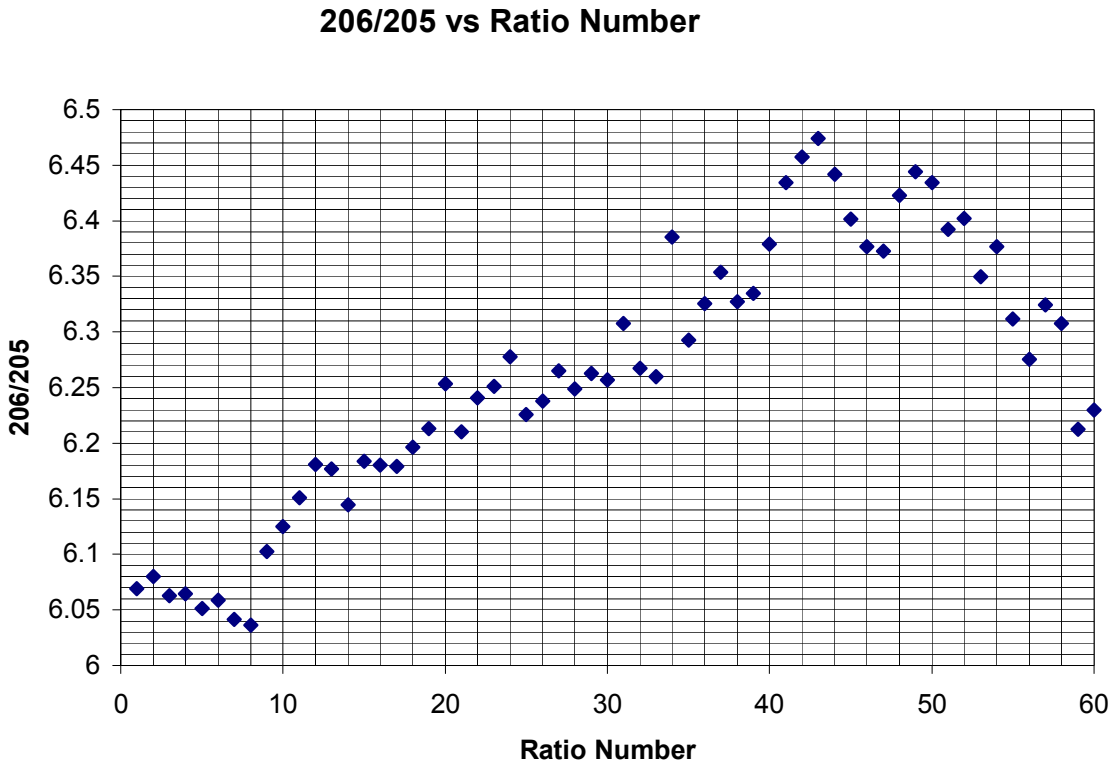

Figure 5.6: Ratios obtained in analysis of NBS-981 Lead

The data sets were re-calculated to give ratios relative to 207, producing the 206/207 and 208/207 ratio results showed in figures 5.7 and 5.8.

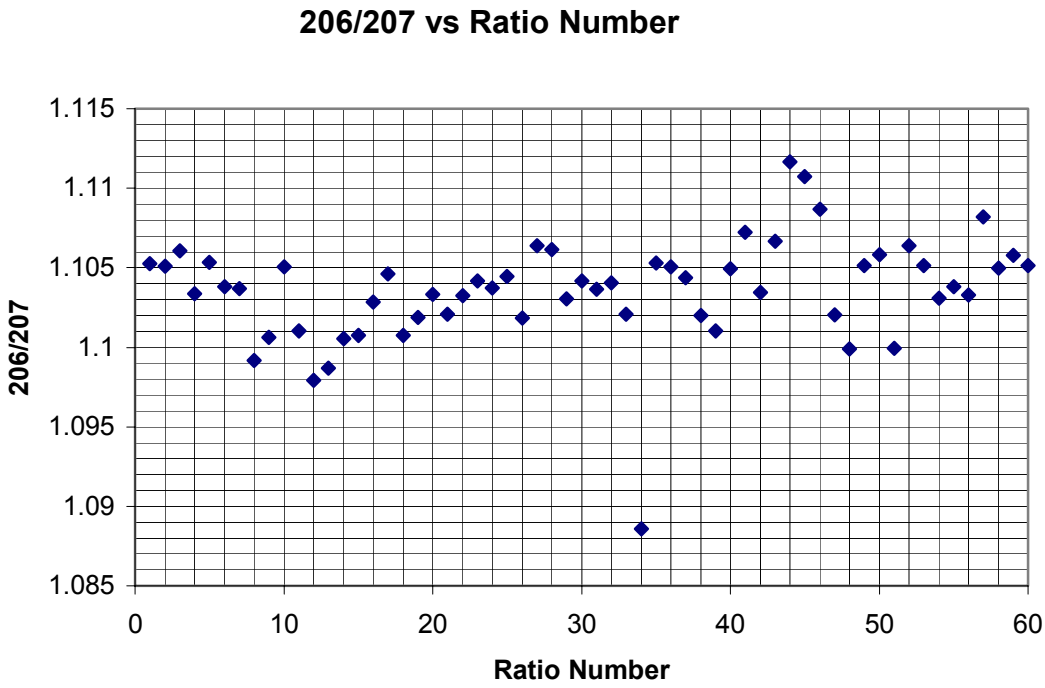

Figure 5.7: Recalculated data for 206/207

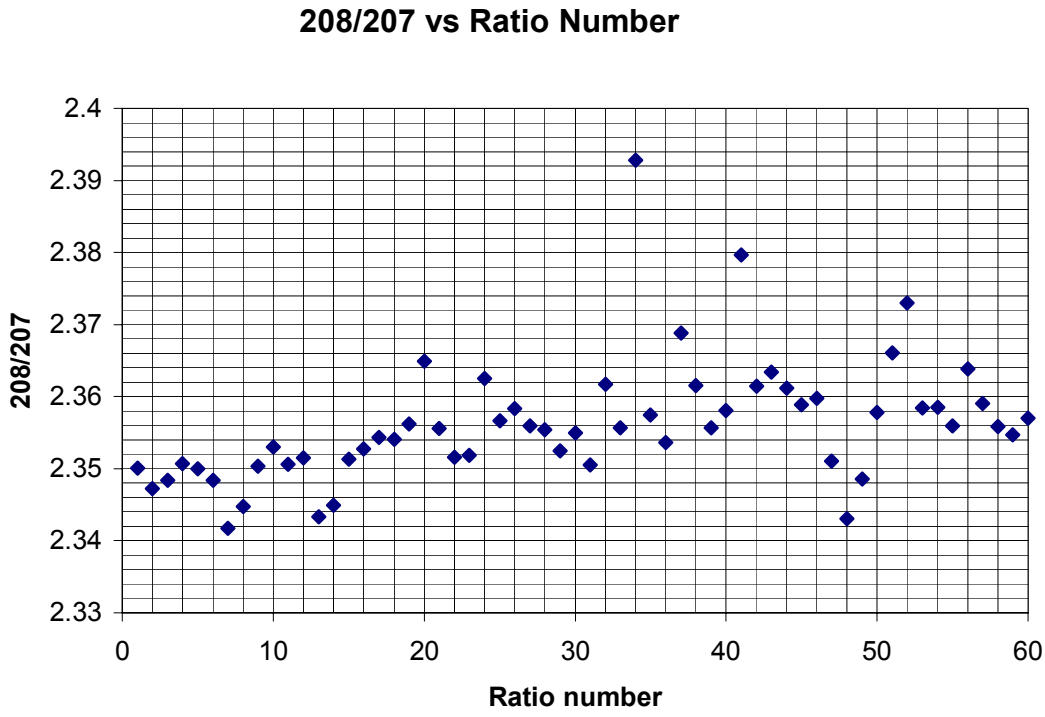

Figure 5.8: Recalculated data for 208/207

Note that the 206/205 ratio changes over time, rising and then falling between almost 6.0 and 6.5, while the two recalculated ratios remain more stable. The overall results calculated by the VG-354 for these data are shown in table 5.2. The results, despite the recalculation, are those obtained from the mass spectrometer under normal conditions.

Table 5.2: Original data calculated by VG-354 for Lead analysis

	Before Rejection		After Rejection		
Ratio	Grand Mean	St Error	Grand Mean	St Error	
204/205	0.37447	0.14 %	0.37444	0.13 %	on 56 of 60
206/205	6.26170	0.28 %	6.26170	0.28 %	on 60 of 60
207/205	5.67378	0.24 %	5.67378	0.24 %	on 60 of 60
208/205	13.3686	0.27 %	13.3573	0.26 %	on 59 of 60

The pre-rejection results, once converted to reference isotope 207, yielded means and standard errors as shown in table 5.3:

Table 5.3: Pre-rejection results recalculated to reference isotope 207

Ratio	Mean	St Error
204/207	0.0660	0.0001
206/207	1.1036	0.0004
208/207	2.3562	0.0011

These results were then compared to those obtained by calculations performed with the new polynomial fit techniques.

The ion beam counts vs. time for each isotope are shown in figure 5.9 while the baseline is shown separately in figure 5.10. The grouped baseline measurements reflect the VG-354's technique of measuring baselines only before the ion beam data is measured.

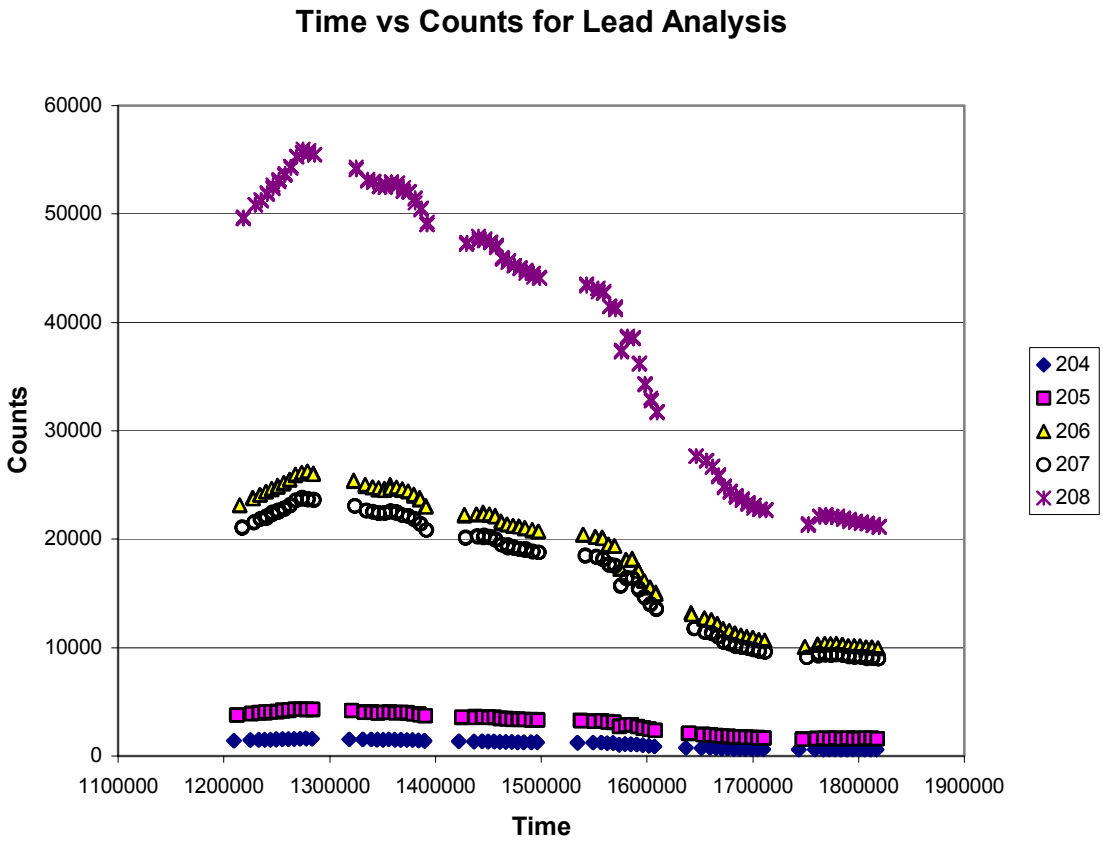

Figure 5.9: Time vs. Ion Beam counts for each Isotope in Lead analysis

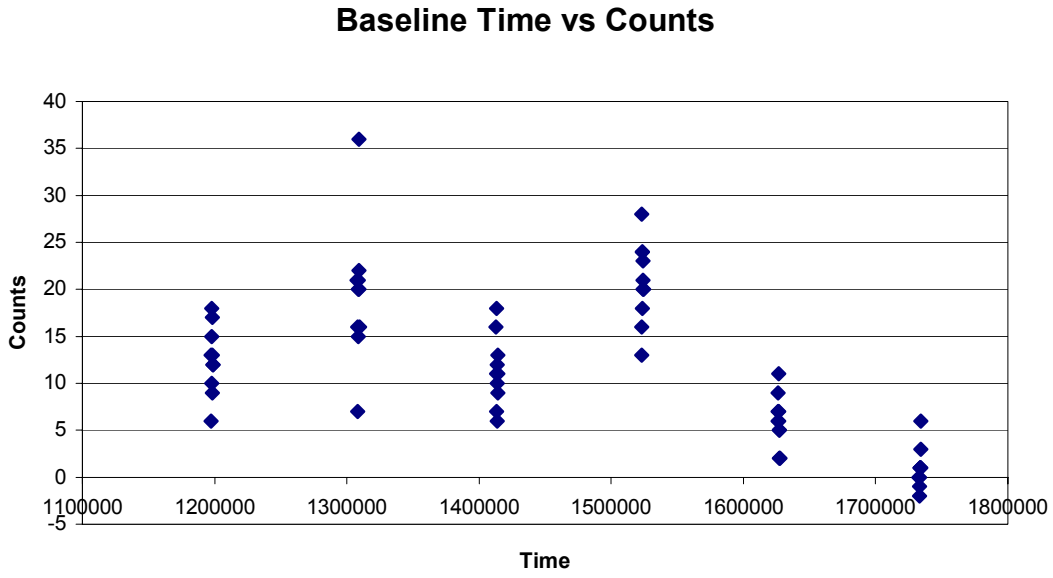

Figure 5.10: Baseline time vs. counts for lead analysis

The polynomial fit VI was modified to calculate lead ratios from the real ion beam data. Ratios were calculated at every point for which there was data. Each one of the fit algorithms

was tested at various orders. Over all of the ratios, the *Householder* algorithm seemed to produce the best results, with ten being the optimal fit order. Higher orders did not produce better results, suggesting there is an optimal order for a given data set. An order of three was used for the baseline, as it had fewer points. For example, the following results were obtained for the 208/207 ratio and its standard error, shown with the VG results for comparison:

Table 5.4: Polynomial fit results for 208/207 ratio

Order	Ratio	Standard Error
5	2.35581	0.00026
6	2.35545	0.00025
7	2.35621	0.00024
8	2.35592	0.00022
9	2.35554	0.00022
10	2.35554	0.00022
11	2.35692	0.00026
12	2.36209	0.00038
VG-354	2.3562	0.0011

The table shows the same ratio result for the nine-order and ten-order fits and similar standard errors for both. The difference between the VG-354 ratio calculation (2.3562) and the 9/10 order fit calc (2.35554) is 0.0007, well below one standard error of the VG-354 results (0.0011). The polynomial standard error is itself a factor of five lower than the VG-354 standard error. Interestingly, the VG software chose to reject one point in the calculation of the 208/205 ratio (from which the 208/207 ratio was calculated). Re-calculation using the post-rejection data gives a result of 2.3542, lower than the pre-rejection result. The optimal polynomial fit also gave a result lower than the pre-rejection value, showing that when including all data, at least in this example, it handles these outlier points better than the standard pre-rejection calculation in the current VG-354 software.

Figure 5.11 shows the 206/207 ratio, calculated through a linear interpolation. Figure 5.12 shows the same ratio obtained with a 10-order polynomial fit calculated with the *Householder* algorithm.

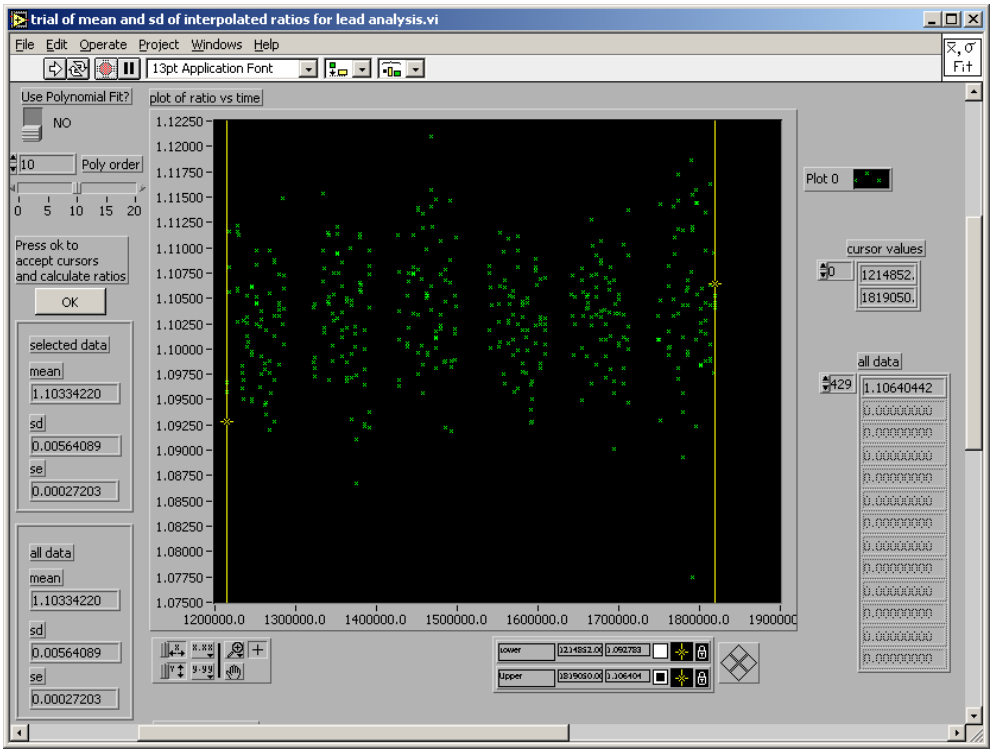

Figure 5.11: Linear interpolation calculation of 206/207 ratio for Lead analysis

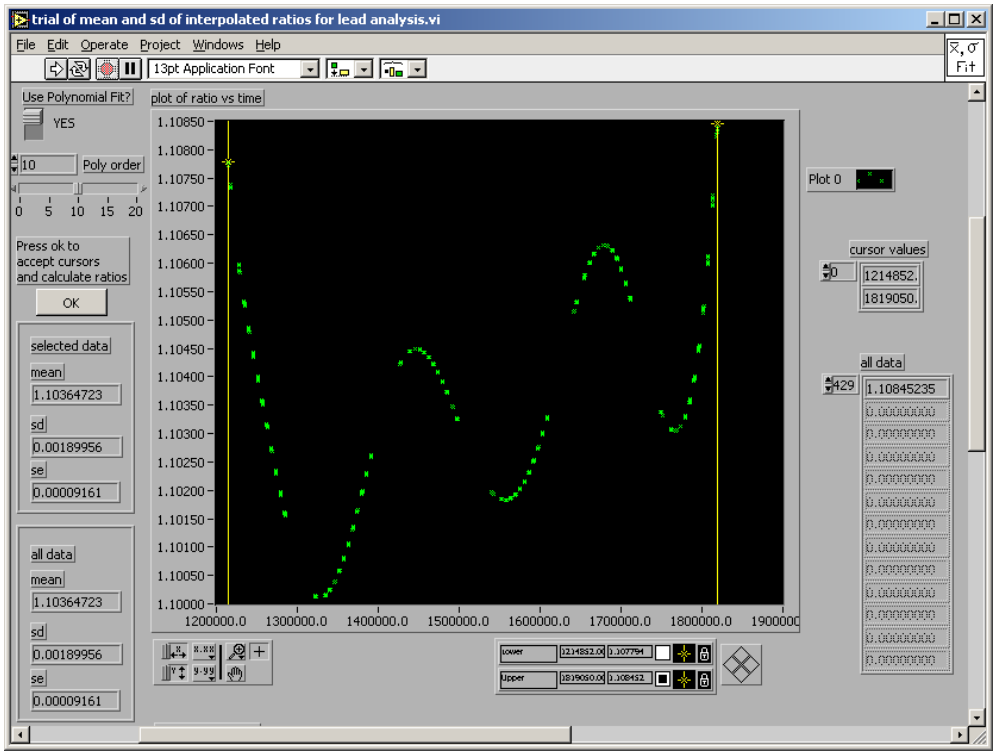

Figure 5.12: Polynomial fit calculation of 206/207 ratio for Lead analysis

The figures show different calculated ratios to the VG-354 results, due to the vastly different methods used. The results are set out in table 5.5.

Table 5.5: Comparison of VG-354, polynomial and linear interpolation calculations for 206/207 isotope ratio

	VG-354	Polynomial Calc	Linear Interpolation
Ratio	1.1036	1.1036	1.1033
Standard Error	0.0004	0.0001	0.0003
Standard Deviation	0.003	0.002	0.006

The results agree within one standard error of each other (despite each looking different from the other in graphical form) with the polynomial fit yielding results closer to the VG-354 results than the linear interpolation. The standard deviation is lower because the fit is reducing the spread of the points used; the standard error is a factor of four lower for the polynomial fit than for the VG-354 data because of this and the fact that more points (seven times more in this case) were used in the calculation. Similar results were obtained with the polynomial fit for the other isotopes, with standard errors a factor of four to five lower than the VG-354 results - this clearly demonstrates the superiority of this technique with these data and under these conditions.

5.3 Analysis Module

The *peak centring* and *ratio calculation* modules were then combined with a *measure* module and the mass spectrometer model to create the core of the *analysis* module. The user input for the Analysis VI included the number of ratios per block, the number of blocks, the masses to measure and the baseline location. It then centred and measured on the peaks, displaying a warning if a peak centre wasn't found properly. The results were plotted and then control was passed to the user to select the ratio to display. The Ratio Selection VI passed the selected ratio to the Ratio Calculation VI with either linear interpolation or polynomial fit isotope ratio calculations selectable by the user. The set of VIs used are in figures 5.13 to 5.15, showing an example of testing performed with the same test spectrum used previously.

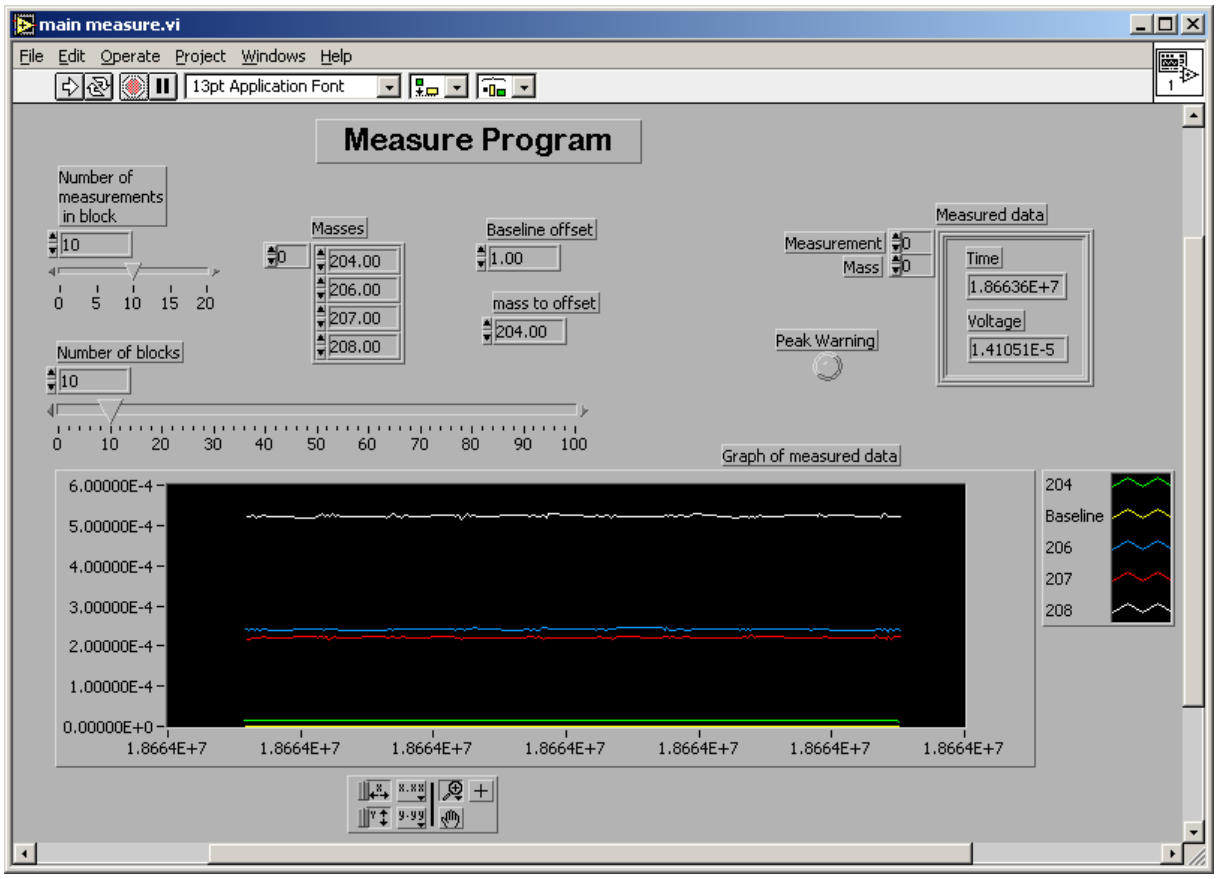

Figure 5.13: Analysis VI showing Lead test measurements

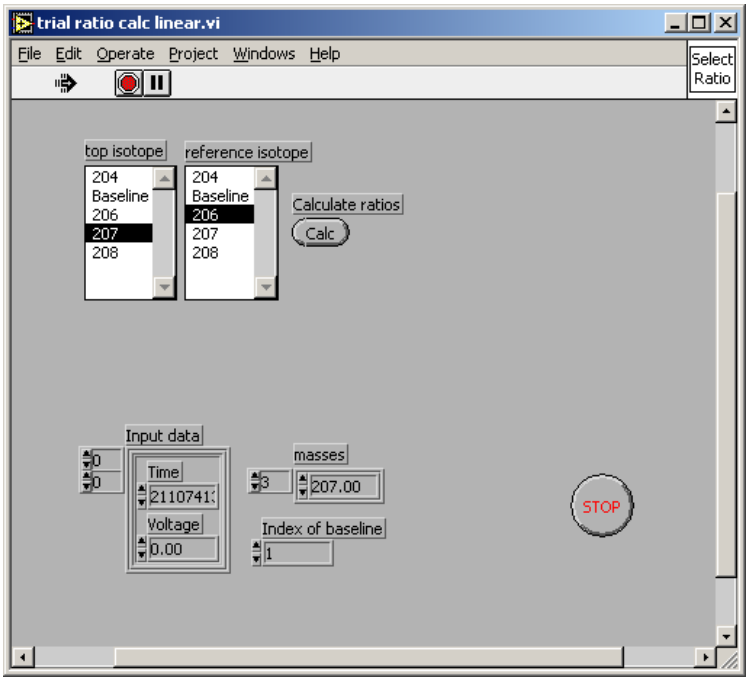

Figure 5.14: 206/207 ratio selection

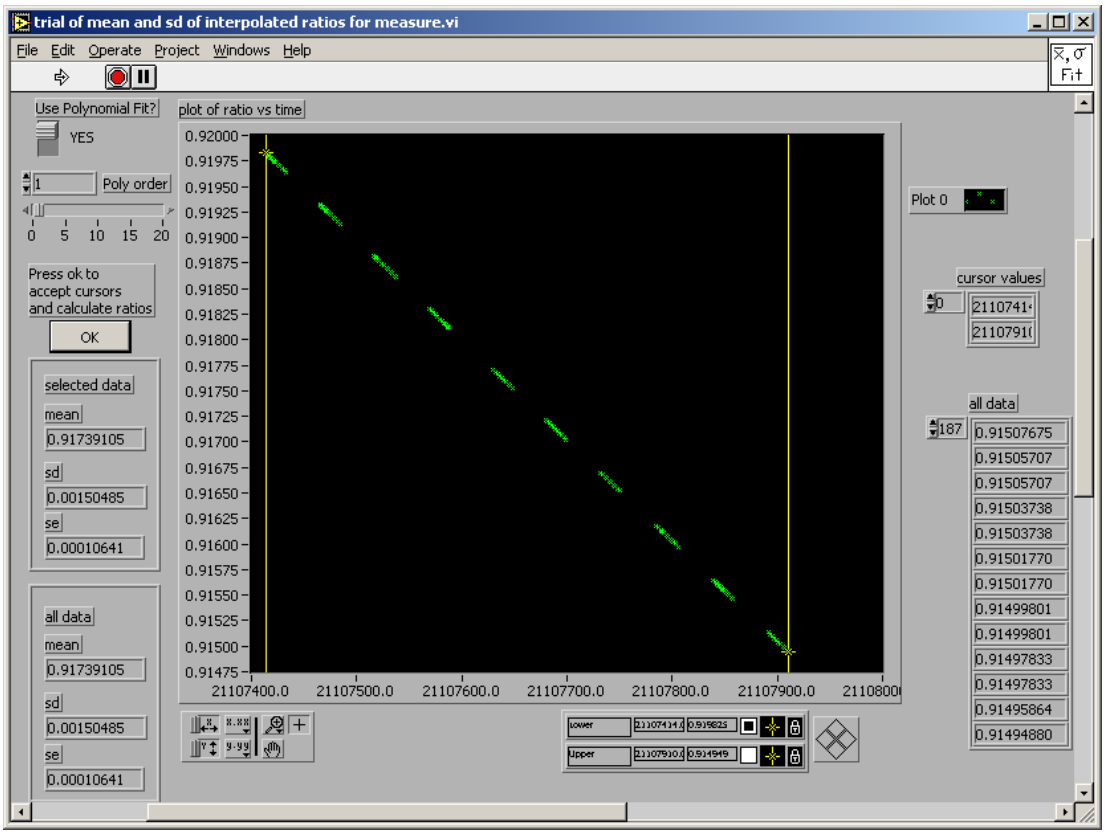

Figure 5.15: Optimal polynomial fit ratio measurement

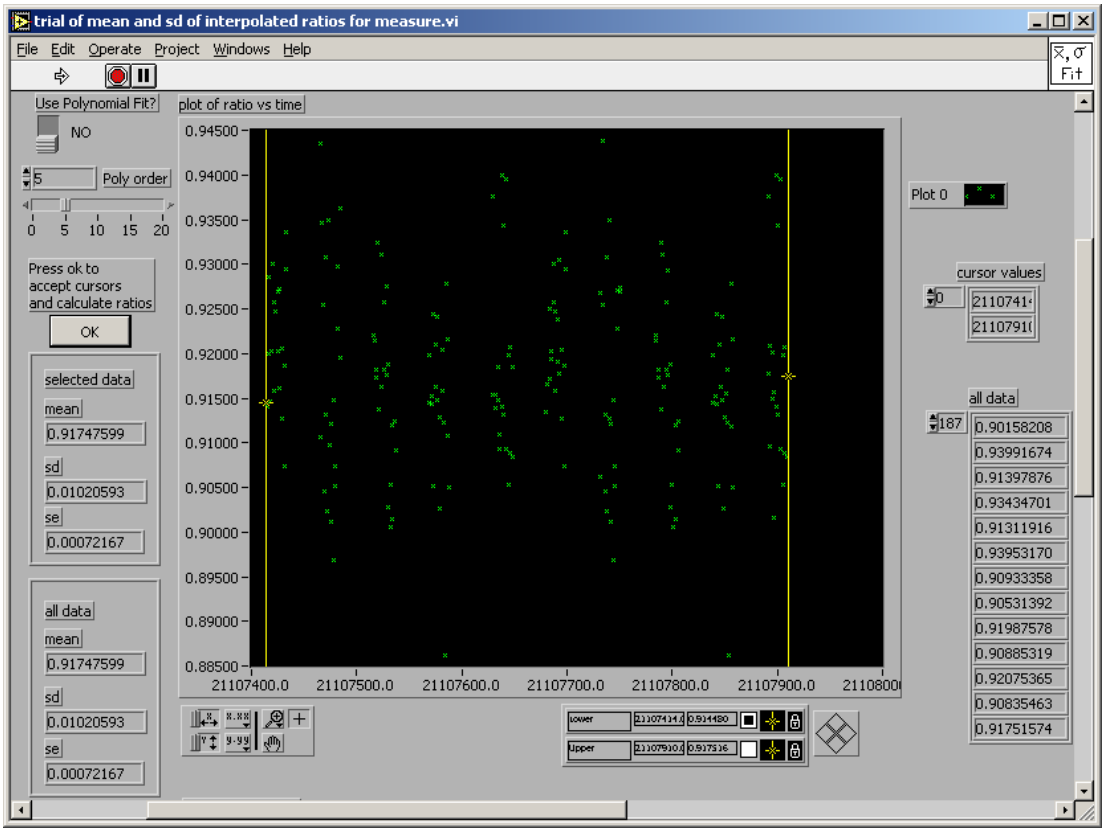

Figure 5.16 Linear fit ratio measurement

The results for the 207/206 ratio, as selected in figure 5.14, are in table 5.6.

Table 5.6: Polynomial fit and linear interpolation results for 207/206 ratio

Order	Ratio	Standard Error
1	0.91755	0.00007
2	0.91755	0.00008
3	0.91763	0.00009
4	0.91413	0.00012
5	0.91523	0.00014
6	0.91472	0.00014
7	0.91434	0.00015
8	0.91217	0.00015
9	0.92940	0.00027
10	0.91870	0.00027
Linear	0.91770	0.00077
Input	**0.917**	

In this case, the order-one polynomial (i.e. a linear regression) gives the most accurate result (0.91755), with the lowest standard error in the table. This should not be surprising as the input data was based on constant level ion currents with noise (i.e. linear). The linear interpolation (which is different to a linear regression) gave the same result, but yielded a higher standard error than the polynomial fit. The improved precision with the polynomial fit was also observed in the test with the VG-354 data as already discussed.

The other isotope ratios showed similar results, with the order-one polynomial fit producing the most accurate results and yielding the lowest standard errors.

In a system with a time-varying ion current, as in the VG-354 test data, higher orders of polynomial would be necessary. Modifications to the model to produce time-varying ion currents would allow further testing of this method.

6. Conclusion

Computer simulations are increasingly being used for a wide variety of purposes. In particular, complex instrumentation can be simulated to provide a replacement for hands-on use in developing operating and analytical procedures. Modern computer-based technology is also allowing the creation of "virtual instruments" where the functions of traditional analog instruments are replaced with computer hardware and graphical software.

The John de Laeter Centre for Mass Spectrometry VG-354 Thermal Ionisation Mass Spectrometer is an excellent example of an instrument that can benefit from such developments. The current software on this instrument utilizes a decade-plus old, inflexible, text-based operating system that has not been ported to modern PC formats because of a host of factors, the most important of which is the very expensive instrumental operational time required to develop and test new or re-written components. This work takes advantage of modern software tools and hardware platforms, and applies Virtual Instrument techniques to the development of new highly flexible simulator and machine control software for this instrument. Most importantly the software was developed by and large without the need for access to the actual mass spectrometer.

The aims of this thesis were to research and develop:

- a numerical model to sufficiently simulate the operation and behaviour of a Thermal Ionisation Mass Spectrometer and
- Virtual Instrument control and measurement software for the Simulated Mass Spectrometer, which did not require the use of the mass spectrometer.

The theory presented in chapters 2 and 3 sets the background requirements for and has been successfully employed to achieve these two objectives.

A Simulated Mass Spectrometer was developed, as detailed in chapter 4. The model was subsequently successfully incorporated into both a mass-spectrum simulator program and an existing VG-354 mass-scanning program. The mass peaks and spectra generated by the model and simulator program realistically simulated those obtained using the actual VG-354 with a stable ion beam. This was limited to ion currents where the Normal distribution

approximation to the Poisson distribution applied to the expected ion counts. Due to time constraints no time-varying characteristics, such as isotopic mass fractionation or major ion beam instability, were incorporated into the model although these are not expected to present major difficulties in any future developments.

The Simulated Mass Spectrometer was used to develop critical measurement modules such as peak centring and isotope ratio calculations. Improved data analysis techniques were developed, which used polynomial fits to find peak centres and to determine isotope ratios. Testing was performed with the Simulated Mass Spectrometer and with data obtained from the existing VG-354 software under normal operating. The major outcomes of these modules were that peak centres were determined to within 1ppm and the standard errors of isotope ratio measurements were reduced by a factor of between 4 and 5 below those achieved with the existing VG-354 software.

7. Recommendations

7.1 Simulated Mass Spectrometer

The Simulated Mass Spectrometer is limited in some ways.

The model simulates a stable ion beam well but does not produce the degree of randomness, range or frequency of temporal variations that provide extra challenges for isotope ratio measurements. Future improvements to the model, introducing instability in the ion beam and fractionation of the sample, would allow more advanced testing of the polynomial fitting techniques.

The ability to realistically simulate low ion currents measured with the Daly system would provide an environment to test how the polynomial fit techniques apply to very small samples. A full Poisson treatment of the measured ion current would be necessary for this.

Simulation of the linearity and relative gains of the Faraday collectors would provide for future development of multiple-collector measurement techniques.

7.2 Measurement Modules

The peak-centring module was tested with Lead spectra. The settings used in the module were therefore manually chosen to provide optimum results for the appropriate mass range. Further testing with a low-mass isotope would allow the development of an “intelligent” algorithm to automatically choose the parameters with which to determine peak centres.

Software could be developed for other modes of mass-spectrometer operation, such as multiple-collector measurement. This would require model enhancements such as a simulation of the relative gains of the Faraday collectors.

7.3 Simulation Replacement and Training Software

The newly developed measurement software and any further enhancements could be converted to work with the VG-354, replacing the existing VG-354 software. At the same time, the simulation-driven modules could be used as training software.

8. References

Alty, J. L. (1993). "Multimedia: we have the technology but do we have a methodology?" Educational Multimedia and Hypermedia Annual **1993**: 3-10.

Berguer, R., R. G. Loeb, et al. (1997). "Use of the virtual instrumentation laboratory for the assessment of human factors in surgery and anesthesia." Studies in Health Technology and Informatics **39**: 187-194.

Bettiol, A. A., J. A. van Kan, et al. (2001). "A LabVIEW(TM)-based scanning and control system for proton beam micromachining." Nuclear Instruments and Methods in Physics Research Section B: Beam Interactions with Materials and Atoms **181**(1-4): 49-53.

Blakey, A. (1994). "Managing Interface Complexity With Mimics." IEE Colloquium on "What are Graphical User Interfaces Good For?" **1994**(021): 5/1-6.

Blaum, K., C. Geppert, et al. (2000). "Peak shape for a quadrupole mass spectrometer: comparison of computer simulation and experiment." International Journal of Mass Spectrometry **202**: 81-89.

Clement, S. and W. Compston (1972). "The design and performance of a Mass Spectrometer Using Ion Beam Transport Theory." International Journal of Mass Spectrometry and Ion Physics **10**: 323-342.

Cross, W. C. (1951). "Two directional focussing of charged particles with a sector shaped uniform magnetic field." Review of Scientific Instruments **22**(717-722).

DeCou, J. M., T. Timberlake, et al. (2002). "Virtual reality modeling and computer-aided design in pediatric surgery: applications in laparoscopic pyloromyotomy." Pediatric Surgery International **18**(1): 72-74.

Delmore, J. E. and A. D. Appelhans (1992). Surface ionization: the chemistry defines the physics?, Los Alamos.

Derra, S. (1998). "Driving simulator focuses on saving lives." R & D **40**(9): 59.

Duckworth, H. E., R. C. Barber, et al. (1986). Mass Spectrometry. London, Cambridge University Press.

Economou, A., S. D. Bolis, et al. (2002). "A "virtual" electroanalytical instrument for square wave voltammetry." Analytica Chimica Acta **467**(1-2): 179-188.

Eng, R. and F. W. Karasek (1983/1984). "Study of the analytical characteristics of an aperiodoc RF mass spectrometer by computer simulation." International Journal of Mass Spectrometry and Ion Processes **55**: 249-261.

Fietzke, J., A. Bollhöfer, et al. (1999). "Proactinium determination in manganese crust VA13/2 by thermal ionization mass spectrometry (TIMS)." Nuclear Instruments and Methods in Physics Research Section B: Beam Interactions with Materials and Atoms **149**: 353-360.

Frew, A. (1998). Programming control modules for use on the VG-354 mass spectrometer using the LabVIEW graphical programming environment. Perth, Department of Applied Physics, Curtin University of Technology.

Garcia-Haro, F. J. and S. Sommer (2002). "A fast canopy reflectance model to simulate realistic remote sensing scenarios." Remote Sensing of Environment **81**: 205-227.

Goonetilleke, R. S., H. Martins Shih, et al. (2001). "Effects of training and representational characteristics in icon design." International Journal of Human-Computer Studies **55**(5): 741-760.

Guo, Z., C. Moulder, et al. (2001). "A virtual instrument for acquisition and analysis of the phonocardiogram and its internet-based application." Telemedicine Journal and e-Health: the Official Journal of the American Telemedicine Association **7**(4): 333-339.

Harrison, I. R. (2001). "Thermal analysis of polymers using virtual instruments; A tool for teaching and training." Thermochimica Acta **367-368**: 85-92.

Hildreth, E. C., E. R. Boer, et al. (2000). "From Vision to Action: Experiments and Models of Steering Control During Driving." Journal of Experimental Psychology: Human Perception and Performance **26**(3): 1106.

Huang, S.-M., K.-K. Shieh, et al. (2002). "Factors affecting the design of computer icons." International Journal of Industrial Ergonomics **29**(4): 211-218.

Jamieson, D. N. and J. M. Pearce (1995). Virtual Laboratory for Ion Scattering to Probe Atomic, Nuclear and Microscopic Structures. Second Australian Conference on Computers in University Physics Education, University of Melbourne, Australia.

Jenness, J. W., R. J. Lattanzio, et al. (2002). "Effects of manual versus voice-activated dialing during simulated driving." Perceptual and Motor Skills **94**(2): 363-380.

Johnson, G. W. (1994). LabVIEW Graphical Programming: Practical applications in instrumentation and control. Sydney, Australia., McGraw-Hill.

Kaelin-Lang, A. and L. G. Cohen (2000). "Enhancing the quality of studies using transcranial magnetic and electrical stimulation with a new computer-controlled system." Journal of Neuroscience Methods **102**(1): 81-89.

Loss, R. D. (1985). Software development on the VG-354 thermal ionisation mass spectrometer. Internal Report no SPG 400/1985/AP 110. Perth, Physics Department, Western Australian Institute of Technology.

Loss, R. D. (1986). Mobility of the Fission Valley Elements from the Oklo Fossil Reactors. Department of Applied Physics. Perth, University of Western Australia.

Meyer, S. L. (1975). Data analysis for scientists and engineers. New York, Wiley.

Microsoft (2001). The history of Windows desktop operating systems. **2002**.

Miller, J. O., R. R. Hill, et al. (2001). Applications of discrete event simulation modeling to military problems. Proceedings of the 2001 Winter Simulation Conference, Arlington, VA.

Müller, W., U. Bockholt, et al. (2000). "VRATS--Virtual Reality Arthroscopy Training Simulator." Der Radiologe **40**(3): 290-294.

National-Instruments (1993). LabVIEW for Windows User Manual. Austin, Texas, National Instruments Corporation.

Patuzzi, R. B. and G. A. O'Beirne (1999). "Boltzmann analysis of CM waveforms using virtual instrument software." Hearing Research **133**(1-2): 155-159.

Platzner, I. T. (1997). Modern isotope ratio mass spectrometry. Chichester, New York, J. Wiley.

Proctor, M. D. and J. C. Gubler (1998). Military simulation worlds and organizational learning. Proceedings of the 1998 Winter Simulation Conference, WSC. Part 1 (of 2).

Reed, M. P. and P. A. Green (1999). "Comparison of driving performance on-road and in a low-cost simulator using a concurrent telephone dialling task." Ergonomics **42**(8): 1015-1017.

Regenstreif, E. (1967). Focussing with Quadrupoles, Doublets and Triplets. Focusing of Charged Particles. A. Septier. New York, Academic Press.

Rigobello, M. P., F. Cazzaro, et al. (1999). "Virtual instrumentation for pH measurements in biological systems." Computer Methods and Programs in Biomedicine **60**(1): 55-64.

Roberts, D. J. (1994). "Getting close to the problem with object oriented interaction (GUIs)." IEE Colloquium on "What are Graphical User Interfaces Good For?" **1994**(021): 5/1-6.

Smith, R. D. (1995). "Wargaming military training via simulations." IEEE Potentials **14**(Oct-Nov): 19-22.

Staggers, N. and D. Kobus (2000). "Comparing response time, errors, and satisfaction between text-based and graphical user interfaces during nursing order tasks." Journal of the American Medical Informatics Association: JAMIA **7**(2): 164-176.

Tollmar, K. and Y. Sundblad (1995). "The design and building of the graphic user interface for the collaborative desktop." Computers & Graphics **19**(2): 179-188.

Toran, F., D. Ramirez, et al. (2001). "Design of a virtual instrument for water quality monitoring across the Internet." Sensors and Actuators B: Chemical **76**(1-3): 281-285.

Turner, J. (1995). Development of a virtual analytical instrument using new generation graphically based software tools. Perth, Department of Applied Physics, Curtin University of Technology.

Turner, J. (1995). Development of a virtual analytical instrument using new generation graphically based software tools. Perth, Department of Applied Physics, Curtin University of Technology.

Walker, H. M. (1989). Computer science 2 : principles of software engineering, data types, and algorithms. Glenview, Illinois, Scott, Foresman.

Waller, J. C. and N. Foster (2000). "Training via the web: a virtual instrument." Computers & Education **35**(2): 161-167.

Werz, R. and P. De Bièvre (1981). Orthodox data reduction and error propagation in isotope ratio measurements. AGMS conference, Amsterdam.

White, F. A. and G. M. Wood (1986). Mass Spectrometry - Applications in Science and Engineering. New York, John Wiley and Sons.

Zubillaga-Elorza, F., C. R. Allen, et al. (1999). "A method for rapid prototyping of instruments using web tools." Microprocessors and Microsystems **23**(4): 235-243.

Appendices

Appendix A – The General Purpose Interface Bus (GPIB)

The General Purpose Interface Bus (GPIB) is an eight-bit parallel digital communications specification originally invented by Hewlett-Packard Corporation in 1965 (called the HP Interface Bus by them). The Institute of Electrical and Electronics Engineers formalised the specifications as IEEE-488 in 1978, when the common name of GPIB was also adopted.

IEEE 488 didn't formalise data formats, status handling and error reporting, so in 1987 the standard was updated to include the hardware definition, IEEE 488.1, and the data specifications, IEEE 488.2.

Important features of the hardware standard include:

- one byte data width
- transfer rates of around 800kB per second
- hardware handshaking
- a maximum separation of 4m between any two devices and an average separation of 2m over the entire bus.
- a maximum bus length of 20m
- up to 15 devices on a single bus

The GPIB uses talkers and listeners to regulate flow of data. The bus is overseen by a controller. The controller addresses the talker and the listener before they can communicate.

There are a total of 16 digital lines in the bus:

- eight data lines DIO1 – DIO8
- three handshake lines DAV, NFRD and NDAC
- five interface management lines ATN, IFC, REN, SRQ and EOI